Functional Labeling of Individualized Post-Synaptic Neurons using Optogenetics and *trans*-Tango

Allison Castaneda

Dissertation submitted to the faculty of the Virginia Polytechnic Institute and State University
in partial fulfillment of the requirements for the degree of

Doctor of Philosophy
In
Translational Biology, Medicine, and Health

Lina Ni, Chair
Shihoko Kojima
Igor Sharakhov
Julia Gohlke

April 27, 2023
Blacksburg, VA

Keywords: neural circuits, thermosensation, optogenetics, transsynaptic tracing

Functional Labeling of Individualized Post-Synaptic Neurons
using Optogenetics and *trans*-Tango

Allison Castaneda

ABSTRACT

Neural circuitry, or how neurons connect across brain regions to form functional units, is the fundamental basis of all brain processing and behavior. There are several neural circuit analysis tools available across different model organisms, but currently the field lacks a comprehensive method that can 1) target post-synaptic neurons using a pre-synaptic driver line, 2) assess post-synaptic neuron morphology, and 3) test behavioral response of the post-synaptic neurons in an isolated manner. This work will present FLIPSOT, or Functional Labeling of Individualized Post-Synaptic Neurons using Optogenetics and *trans*-Tango, which is a method developed to fulfill all three of these conditions. FLIPSOT uses a pre-synaptic driver line to drive *trans*-Tango, triggering heat-shock-dependent expression of post-synaptic optogenetic receptors. When heat shocked for a suitable duration of time, optogenetic activation or inhibition is made possible in a randomized selection of post-synaptic cells, allowing testing and comparison of function. Finally, imaging of each brain confirms which neurons were targeted per animal, and analysis across trials can reveal which post-synaptic neurons are necessary and/or sufficient for the relevant behavior.

FLIPSOT is then tested within *Drosophila melanogaster* to evaluate the necessity and sufficiency of post-synaptic neurons in the *Drosophila* Heating Cell circuit, which is a circuit that functions to drive warmth avoidance behavior. FLIPSOT presents a new combinatory tool for evaluation of behavioral necessity and sufficiency of post-synaptic cells. The tool can easily be utilized to test many different behaviors and circuits through modification of the pre-synaptic driver line. Lastly, the success of this tool within flies paves the way for possible future adaptation in other model organisms, including mammals.

Functional Labeling of Individualized Post-Synaptic Neurons
using Optogenetics and *trans*-Tango

Allison Castaneda

GENERAL AUDIENCE ABSTRACT

The human brain is made up of billions of neurons, each of which are interconnected in various ways to allow communication. When a group of connected neurons work together to carry out a specific function, that group is known as a neural circuit. Neural circuits are the physical basis of brain activity, and different circuits are necessary for all bodily functions, including breathing, movement, regulation of sleep, memory, and all senses. Disruptions in neural circuits can be found in many brain-related diseases and disorders such as depression, anxiety, and Alzheimer's disease.

One example of a neural circuit is that of temperature sensation. When someone holds a cube of ice, temperature-sensing neurons in the hand pass signals along neurons in the spine until they reach the brain. There, the signals are carried to various brain regions to be processed and recognized as cold, and eventually, pain. When the sensory signals of cold and pain grow too prominent to ignore, the person may move to avoid the feeling. In this case, the brain will send signals back down to neurons responsible for movement in the arm, allowing the person to drop the ice cube. Avoidance of temperatures that are too warm or cold is an evolutionary trait that is important in preventing the body from harm.

Even in a relatively simple system like temperature sensation, neural circuits can be complex and difficult to study, especially in higher order organisms such as mammals. For this reason, it can be beneficial to use simpler animals such as *Drosophila melanogaster*, or the common fruit fly. Flies have far fewer neurons than humans, meaning their neuronal connections are also significantly less complicated, and there are many genetic tools available in flies that aren't available in mammalian models such as mice. Additionally, flies are inexpensive, easy to raise, and grow quickly, making them ideal for troubleshooting new tools and replicating experiments. Though somewhat different in anatomy, fly brain function is similar enough to humans and other mammals that findings can often be applied across species. Studies in flies can also be applied in other insects, such as mosquitoes, which are notorious for carrying deadly diseases.

Though there are several available tools in flies to study neural circuits, many tools are better for usage in sensory neurons themselves than in the neurons that carry signals in the brain afterward. This work presents a new tool, abbreviated as FLIPSOT, that modifies and combines several existing genetic methods in order to help examine those higher order neurons. FLIPSOT allows users to determine which higher order neurons are important in leading to behavioral responses, as opposed to carrying the signal to other brain regions, such as those associated with memory. Then, FLIPSOT is implemented in a warmth-sensing neural circuit known as the Heating Cell (HC) circuit and used to identify the higher order neurons needed for fly warmth avoidance.

Development of tools such as FLIPSOT helps to expand our knowledge in the fields of neural circuits and behavior. Genetic tools can also be more easily tested in flies prior to attempting to implement them in other organisms, such as mice. Finally, studying temperature in flies can help create a deeper understanding of how temperature sensation works in all animals, including humans.

For teachers.

ACKNOWLEDGEMENTS

There are so many people who I could not have completed my Ph.D. work without. I owe my greatest thanks to Lina, for your intelligent and compassionate mentorship, for always giving helpful advice and being willing to answer questions every step of the way. I have learned so much from you. The Ni Lab has been a wonderful workplace for the years I have been here. Thank to Ainne, Hua, Thomas, Jackson, Jordan, and Iona, for your camaraderie and assistance with so many things in the lab. Thank you to my undergraduate researchers, especially Julianne and Grace, for helping me to improve my mentorship skills as well as contributing to this research. Finally, thank you to Alisa, for being a fantastic lab manager, friend, and pandemic buddy – I miss chatting with you while sorting our flies!

Thank you to Shihoko Kojima, for your continuous support during my undergraduate throughout my graduate years – I have learned much about research and science from you! Thank you as well to Igor Sharakhov and Julia Gohlke for your invaluable advice as members of my committee. I would have had much more trouble getting through even my first year without support from some of my fellow TBMH cohort members, and there are several people in my GPP cohort who helped me make it through the final dissertation push – thank you!

To my family and friends – thank you so much for your support and kindness throughout the years. Thank you to especially to Victoria, for being there whenever I needed a listening ear, helping hand, or a distraction. Thank you to Kevin, for your stability and willingness to help, sometimes even before I know I need it. Lastly, thank you to Sophia, my sweet furry companion through my time in graduate school.

TABLE OF CONTENTS

ABSTRACT ii

GENERAL ABSTRACT iii

DEDICATION iv

ACKNOWLEDGEMENTS v

LIST OF FIGURES viii

ABBREVIATIONS ix

CHAPTER 1: INTRODUCTION

1.1 Neural circuits are fundamental units of brain function 1

1.2 *Drosophila* is an excellent model for studying neural circuits 1

1.3 Drosophila Heating Cells activate a neural circuit with a simple behavioral output 4

1.4 Current neural circuit analysis tools 9

1.5 Developing a tool to allow behavioral assessment of post-synaptic neurons 14

CHAPTER 2: DEVELOPING FLIPSOT

2.1 Introduction 16

2.2 Establishment of FLIPSOT components 16

2.3 Creating FLIPSOT flies 27

2.4 Methods 33

2.5 Discussion & Conclusions 36

CHAPTER 3: USING FLIPSOT TO FIND NECESSARY AND SUFFICIENT HEATING CELL PROJECTION NEURONS

3.1 Introduction 38

3.2 Establishing experimental controls 38

3.3 Using FLIPSOT to determine necessity and sufficiency 48

3.4 Methods 60

3.5 Discussion & Conclusions 62

CHAPTER 4: GENERAL DISCUSSION

4.1 Summary of findings 65

4.2 Strengths and weaknesses of FLIPSOT 65

4.3 Future Directions 68

4.4 Conclusions 69

REFERENCES 70

APPENDICES 77

LIST OF FIGURES

1. *Drosophila* binary expression systems 3

2. *Drosophila* Heating Cells project from the arista to the brain 6

3. The *trans*-Tango system 18

4. CsChrimson does not negate the effects of Kir inhibition 21

5. GtACR2 and Kir drive comparable avoidance responses 22

6. Single-fly behavior of *HC>GtACR2/CsChrimson* 24

7. Heat shock driving FLP Out 26

8. Using heat shock to drive FLP Out randomizes gene expression 27

9. Effect of genotype and heat shock length on “FRT-stop” cassette removal 29

10. The FLIPSOT system 32

11. Single fly temperature/optogenetic avoidance behavior 40

12. Verification of behavioral assay conditions 43

13. Heating Cell projection neurons 45

14. Effects of arista ablation on warmth avoidance and PNs 47

15. FLIPSOTi experimental workflow 48

16. *HC>FLIPSOTi* indicates necessary PNs for warmth avoidance 50

17. FLIPSOTa experimental workflow 54

18. *HC>FLIPSOTa* indicates sufficient PNs for warmth avoidance 55

19. Age of flies affects thermal preference 59

ABBREVIATIONS

ATR	all-trans retinal
BAcTrace	botulinum activated tracer
ChR	channelrhodopsin
DOCCs/DOG	dorsal organ cool cells/dorsal organ ganglion
EM	electron microscopy
FLIPSOT	functional labeling of individualized post-synaptic neurons using optogenetics and *trans*-Tango
GPCR	G protein coupled receptor
GR	gustatory receptor
GRASP	GFP reconstitution across synaptic partners
GtACR2	*Guillardia theta* anion-conducting channelrhodopsin 2
HC	Heating Cell
IR	ionotropic receptor
Kir	inwardly rectifying potassium channel
lACA	lateral accessory calyx
lALT	lateral antennal lobe tract
MARCM	mosaic analysis with a repressible cell marker
mALT	medial antennal lobe tract
mlALT	mediolateral antennal lobe tract
tALT	transverse antennal lobe tract
TRACT	transsynaptic control of transcription
TRP	transient receptor potential
PA-GFP	photoactivatable green fluorescent protein
PAL	posterior antennal lobe
PI	preference index
PLP	posterior lateral protocerebrum
PN	projection neuron
TEV	tobacco etch virus
VP	ventroposterior
WT	wild type

CHAPTER 1: INTRODUCTION

1.1 Neural circuits are fundamental units of brain function

Primitive brains can be found in animals as simple as the planarian, a type of flatworm capable of responding to several types of stimuli. Despite the obvious differences between flatworms, humans, and all of the organisms in between, their nervous systems show some surprising similarities: sensory neurons synapse onto other neurons in the brain using neurotransmitters, creating a chain reaction of sensory integration that culminates in a behavioral response (Sarnat & Netsky, 1985). Systems of neurons that communicate with each other to execute a common function are known as 'neural circuits' (Bear et al, 2020).

Neural circuits are imperative for all brain functions, from reflexes and breathing to more complex processes such as learning and memory. Disruptions in neural circuitry have been linked with mental illnesses such as depression/anxiety, neurodevelopmental disorders, and neurogenerative disorders such as Alzheimer's disease (McTeague et al, 2017; Sahin & Sur, 2015; Werner et al, 2019). Despite their importance, the neural circuitry for most brain processes is not well described. Neural circuits can be difficult to study, as they often span several regions of the brain and can feature neurons with long, thin processes that are tricky to visualize. Studying these circuits can help to further explain behaviors, give context to less well-known regions of the brain, and help to understand the molecular mechanisms of the neurons that make up each circuit (Olsen & Wilson, 2008).

1.2 *Drosophila* is an excellent model for studying neural circuits

Drosophila melanogaster, a species of common fruit fly, is an extremely valuable model organism for studying neural circuitry. They possess far fewer neurons than more complex models, have a vast array of genetic manipulations available, and display a wide

range of behaviors that can be correlated with higher order organisms (Olsen & Wilson, 2008; White, 2019). Despite their small size, flies have a large variance in neuronal cell types and utilize similar kinds of neurotransmitters and ion channels to the ones mammals do (Venken et al, 2011.) They are inexpensive, have a fast generation time with many offspring, and are well-characterized, both genome and anatomy-wise (Jeibmann & Paulus, 2009). Investigating neural circuitry and behavior in *Drosophila* can provide important insights into the evolution of behavior as well as brain function in higher order organisms (White, 2019).

Studying animals with fewer neurons is advantageous because it reduces the complexity of the brain while still allowing for an observable behavioral response. A neural circuit by definition must span multiple brain regions in order to integrate incoming signals and subsequently perform its designated function; therefore, the fewer neurons in the brain, the smaller the typical circuit, and the easier it is to study and characterize. Additionally, because the Drosophila brain is physically compact, it is possible to image and analyze the whole adult brain at once instead of requiring slicing (White, 2019). When combined with certain circuit visualization techniques, this allows easy visualization of connections between neurons as well as circuit shape and morphology (Ni, 2021.)

The abundance of genetic tools available in Drosophila makes visualizing neural circuits as well as testing their function much easier. Binary expression systems, which are genetic systems that use a transcriptional activator paired with a specific binding site to activate the expression of a gene, allow a high degree of manipulation of groups or even singular neurons through use of neuron-specific promotors (Figure 1; Venken et al, 2011). Optogenetic techniques allow control of behavior through genetic means, permitting the assessment of the necessity and/or sufficiency of specific neurons for certain behaviors (Klapoetke et al, 2014; Mauss et al, 2017). These tools rely on the relative ease of genetic

manipulation of Drosophila and can be implemented through genetic crosses, recombination, and the usage of balancer chromosomes (Miller et al, 2019).

Figure 1: *Drosophila* binary expression systems

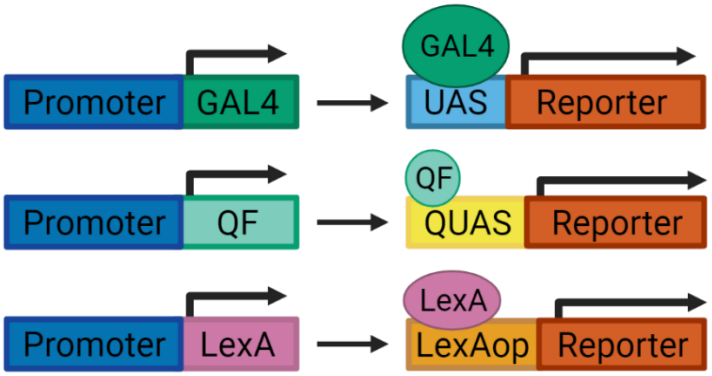

Figure 1. *Drosophila* binary expression systems feature usage of a promoter of choice to drive expression of a transcription factor (GAL4, QF, or LexA). Each transcription factor can then bind to a specific corresponding sequence (UAS, QUAS, or LexAop, respectively) to drive transcription of a reporter or other gene of interest. In this way, binary expression systems limit expression of that gene to cells with the desired promoter, allowing users to restrict gene expression spatially, temporally, or in numerous other ways.

The *Drosophila* nervous system has been used to study circuits involved with all five senses: sight, smell, taste, touch, and hearing (Larderet et al, 2017; Couto et al, 2005; Kim et al, 2017; Tuthill & Wilson, 2016; Boekhoff-Falk & Eberl, 2014). Locomotion and flight, along with more complex circuits such as those associated with courtship, memory, pain, and circadian rhythms have also been studied (Lehmann & Bartussek, 2017; Takayanagi-Kiya and Kiya et al, 2019; Keene & Waddell, 2007; Neely et al, 2011; King & Sehgal, 2020).

However, not all of these circuits are fully understood, and there are many facets of the nervous system left to explore. One such group of circuits that have not yet been fully described are those involving temperature sensation. Though there are several known temperature receptors as well as thermosensory neurons, much less is known about the circuits involved thereafter (Hamada et al 2008; Ni et al 2013; Ni et al 2016). Investigating these systems in *Drosophila*, with its relatively simple brain, gives an excellent foundation for studying the circuits behind similar behaviors in more complex organisms.

1.3 *Drosophila* Heating Cells activate a neural circuit with a simple behavioral output

Temperature is an important part of survival for all animals; if it is too hot or too cold, even humans can experience weakness, fatigue, illnesses like heat stroke, and death (Seltenrich 2015). Rising temperatures due to climate change have been predicted to cause overwhelmingly negative physiological and metabolic disruptions in mammals such as livestock animals, as well as many other animals, particularly those in warmer latitudes (Lacetera, 2019; Deutsch et al, 2008; Burraco et al, 2020). Heat failure rates in terrestrial ectotherms have been modelled to increase by as much as several hundred percent in the next century (Jørgensen et al, 2020). As our planet increases in temperature, it is important to study the basis of temperature sensation so that we can work to understand these physiological effects on both people and animals.

External temperature is especially important for those animals who cannot regulate their own internal body temperatures, like *Drosophila*. Flies' small size means that their internal body structures will quickly reach the temperature of their environment (Garrity et al, 2010). Placing flies in a vial at 40ºC for 10 minutes begins to incapacitate the animals and causes death shortly afterward (Neely et al, 2011). Thus, it is vital for them to be able to avoid noxious temperatures. There are also more sophisticated behaviors that rely on

temperature, such as mating and food preference (Miwa et al, 2018; Brankatschk et al, 2018). Females respond to courtship at much lower rates as temperature increases, eventually stopping altogether at 36ºC, and may choose different places to lay eggs depending on temperature (Miwa et al, 2018; Dillon et al, 2009). This makes temperature extremely important for both reproduction and individual fitness of the species, even when it is not a temperature that is fatal to the animal.

The impact of temperature on *Drosophila* evolution can be inferred by their extraordinarily sensitive evasive response to non-optimal temperatures. Wild type flies highly prefer 25ºC (about room temperature) over higher or lower temperatures, even ones differing by just a few degrees (Dillon et al, 2009). Flies will quickly avoid unfavorable temperatures in a process termed thermotaxis (Garrity et al, 2010). In order to produce such a rapid behavioral output, flies use several different types of thermosensory neurons to sense non-optimal temperatures. When these neurons activate, they trigger the activation of their respective neural circuits, which ultimately can lead to avoidance behavior (Hamada et al, 2008; Ni et al, 2013; Ni et al, 2016). Thus, thermosensory avoidance circuits are an example of relatively simple circuits with a sensory input that leads eventually to a motor output, i.e. moving away from the aversive temperature. This avoidance can also be integrated to create a memory and learned response (Putz & Heisenberg, 2002).

The *Drosophila* Heating Cell circuit is one such example of a thermosensory avoidance circuit. Heating cells, or HCs, are located in the arista of the fly, which is a thin, hair-like structure that protrudes from the third segment of the antenna. In order to sense warm temperatures, HCs express a thermosensory receptor called GR28b(D). GR28b(D) is a member of the gustatory receptor family; it has been demonstrated as thermosensitive to temperatures starting at about 26ºC (Ni et al, 2013). GR28b(D) is one of several thermoreceptors that have been described in *Drosophila*, a category that also contains

transient receptor potential (TRP) channels such as TRPA1 and ionotropic receptors (IRs) such as IR21a (Hamada et al, 2008; Ni et al, 2016). GR28b(D) itself has been described as a nonspecific cation channel, and it confers temperature sensitivity to other neurons when ectopically expressed, proving its sufficiency as a thermosensor (Ni et al, 2013; Mishra et al, 2018). GR28b(D) is also necessary for rapid negative thermotaxis (Ni et al, 2013). Thus, once GR28b(D) is activated by warm temperatures, it drives activation of the HCs which then triggers the HC neural circuit.

The HCs have long, thin processes that allow them to travel, or project, from the arista into the brain (Figure 2). There, they converge on a region called the Posterior Antennal Lobe (PAL) in a specific glomerulus called VP2 (VP, ventroposterior; Gallio et al, 2011). The second-order neurons of the circuit, or the neurons that are post-synaptic to the HCs, consist of local interneurons (which connect to other areas in the antennal lobe) as well as far-reaching projection neurons (PNs). These PNs project and carry information to other regions of the brain.

Figure 2: *Drosophila* Heating Cells project from the arista to the brain

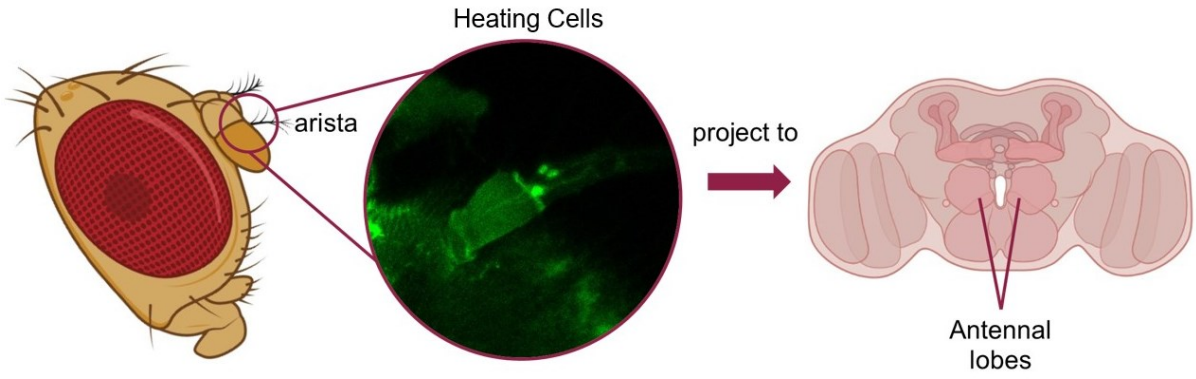

Figure 2. The three Heating Cells (HCs) located at the base of each arista project to the VP2 glomerulus, which is located in the medial posterior region of the antennal lobe.

Several HC PNs that project from the antennal lobe to other brain regions have been previously described; they will be referred to here as antennal lobe tracts (ALTs) based on their relative morphology and positioning in the brain. Frank et al depicted warm-responsive neurons that follow three general tracts: a medial tract (mALT) that curves up through the mushroom body and lateral horn, then back down the lateral side of the brain; a lateral tract (lALT) with neurons that curve outwards and upwards toward the lateral horn, sometimes with a sharp bend back downwards toward the posterior lateral protocerebrum (PLP); and a transverse mediolateral tract (mlALT) that starts upwards along the medial path before cutting diagonally outwards toward the lateral horn. The mushroom body and lateral horn are both regions of the brain that are known for sensory processing, while the PLP is a less well-known region that can thus be inferred as important in temperature processing. The described medial tract PNs were shown to be necessary for rapid avoidance of 30ºC; however, whether the neurons were sufficient for this behavior was not tested. Additionally, although the driver line for the behavioral experiments was tested for synaptic connection to the HCs, the behavioral response was not tested for reliance on the HCs nor GR28b(D) (Frank et al, 2015).

Liu et al describe two warm-responsive PN types: one PN type which follows a similar path as Frank et al's medial tract, arcing up and around through the mushroom body and lateral horn before curving back down laterally toward the PLP, and a more lateral PN type that curves outward through the PLP and up toward the lateral horn. The neurons' responses to warmth were eliminated after removal of the arista, but interestingly, they continued to respond to warmth even in a *Gr28b.d* mutant background, a process explained by potential disinhibition by the cool-responsive circuits (Liu et al, 2015). However, behavioral responses were not tested in this study, and since the initial search for PNs was

done through screening driver lines, it is highly possible that there are additional warm responsive PNs not described here.

Marin et al took a different approach to identify several thermosensory PNs, using electron microscopy data to find neurons that project from the VP2 to other areas of the brain. They were able to reconstruct at least 13 different PNs, some of which also receive input from other VP areas, and many of which are similar in morphology to those described by either Frank et al or Liu et al. One notable exception is a mediolateral transverse neuron (tALT) that follows a path to the lateral horn similar to Frank et al's transverse tract; however, instead of cutting straight across to the lateral horn, there is a recognizable bend in the middle. They also define a new small brain region, called the lateral accessory calyx (lACA), which is a part of the mushroom body that receives input from several thermosensory PNs (Marin et al, 2020). This study thoroughly described the morphology of many VP2 PNs, but did not experimentally assess PN function, behaviorally or otherwise.

Despite the studies that have been done to investigate the HC PNs, more work will need to be done to firmly assess which PNs are necessary and/or sufficient for behavior driven by HC activation. From there, further advances can be made in determining the next neurons important for driving the behavioral circuit, both third-order and beyond. Studying circuits like the HC circuit in *Drosophila* can help us to understand temperature responses in similar ectotherms such as mosquitoes, who also rely on temperature in order to seek hosts for blood feeding (Wang et al, 2009; Corfas & Vosshall, 2015). Additionally, *Drosophila* serves as a simpler, more genetically tractable model for elucidating temperature circuits, and these circuits can then be used as a basis to study those in higher order organisms such as mammals.

1.4 Current neural circuit analysis tools

The many tools currently available to help examine neural circuits can be broadly divided into two categories: those that allow visualization of circuit morphology and/or synaptic connections, and those that allow functional analysis of the neurons. Though all of these tools are useful in different ways, each of them has different strengths as well as limitations to their usage. Additionally, there are certain desirable capabilities that the current available tools lack, such as the ability to concurrently assess morphology and function. Below is a general discussion of some of these tools; PA-GFP, GRASP, TRACT, *trans*-Tango, BAcTrace, and electron microscopy are tools that are typically used to assess morphology and/or synaptic connections, while calcium imaging, paired recording, and thermo/optogenetics are tools that are used to assess function.

Photoactivatable GFP (PA-GFP) is a green fluorescent protein variant that increases in fluorescence after exposure to both irradiation and excitation. This method was first tested in cell lines, but has later seen use in several models, including *Drosophila* and mice (Patterson & Lippincott-Schwartz, 2002; Frank et al, 2015; Peter et al, 2013). This method is useful in visualization of post-synaptic neuron morphology by expressing PA-GFP in all neurons, then targeting certain pre-synaptic terminals in order to photoconvert the GFP. Neurons with post-synaptic terminals in the same region will also experience photoconversion, and the GFP will diffuse along the length of the cell, hence allowing visualization (Venken et al, 2011). This method is useful in that the photoconversion can be very specifically targeted to a certain area. However, it has drawbacks in that it is relatively invasive. It also does not truly confirm synaptic connections, as cells are photoconverted based on proximity rather than activity, function, or ligand binding.

GRASP, or GFP Reconstitution Across Synaptic Partners, is a system that involves expressing paired fragments of GFP the membrane of different neurons. When cells are

close enough for the complementary fragments to unite, such as at the synapse, GFP will fluoresce and allow visualization of those areas. GRASP was a tool initially created in *Caenorhabditis elegans*, but it has since been used successfully in *Drosophila* as well as in mice (Feinberg et al, 2008; Shearin et al, 2018). Different variants of GRASP have also been developed, such as t-GRASP, which pairs its split GAL4 fragments with proteins that localize them specifically to either the pre- or post-synaptic membrane. This allows for a more confident assessment of synaptic connections (Shearin et al, 2018). GRASP is an excellent tool for validation of synapses and can even predict the directionality of a synapse if variants such as t-GRASP are used, though the tool is limited in that it requires a driver for both the pre- and post-synaptic neuron in order to enable expression of the GFP fragments.

TRACT (transsynaptic control of transcription) and *trans*-Tango are two methods that use pre-synaptic drivers to express reporters in post-synaptic neurons. They do this through usage of multiple fusion proteins, one of which is an exogenous ligand that is selectively localized to pre-synapses. The fusion protein receptor for the ligand is expressed in all neurons and is localized to post-synapses. When expression of the ligand is driven in a pre-synaptic neuron, the ligand will bind only to receptors expressed on cells that are post-synaptic to the original neuron. The receptor binding triggers a cleavage event, freeing an attached transcription factor that can then translocate to the nucleus and activate reporter expression. These two methods differ in several ways. Firstly, the exogenous fusion proteins and receptors are different; TRACT relies on the mouse CD19 antibody and its receptor, as well as parts of the *Drosophila* Notch pathway, while *trans*-Tango uses human glucagon and its receptor. The portions of the fusion proteins used to localize the ligand and receptor to the pre- and post-synapse respectively are also different between the systems. Finally, *trans*-Tango utilizes GAL4-UAS as the primary driver expression system and the Q system as a means to express the reporter, while TRACT uses LexA-LexAop as its primary system

and a modified GAL4 to express the reporter (Huang et al, 2017; Talay et al, 2017). Despite the relative similarities between the two methods, *trans*-Tango has seen much more usage than TRACT; the *trans*-Tango study has roughly five times the amount of citations as the TRACT study on PubMed (98:20 at the time of this writing) and has been used to study a wide range of circuit types (Ni 2021). This is more likely due to the compatibility of *trans*-Tango with GAL4 than to an issue with the TRACT system as a whole, as there is a large abundance of pre-existing GAL4 driver lines compared to that of LexA, so the likelihood of finding a GAL4 driver for a primary neuron of interest is much higher (del Valle Rodríguez et al, 2012). However, both TRACT and *trans*-Tango are useful tools for confirming anterograde synaptic signaling, and while neither include a functional component on their own, the reporter in the post-synaptic cell could easily be replaced with a genetic component that allows for functional assessment.

In contrast to anterograde tracers such as TRACT and *trans*-Tango, BAcTrace (which stands for botulinum activated tracer) is used for retrograde tracing, or post-synaptic to pre-synaptic. The tool is based on a botulinum toxin mechanism that allows the fusion protein, which is initially expressed on the outside of the post-synaptic cell, to cross to the pre-synapse. There, it binds to another fusion protein, which is a receptor that is made available on the inside of the synaptic vesicle during vesicular neurotransmitter release. Then, the vesicle is reabsorbed into the pre-synaptic cell, and the transcription factor originally attached to the receptor is released by a cytosolic protein and translocates to the nucleus to activate reporter expression. Besides acting in the opposite direction from the other trans-synaptic tracers, BAcTrace also differs in that it requires a separate, non-overlapping driver line for expression of the ligand (GAL4) and the receptor (LexA) instead of just the ligand (Cachero et al, 2020). This is due to the toxicity of the receptor when expressed in all neurons, but unfortunately it also limits the tool in that discovery and

verification of synaptic connections can only occur if both a specific post-synaptic driver as well as a less specific pre-synaptic driver exist. This also may lead to confirmation bias on the part of the experimenter, since choice of pre-synaptic driver may accidentally exclude other possible pre-synaptic neurons. Additionally, as with TRACT, availability of LexA lines is more limited compared to GAL4. BAcTrace is a useful method for confirming pre-synaptic connections, but it does not inherently include a functional component and may be best used alongside another method for validation.

Electron microscopy (EM) can be used for neural circuit analysis by taking partial or entire volumes of the brain, then analyzing the processes of neurons to find visible indicators of synaptic activity. The first full adult fly brain EM volume was completed in 2018 and has been pivotal in broad connectomics studies (Zheng et al, 2018; Marin et al, 2020). Other partial volumes of the fly brain also exist and have been used to study circuits and synaptic connections (Scheffer et al, 2020). However, the low number of volumes available makes comparative analysis either difficult or impossible depending on the brain region of interest, and analysis is specialized and time consuming. EM analysis is useful for discovery of synaptic connections and comparison to genetic tracing methods, but it cannot confirm functional connectivity, nor does it currently account for variation between animals.

Paired recording and calcium imaging are two methods that are often used for functional analysis of neurons. Paired physiological recording does not necessarily require a driver line and allows a side-by-side comparison of the change in membrane voltage of two neurons, which can help elucidate information about the synapse as well as about functional response to a stimulus. (Bykhovskaia & Vasin et al, 2017). However, *in vivo* paired recording in the brain is extremely challenging due to the small size of *Drosophila* neurons, so it is often not as feasible as other methods. Calcium imaging involves the usage of fluorescent calcium indicators to measure the amount of calcium influx into the neuron, thereby

measuring neuronal activity. Synaptic or circuit activity can be assessed through expression of the calcium indicator using a driver line that labels multiple cells in the circuit (Vajente, 2020). Calcium imaging is a good method for both confirmation of synaptic activity and functional assessment of neurons, but it is not as useful for investigation of morphology. However, pairing of calcium imaging with other trans-synaptic tracing techniques such as *trans*-Tango allows the assessment of morphology, synaptic connection, and neuronal activation in tandem (Guo et al, 2018; Snell et al, 2022).

Optogenetics and thermogenetics are techniques that involve using driver lines (the "genetic" component) to target expression of a receptor that can be activated by light or temperature, respectively. This allows external activation of the neuron, after which any potential behavioral changes can be assessed (Mauss et al, 2017; Mishra et al, 2018). Neurons can then be visualized after the fact, since these receptors are typically tagged with fluorescent reporters. These techniques can also be used in combination with calcium imaging as a source of stimulation for a circuit or group of neurons. Optogenetics is more widely used and has been utilized in several different models including mice, but its ability to assess mouse behavior is hindered by the need for an intracranial implant to deliver light (Moulin et al, 2021). *Drosophila* are much more conducive to optogenetic behavioral manipulation, as their smaller size and relatively thin cuticle allows light to penetrate the brain without invasive surgery. Since opto- and thermogenetics require driver lines, they are not very useful for initial screens of synaptic connections, but they can be used for confirmation of connections as well as for functional assessment of different parts of a circuit.

The above tools have allowed for many discoveries in the field of neural circuit analysis in both *Drosophila* and other models. However, many methods require specific driver lines, intricate experimental methods, or are limited in what they are able to help

assess. Creating new combinations of existing tools, such as the addition of calcium imaging to *trans*-Tango, can help to fill these gaps and further facilitate the study of neural circuits (Snell et al, 2022).

1.5 Developing a tool to allow behavioral assessment of post-synaptic neurons

The HC neural circuit still has several associated unanswered questions. There are not yet proper candidates for which PNs are necessary or sufficient to drive avoidance behavior, and information is not yet available about third-order neurons of the circuit and beyond. In order to “crack” the warmth avoidance circuit driven by the HCs, it is imperative to deduce the necessary and/or sufficient PNs, after which necessary and/or sufficient third-order neurons, etc. can be studied and defined. Eventually, tracing far enough along the circuit will lead to motor output neurons, at which point the full warmth avoidance circuit would be completed.

Though many useful tools exist for neural circuit tracing and functional analysis, there is not yet an existing tool that allows for both behavioral analysis of post-synaptic neurons as well as assessment of pre-synaptic connection. Additionally, many tools require driver lines, which are sometimes limited in availability and can bias the resultant outcome. Sensory neurons lend themselves more easily to creation of new driver lines due to the prominence of receptors that can be used as markers as well as distinctive locations outside the brain, but PNs tend to have more complicated, less unique brain paths as well as less distinctive expression of possible markers. Thus, isolating possible promoters to create PN driver lines from is difficult, and though many studies screen randomized collections of driver lines to find drivers specific to PN expression, this method often yields lines with additional expression in unrelated neurons or lines that do not illuminate all of the PNs at once (Liu et

al, 2015; Frank et al, 2015). Using a trans-synaptic tool like *trans*-Tango negates the need for PN-specific driver lines, but the current iterations of *trans*-Tango do not involve a behavioral component.

The second chapter of this work describes the conceptualization and creation of a tool called FLIPSOT, or Functional Labelling of Individualized Post-Synaptic Neurons using Optogenetics and *trans*-Tango. FLIPSOT is a *trans*-Tango and optogenetics based tool that allows usage of a pre-synaptic driver line to target and assess behavioral function of post-synaptic neurons. It also includes a randomization component, which is important for ensuring that functional assessment of post-synaptic neurons can be isolated and compared. Finally, it includes a fluorescent reporter as well as a control reporter for visualization of morphology. The third chapter of this work goes on to describe the usage of FLIPSOT to evaluate which HC PNs are necessary or sufficient to drive warmth avoidance behavior. The HC PNs are characterized and described, and the necessary or sufficient PNs are elucidated through single-fly behavioral experiments followed by imaging.

Drosophila is an optimal model for implementing new tools such as FLIPSOT because of the extensive genetic resources and knowledge already available. Using tools like FLIPSOT to explore the neural circuitry of temperature sensation will help to deepen understanding of sensory systems as well as behavior and fly neural anatomy. Finally, tools that are created and tested in *Drosophila* first can be more easily implemented in other model systems, aiding the research community as a whole.

CHAPTER 2: DEVELOPING FLIPSOT

2.1 Introduction

The neural circuitry of temperature sensation in *Drosophila*, particularly where it involves third-order neurons and beyond, is not well described. Even second-order PNs are surrounded by uncertainty as to their exact function within their circuits (Marin et al, 2020). Sensory neurons, such as those that sense temperature, are typically the most well-characterized neurons in their respective circuits due to unique receptors that can be used as markers, as well as spatial positioning toward the outside of the brain, head, or even on the body. However, neurons post-synaptic to the sensory neurons are much more difficult to target due to less obvious markers, complex inner brain circuitry, and high degrees of similarity in morphology between neurons that are part of different circuits altogether (Marin et al, 2020).

While there are currently tools available to help describe morphology of post-synaptic neurons using a pre-synaptic driver, none exist that work to assess the behavioral necessity or sufficiency of these neurons (Talay et al, 2017; Huang et al, 2017). This work aims to establish a method that will allow the possibility of such testing.

2.2 Establishment of FLIPSOT components

The first task in creation of the FLIPSOT tool was to decide on a method of targeting the post-synaptic neurons. Two tools, TRACT and *trans*-Tango, were available for usage and could be modified to suit our needs. In the end, *trans*-Tango was selected for use due to its reliance on GAL4 driver systems compared to TRACT's reliance on LexA. GAL4 is a far more common driver, and many GAL4 lines exist for isolated expression in small sets of pre-

synaptic neurons. However, TRACT was and still is a viable alternative, and could potentially be used to extend the system in the future (see Discussion).

trans-Tango requires expression of several different genetic components in neurons of interest (Figure 3). The first component is the *trans*-Tango ligand, which is a fusion protein under GAL4-UAS control. It consists of a human glucagon protein, the extracellular domain of human ICAM1 for length, and parts of Neurexin1, a *Drosophila* protein that functions to localize the entire ligand to the pre-synaptic membrane. Usage of primarily human proteins helps ensure that the system will not have off-target effects within the cell. All of these parts combine to create a ligand which can be expressed specifically in pre-synaptic neurons, localizes to the pre-synaptic membrane, and bridges across the synapse. The second component of the system is the *trans*-Tango receptor. This fusion protein contains the human glucagon receptor (a GPCR, G-protein coupled receptor) linked by a tobacco etch virus (TEV) cut site to the transcription factor QF. Though this component is expressed in all neurons, the receptor will only be bound and activated in neurons that are post-synaptic to those that express the *trans*-Tango ligand. The third system component, a protease, is also expressed in all neurons. It consists of a TEV protease linked to human beta-arrestin2, which is a protein recruited upon activation of GPCRs such as the human glucagon receptor. Once recruited, the TEV protease will cut at the TEV cut site, releasing the QF transcription factor from the *trans*-Tango receptor. Finally, the system requires a fluorescent reporter under QUAS control, which will be expressed once QF is free to translocate to the post-synaptic nucleus. A separate pre-synaptic reporter under UAS control marks pre-synaptic neurons for comparison (Talay et al, 2017). In sum, the system includes a ligand expressed using a GAL4 driver in pre-synaptic cells, which will then bind to its receptor only in post-synaptic neurons. Binding of the receptor recruits the protease, which allows transcription factor QF to move to the nucleus and activate reporter expression in post-

synaptic neurons. Thus, the *trans*-Tango system can be easily activated using pre-synaptic drivers to reveal post-synaptic neuronal morphology.

Figure 3: The *trans*-Tango system

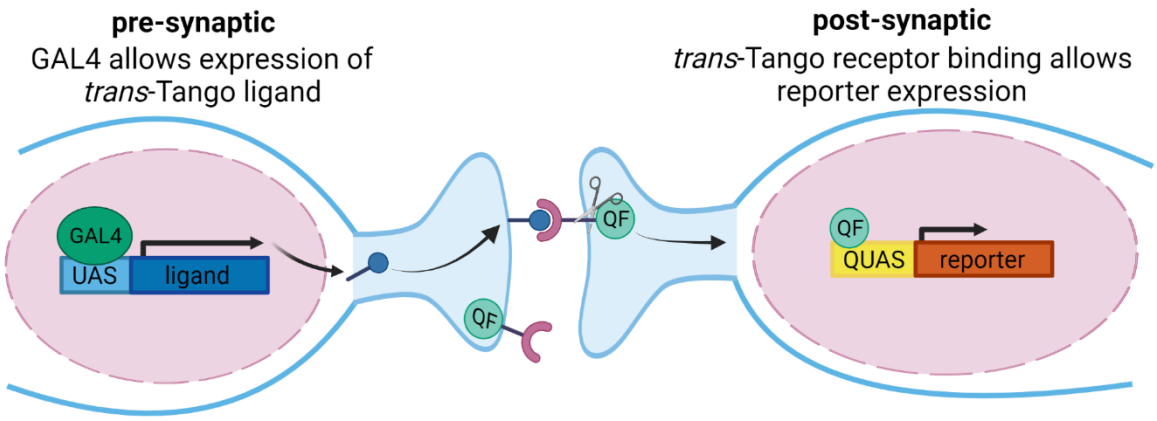

Figure 3. GAL4 expressed using a pre-synaptic promoter binds to UAS and drives expression of the *trans*-Tango ligand (dark blue). The ligand translocates to the pre-synaptic membrane, where it binds to the *trans*-Tango receptor (purple). Receptor binding recruits the presence of a protease, which cleaves at the TEV cut site and frees the QF transcription factor to move to the nucleus and activate reporter transcription.

Our interest in the *trans*-Tango system stemmed from the fact that its post-synaptic reporter is under simple QUAS control. Though the Q system is not as widely used as GAL4 or LexA, it is becoming more common as a method for expression alongside either of the latter systems (del Valle Rodríguez, 2012). More interestingly, in this case it represented an opportunity to add a behavioral component to the *trans*-Tango system, as using *trans*-Tango-driven QF-QUAS to control a method of behavioral manipulation would thereby

restrict that method to the post-synaptic neurons. The next goal was thus to decide on a method of manipulating behavior. To achieve the target of determining necessity and sufficiency of post-synaptic neurons, two different methods were required: a way to inhibit the neurons (to evaluate necessity) and a way to activate the neurons (to evaluate sufficiency).

CsChrimson is a robust, well-tested, and widely used optogenetic activator in *Drosophila*. It is a channelrhodopsin, which is a class of light-activated ion channels, and was derived from the algae *Chloromonas subdivisa*. CsChrimson responds to red light and allows an influx of positive ions when activated, causing strong depolarization and thus activation of the neuron (Klapoetke et al, 2014). Since its conception, its establishing paper has garnered over five hundred citations on PubMed, and there are multiple fly stocks including CsChrimson that are publicly available. Thus, we decided to build upon CsChrimson as our activator.

Choosing a method of inhibition was slightly more difficult, as it had to fulfill several criteria: 1) it could not interfere with the function of CsChrimson, and vice versa, 2) it needed to either be activated separately from CsChrimson or potentially overridden by CsChrimson, and 3) it had to drive a robust response. We considered Halorhodopsin, which is a different optogenetic channel that drives neuronal inhibition; however, it responds to yellow light, which overlaps more closely in spectra to CsChrimson's activation range than is desirable (Inada et al, 2011). Ultimately, two different potential methods of inhibition were investigated: inwardly rectifying potassium channels (Kir) and GtACR2 (*Guillardia theta* anion-conducting channelrhodopsin 2).

Kir channels are channels that, when overexpressed, allow an increased amount of potassium to leave the neuron. This causes hyperpolarization of the membrane, which makes it increasingly hard to cause an action potential, and so overexpression of Kir is

commonly used as a genetic method of neuronal inactivation (Hodge 2009). GtACR2 is from a family of Channelrhodopsins that allows negative chloride ions into the cell instead of positive ions, causing the cell to hyperpolarize and inhibiting the neuron. GtACR2 was chosen over a similar channel, GtACR1, because GtACR2 is activated by blue light and as such does not have an activation spectrum that overlaps as much with CsChrimson (Meloni et al, 2020).

We theorized that the strong activation caused by CsChrimson may be enough to overcome the hyperpolarization caused by Kir. To assess the possibility of using Kir along with CsChrimson in this manner, we expressed both in Gr66a positive neurons; Gr66a is a bitter sensing receptor that drives aversion to bitter tastes (Dweck & Carlson, 2020). Driving CsChrimson in Gr66a+ neurons alone typically causes flies to display a strong aversive response to red light (Aso et al, 2014). However, larvae expressing CsChrimson along with Kir in Gr66a+ neurons neglected to show a statistically significant aversive response to light compared to larvae raised without dietary all-trans-retinal (ATR), which is required for optogenetic receptor function (Figure 4). This suggested that unfortunately the depolarization of Kir+ prevented optogenetic activation by CsChrimson.

Figure 4: CsChrimson does not negate the effects of Kir inhibition

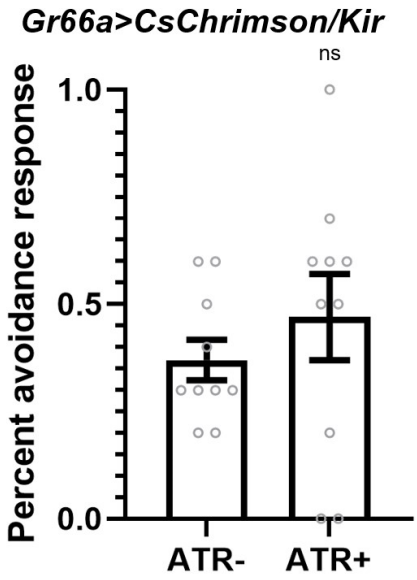

Figure 4. *Gr66a-GAL4* was used to drive expression of both CsChrimson and Kir in larvae. Larvae that were raised with (+) or without (-) dietary retinal were evaluated for avoidance responses such as turns and stops when presented with short periods of red light. Mann-Whitney test, n=10.

Therefore, we turned to GtACR2. GtACR2 was a relatively new optogenetic tool in flies during the development of this system, with the first studies in *Drosophila* adults only being completed a few years prior to FLIPSOT conception (Mohammad et al, 2017). We tested GtACR2's inactivation capabilities in comparison with Kir by expressing either one in the Heating Cells (HCs) and found that GtACR2 inhibited warmth avoidance at similar rates to Kir (Figure 5).

Figure 5: GtACR2 and Kir drive comparable avoidance responses

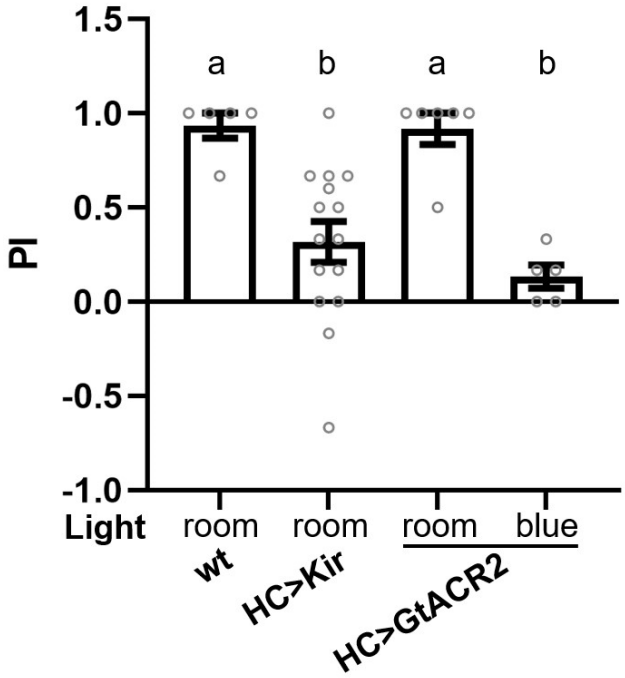

Figure 5. *HC-GAL4* was used to drive expression of either Kir or GtACR2. Flies were examined for warmth avoidance under ambient room or blue light. GtACR2-expressing flies under blue light displayed a defect in warmth avoidance similar to those expressing Kir; GtACR2-expressing flies under room light were indistinguishable from wild type. n=5-15, data represent means ± SEM, Kruskal-Wallis followed by Dunn's multiple comparisons test; letters denote statistically significant groups of $p<0.05$.

To test the possibility of using both CsChrimson and GtACR2 together in the same fly line, we expressed both receptors in the HCs and examined either single fly optogenetic avoidance behavior or single fly warmth avoidance behavior, respectively. Flies of the same genotype with an absence of dietary ATR were used as a control. *HC>GtACR2/CsChrimson* flies displayed an aversion to red light as well as an absence of aversion to warmth in blue light, suggesting that both CsChrimson and GtACR2 were able to be activated in isolation and without strongly interfering with one another (Figure 6B-C). Though there was a statistical difference in room light avoidance between the ATR- and ATR+ flies (Figure 6A), both groups still displayed satisfactory warmth avoidance, so this did not have an overall effect on experimental outcome. Therefore, we confirmed that GtACR2 fulfilled the requirements as an inhibitor for our system.

Figure 6: Single-fly behavior of *HC>GtACR2/CsChrimson*

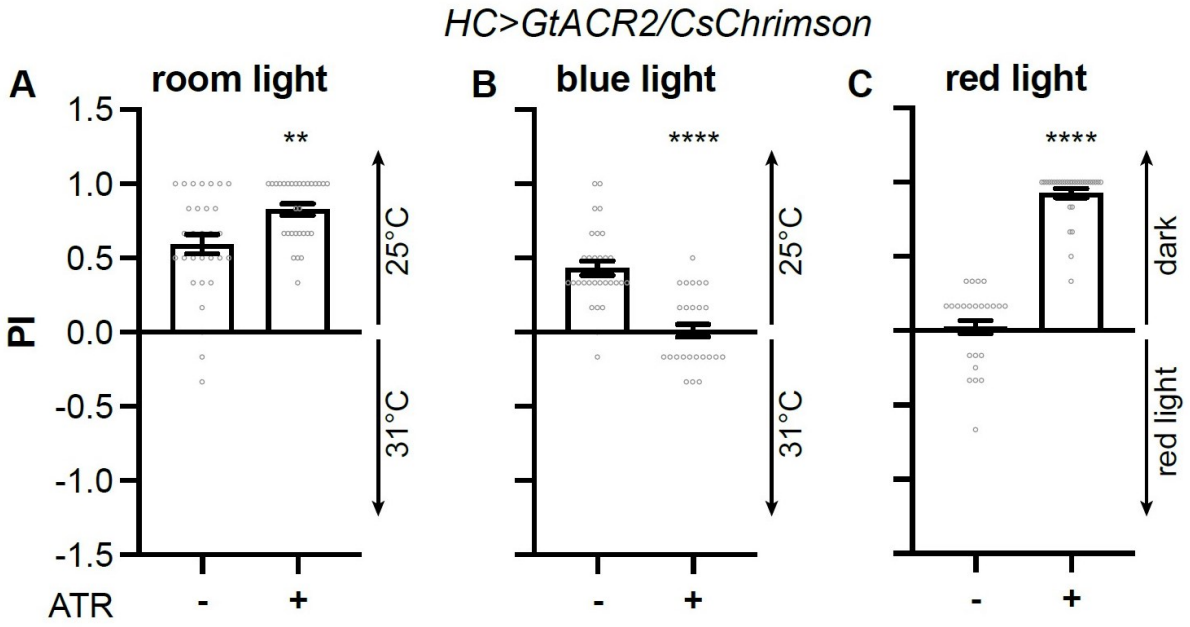

Figure 6. *HC-GAL4* was used to drive *UAS-GtACR2;UAS-CsChrimson*. Flies were examined for warmth avoidance in ambient room light and blue light, and for red light avoidance at room temperature.

(A) Preference to room temperature of *HC>GtACR2/CsChrimson* that were raised with (+) or without (-) dietary retinal (ATR) under ambient room light. n = 30, data represent means ± SEM, Mann-Whitney test, ** $p < 0.01$.

(B) Preference to room temperature of *HC>GtACR2/CsChrimson* that were raised with (+) or without (-) dietary retinal (ATR) under blue light. n = 30, data represent means ± SEM, Mann-Whitney test, **** $p < 0.0001$.

(C) Preference to dark of *HC>GtACR2/CsChrimson* that were raised with (+) or without (-) dietary retinal (ATR) under red light. n = 30, data represent means ± SEM, Mann-Whitney test, **** $p < 0.0001$.

The last component necessary to add to the system was one of randomization. Because activation or inhibition of all post-synaptic neurons would only recapitulate the response of the original pre-synaptic neuron, it was necessary to isolate the expression to a limited group of post-synaptic neurons at once. Ideally, expression would be randomized per single fly so that the functions of each post-synaptic neuron could be compared by examining behavior and receptor expression across multiple animals. One method of randomization that has been used previously in neuronal circuit tracing studies is called MARCM, or mosaic analysis with a repressible cell marker (Marin et al, 2002). However, MARCM requires expression of genetic components on multiple chromosomes, which is difficult in tandem with *trans*-Tango, which already requires substantial genetics. Additionally, a fundamental part of MARCM function is the usage of GAL80 to repress GAL4, which in the scope of MARCM is part of the mechanism that blocks expression of a gene or mutation of interest in some cells. However, usage of GAL80 along with *trans*-Tango would repress the GAL4 needed to activate expression of the *trans*-Tango ligand, making MARCM overall unusable for our system.

Instead, we turned to a different tool called FLP Out, which relies on usage of the FLP recombinase. FLP targets specific sites in DNA (FRT sites), and when two FRT sites are placed on either side of a stop sequence, the genes encoded afterward will not be transcribed until FLP recombines the stop sequence out (aka it “flips out”). FLP can be heat induced by placing it downstream of a heat shock (hs) promoter, and shortening the length of the heat shock will reduce the amount of cells expressing FLP (Golic & Lindquist, 1989). Thus, with a heat shock of the right length of time, stop sequences will be flipped out of a small, randomized amount of cells, allowing expression of a gene of interest only in the cells with FLP expression (Figure 7).

Figure 7: Heat shock driving FLP Out

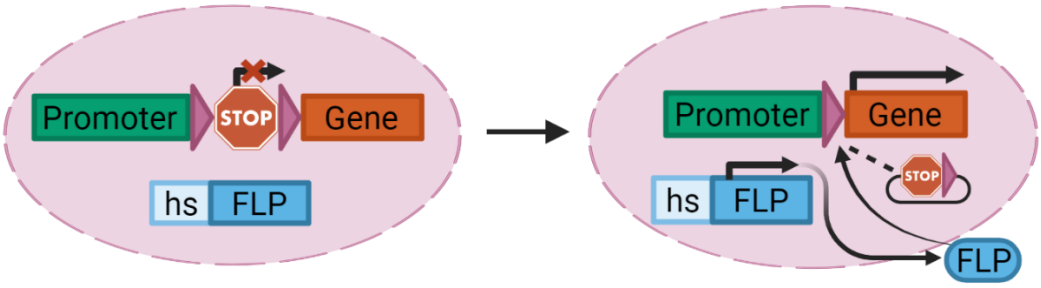

Figure 7. FLP Out involves the placement of two FRT sites (purple triangles) on either side of a stop sequence. This *FRT-stop-FRT* cassette can be placed anywhere after a promoter to stop transcription at the stop sequence. In the presence of *hs>FLP*, heat shock of the animal drives expression of FLP recombinase, which flips out the stop sequence and allows downstream gene transcription.

We tested the efficacy of FLP Out by driving *UAS-FRT-stop-FRT-GFP* in the HCs along with hs>FLP. The HCs are located in the arista and only number three on each side, making them an easy model in which to attempt the system. Heat shock for two hours at 35ºC resulted in GFP expression in approximately two-thirds of HCs, demonstrating the viability of the tool in randomizing expression in a small number of neurons (Figure 8). Varied numbers of HCs were targeted per animal, and results did not differ between sexes (data not shown). Based on this experiment as well as the relative ease of adding an *FRT-stop-FRT* cassette prior to other genes, we chose heat shock driving FLP Out as our randomization method.

Figure 8: Using heat shock to drive FLP Out randomizes gene expression

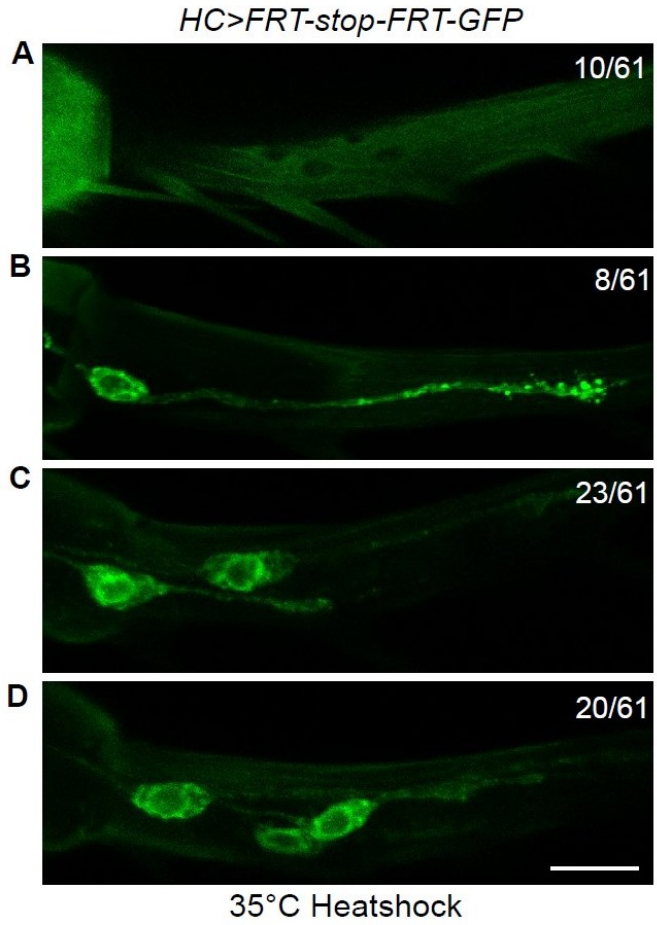

Figure 8. Heat shock randomly removes the "FRT-stop" cassette in HCs. Among 61 aristae observed, 10 had zero HCs (A), 8 had one HC (B), 23 had two HCs (C), and 20 had three HCs (D). Scale bars: 10 μm.

2.3 Creating FLIPSOT flies

Once the components for the system were chosen, a DNA vector was created containing the sequence *QUAS-FRT-stop-FRT-GtACR2-T2A-CsChrimson.mCherry*, where T2A is a site that pauses and restarts translation in order to allow the creation of two separate proteins from one promoter (Lee et al, 2018). Additional constructs were created

including either *QUAS-FRT-stop-FRT-CsChrimson.mCherry* or *QUAS-FRT-stop-FRT-GtACR2.EYFP*. After vector injection, each line was examined for reporter expression in projection neurons through combination with *hs>FLP* along with *Ir21a-QF*. IR21a is expressed in three cool-responsive cells known as the dorsal organ cool cells (DOCCs, Ni et al, 2016), and since the cells are visible in whole larval heads, they are simple and quick to visualize. The CsChrimson.mCherry and GtACR2.EYFP variants positively identified DOCCs (Figure 9A/C); however, the *GtACR2-T2A-CsChrimson.mCherry* variant lacked signal entirely (data not shown). Though insertion sequences were verified by PCR, it is unclear why the joint CsChrimson and GtACR2 construct did not display reporter expression. However, since the CsChrimson.mCherry and GtACR.EYFP variants both had reporter expression, we decided to move onward with usage of the two behavioral components in separate fly lines.

We then continued to use *Ir21a-QF* to test the ratio of cells with reporter expression in our fly lines at different heat shock timepoints. Using *Ir21a-QF* to drive *QUAS-FRT-stop-FRT-CsChrimson.mCherry* or *QUAS-FRT-stop-FRT-GtACR2.EYFP* established that a 30 minute heat shock at 35ºC was sufficient to drive reporter expression in approximately fifty percent of cells (Figure 9B/D).

Figure 9: Effect of genotype and heat shock length on "FRT-stop" cassette removal

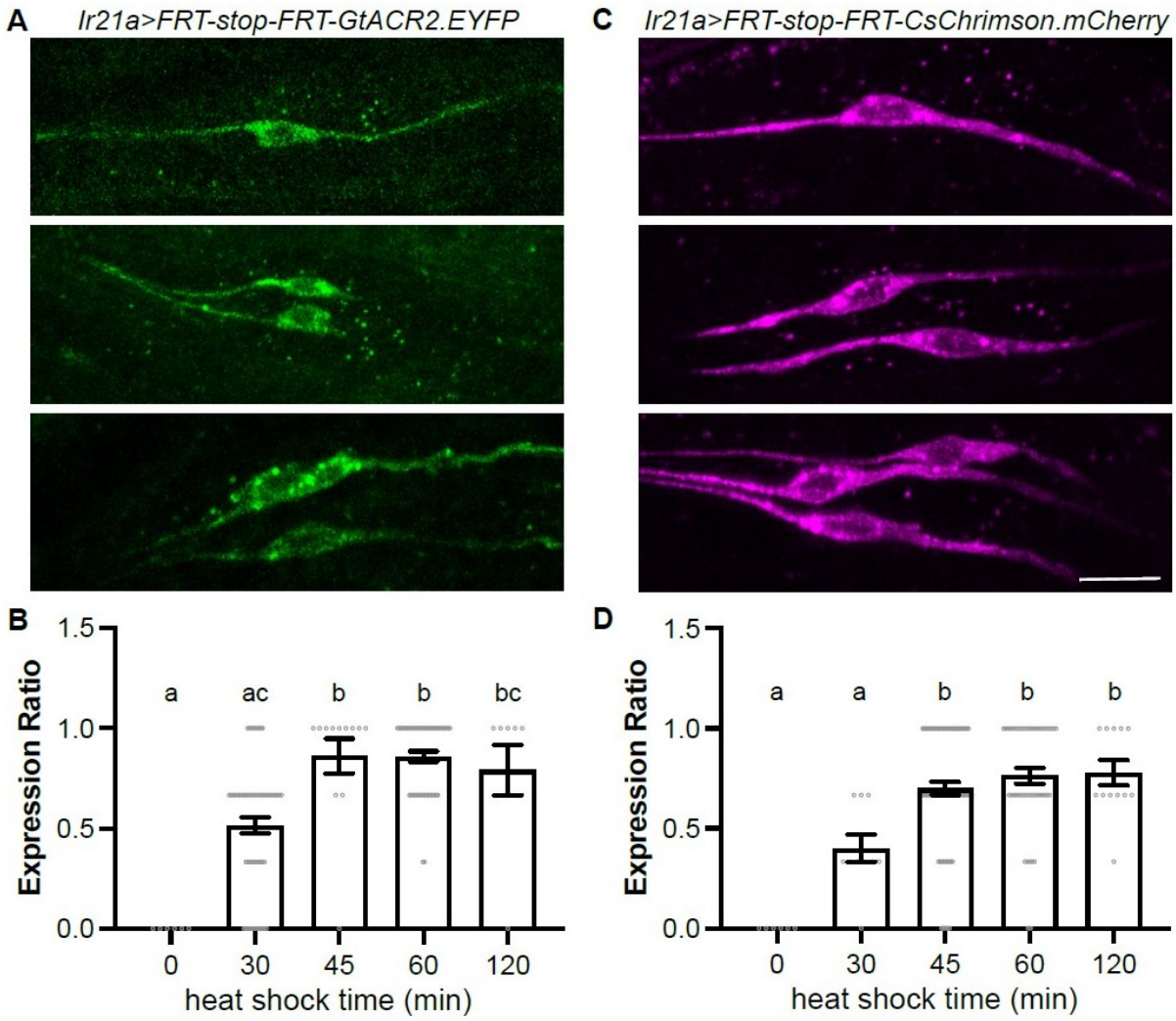

Figure 9. *Ir21a-QF* was used to drive either *QUAS-FRT-stop-FRT-GtACR2.EYFP* (A-B) or *QUAS-FRT-stop-FRT-CsChrimson.mCherry* (C-D) in the presence of *hs>FLP*. Dorsal organ ganglion (DOG) containing the DOCCs were imaged in 2nd instar larvae and DOCCs were quantified.

(A) After heat shock, each DOG may contain zero, one (upper), two (middle), or three (lower) GtACR2.YFP-positive DOCCs.

(B) The percentage of GtACR2.YFP-positive DOCCs in each DOG after incubating larvae at 35°C for the indicated periods. *n* = 6-62; data represent means ± SEM; Kruskal-Wallis test followed by Dunn's multiple comparisons test; letters denote statistically distinct groups, $p < 0.05$.

(C) After heat shock, each DOG may contain zero, one (upper), two (middle), or three (lower) CsChrimson.mCherry-positive DOCCs.

(D) The percentage of CsChrimson.mCherry-positive DOCCs in each DOG after incubating larvae at 35°C for the indicated periods. *n* = 6-80; data represent means ± SEM; Kruskal-Wallis test followed by Dunn's multiple comparisons test; letters denote statistically distinct groups, $p < 0.05$.

After generation and validation of the *QUAS-FRT-stop-FRT-CsChrimson.mCherry* and *QUAS-FRT-stop-FRT-GtACR2.EYFP* fly lines, both were crossed to an additional QUAS-driven reporter (*QUAS-GFP* and *QUAS-mtd.Tomato*, respectively) to serve as an internal control. To complete the FLIPSOT tool, these flies only need to be crossed with flies containing *hs>FLP*, *UAS-trans-Tango*, and a GAL4 driver of interest.

The full FLIPSOT system includes *hs>FLP*, which allows heat shock-dependent generation of FLP recombinase; *trans*-Tango, which allows targeting of the post-synaptic neurons; *FRT-stop* cassettes, which will be "flipped out" in randomized post-synaptic neurons due to variance in FLP expression; an internal reporter, which will allow visualization of all post-synaptic neurons; and a channelrhodopsin tagged with a separate reporter, which will allow optogenetic activation or inhibition of targeted post-synaptic

neurons as well as visualization of the same (Figure 10). Since this system uses optogenetics and *trans*-Tango along with FLP Out to label individualized populations of post-synaptic neurons per fly, we called it FLIPSOT: functional labelling of individualized post-synaptic neurons using optogenetics and *trans*-Tango. To indicate the difference between the two variants, FLIPSOTa (for activation) will refer to the version including CsChrimson, and FLIPSOTi (for inhibition) will refer to the version including GtACR2.

Figure 10: The FLIPSOT system

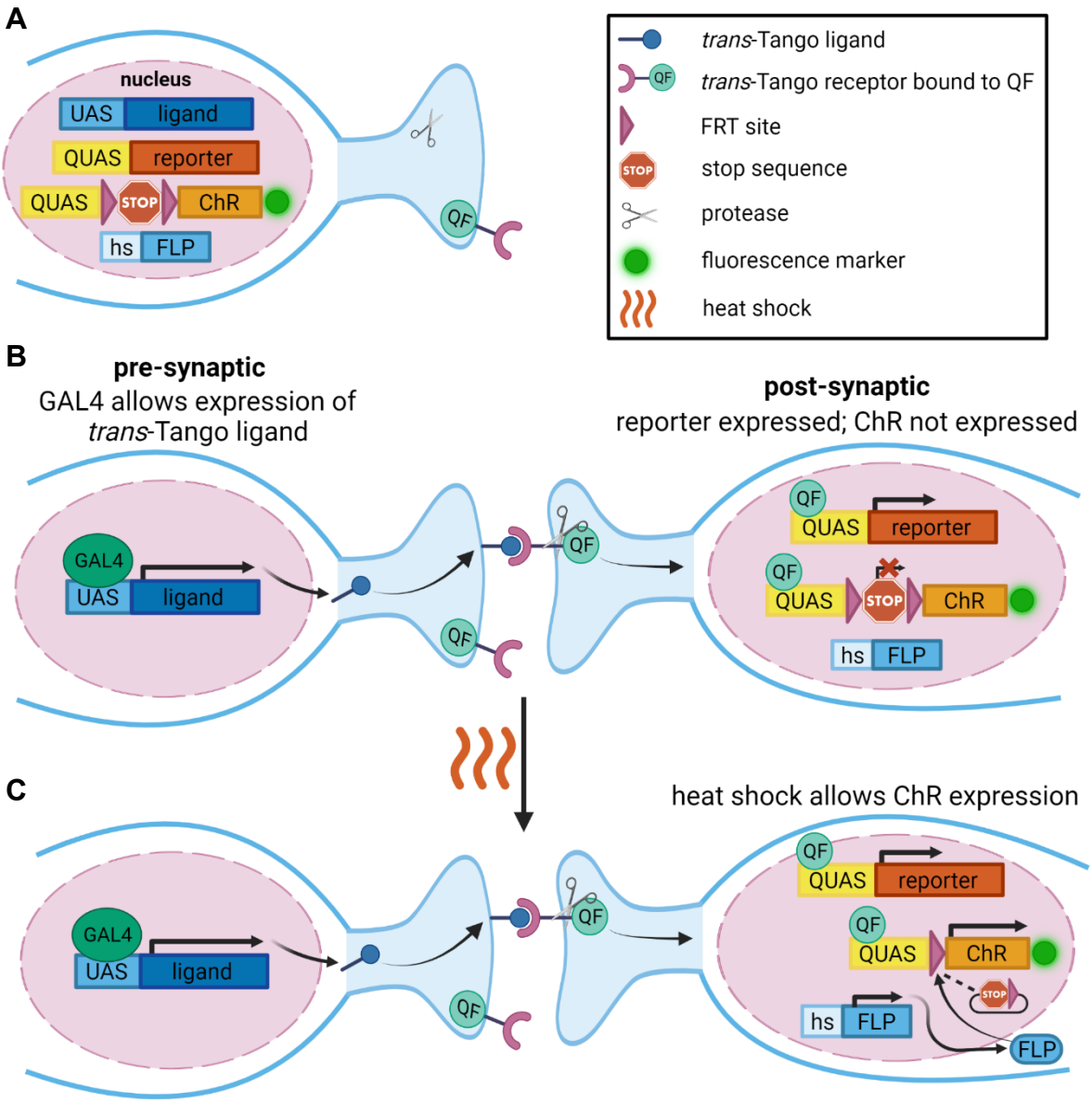

Figure 10. Full schematic of the FLIPSOT system.

(A) FLIPSOT components.

(B) FLIPSOT begins with the *trans*-Tango system. GAL4, driven by a promoter of choice, allows the expression of the *trans*-Tango ligand. When the *trans*-Tango ligand binds to its receptors only on post-synaptic cells, a protease is recruited to cleave off QF and allow its

translocation to the nucleus. In cells unaffected by heat shock, QF will only drive reporter transcription due to the stop sequence prior to the channelrhodopsin (ChR).

(C) In cells affected by heat shock, FLP recombinase will be expressed and will flip out the stop sequence prior to the channelrhodopsin, allowing the ChR (either GtACR2 or Cs.Chrimson) and its fluorescent reporter to be expressed.

2.4 Methods

Fly lines

The wild-type control used for all behavioral assays was w^{1118}. *UAS-GtACR2* (Mauss et al, 2017) was previously described and was a kind gift from the Gaudry Lab. *HC-GAL4* (Gallio et al, 2011), *UAS-CsChrimson* (BDSC 55135 & 55136, Klapoetke et al, 2014), *Gr66a-GAL4* (Dunipace et al, 2001), UAS-Kir (BDSC 6596), *hs-FLP* (BDSC 6938, Golic et al, 1989), *UAS-FRT-stop-FRT-GFP* (BDSC 30032, Hong et al, 2009), *QUAS-GFP* & *QUAS-RFP* (BDSC 30002 & 30004, Riabinina et al, 2016), and *UAS-trans-Tango* (BDSC 77123 & 77124, Talay et al, 2017) were previously described.

To create the *QUAS-FRT-stop-FRT-CsChrimson-mCherry, QUAS-FRT-stop-FRT-GtACR2.EYFP*, and *QUAS-FRT-stop-FRT-GtACR2-T2A-Chrimson.mCherry lines*, the *FRT-stop-FRT* sequence (addgene 64716) was cloned into the *pQUAST-attB* (DGRC_1438) vector. Then, either the *CsChrimson.mCherry* (addgene 111547) sequence or the *GtACR2.EYFP* (addgene 67877) sequence was cloned into the vector, respectively; the *T2A* sequence was added using a PCR primer overhang during one of the DNA isolation steps. The final plasmids were each injected by Rainbow Transgenic Flies, Inc. into fly line R8622, which features an *attP* site on the third chromosome.

Ir21a-QF was created by replacing the synaptobrevin promoter in a *Nsyb-QF* vector with an *Ir21a* promoter prior to the *QF2w* sequence (Ni et al 2016; addgene 46116). The final plasmid was injected by Rainbow Transgenic Flies, Inc. using the *attP2* site on the third chromosome.

Heat shock

Heat shock was performed at first to second instar with larvae in regular food vials. Vials were then submerged in a water bath set to 35ºC for the time described per each experiment.

Behavioral assays

All flies were maintained at about a 12:12 hour light:dark cycle and crossed at 23.5ºC. Two days before behavioral experiments, flies were placed on food containing 40 µM all-trans retinal (ATR, Sigma-Aldrich) and moved to 24-hour dark conditions until testing. Control experiment flies were tested at 2-10 days old.

Single fly two-choice warmth avoidance assays were set up using a sheet protector taped over top of two contiguous metal plates, with one plate warmed on a heat source to 31ºC and the other at room temperature (25ºC). Flies were placed under a small plastic cover and allowed to acclimate for 15-25 seconds before starting the experiment; all experiments were started with flies on the 25ºC side of the assay. The position of the fly was recorded every 5 seconds for 1 minute. Flies that did not move for more than 30 seconds were discarded. For control experiments, a centered desk lamp (22lux) was used as ambient lighting. For blue light optogenetic experiments, a blue light source (20Klux) was built using similar specifications to a previously described red light source (Tyrrell et al, 2021), though modified to use a triple blue LED light instead (470nm, Luxeon Star LEDs SP-03-B3).

Preference index to room temperature was calculated using the formula:

$$\frac{(\text{\# of times in 25ºC} - \text{\# of times in 31ºC})}{\text{total \# of times}}$$

Single fly red light optogenetic assays were conducted at 25ºC, and the base of the experiment consisted of a sheet protector overlaid on a black background. Flies were placed on the sheet protector under a small plastic cover, with two quadrants of the cover blocked from light with opaque, black electrical tape. Flies were given 10 seconds to acclimate, and all experiments started with flies in one of the visible quadrants; flies that did not move for more than 30 seconds were discarded. The red light source (32Klux) was previously described; larval red light optogenetic assays were also conducted as described (Tyrrell et al, 2021).

Preference index to dark quadrants was calculated using the formula:

$$\frac{(\text{\# of times in dark} - \text{\# of times in red light})}{\text{total \# of times}}$$

Imaging

Samples were either fixed for 30 minutes in 4% paraformaldehyde in PBS, then mounted (aristae), or simply mounted (larval heads) in a solution of 90% glycerol in PBS.

Statistical Analysis

Statistical analysis details of each experiment can be found in the figure legends. Statistical comparisons were performed by either the Mann-Whitney test (for two samples) or the Kruskal-Wallis test followed by Dunn’s multiple comparisons test. Data were plotted using bar graphs representing mean ± SEM with the inclusion of scatterplots representing individual data points. Analysis was performed using GraphPad Prism 9.

2.5 Discussion & Conclusions

Various components were tested, optimized, and combined in order to create the full FLIPSOT system. *trans*-Tango was chosen over TRACT due to its higher driver line versatility. CsChrimson and GtACR2 were chosen as methods of optogenetic activation and inhibition, respectively, due to driving robust changes in behavioral response as well as their capability to work together within the same organism. Finally, heat shock driving FLP Out was chosen as a way to randomize expression due to its relative genetic simplicity, potential for fine-tuning, and ability to integrate with the other parts of the system.

Though TRACT was not chosen as a base for this system, it would serve as a valid alternative if a situation arises where only a LexA driver could be used, or if *trans*-Tango failed to be compatible with the other components. TRACT could also be used to extend the system's usage to third order neurons by using a LexA driver to drive TRACT in pre-synaptic neurons, allowing the TRACT-generated GAL4 in post-synaptic neurons to subsequently drive expression of *UAS-trans-Tango*. In this case, the *trans*-Tango ligand would be expressed in post-synaptic neurons, thereby binding to the *trans*-Tango receptor in third-order neurons and allowing optogenetic stimulation and reporter expression in those third-order neurons instead. This would thus potentially allow visualization as well as behavioral manipulation of previously unknown third-order neurons.

The heat shock duration was set in place to allow FLIPSOT expression in some, but not all post-synaptic neurons. We chose a duration that resulted in expression in about fifty percent of cells, which we believed would maximize the trade-off between providing adequate comparisons between animals while still allowing enough expression to heighten the chance of a behavioral response. However, heat shock timing could be increased or decreased depending on the goal of the experiment.

The reasons for the failure of the *QUAS-FRT-stop-FRT-GtACR2-T2A-Chrimson-mCherry* flies to display mCherry expression are unclear. Though the DNA sequences, including the *T2A* sequence, were validated using PCR, there is still a possibility that there was an error concerning the *T2A* function. It is possible in this case that GtACR2 is expressing but not Chrimson.mCherry, but that is difficult to determine due to a lack of a GtACR2-specific reporter. The issue may also have resulted from interactions at that specific insertion site, though we tried to minimize that possibility by inserting the sequence at the same site as in the *QUAS-FRT-stop-FRT-CsChrimson.*mCherry and QUAS-*FRT-stop-FRT-GtACR2.EYFP* lines. Unfortunately, this specific line did not function as planned; however, it may still be possible to combine the FLIPSOTa and FLIPSOTi variants into one tool in the future with further investigation.

This chapter describes the testing and optimization of potential FLIPSOT components as well as the creation and validation of fly lines for both FLIPSOTa and FLIPSOTi. Chapter 3 will demonstrate the implementation of FLIPSOT within a thermosensory circuit as well as validate the possibility of its usage to evaluate necessity and sufficiency of post-synaptic neurons.

CHAPTER 3: USING FLIPSOT TO FIND NECESSARY AND SUFFICIENT HEATING CELL PROJECTION NEURONS

3.1 Introduction

Temperature response in flies is characterized by aversion to both coolness and warmth. As ectotherms, avoiding suboptimal external temperatures is crucial to the survival and fitness of the species. The Heating Cells (HCs) are a set of thermosensory neurons that drive an innocuous warmth avoidance circuit; they express the thermosensor GR28b(D) and are located in the arista. The HC axons extend from the arista to a small region in the antennal lobe of the brain called the VP2, from which projection neurons (PNs) receive the signal and direct it toward other brain regions for sensory integration and processing. Some previous studies have analyzed the HC PNs, but there is not a clear consensus on which of these PNs are necessary or sufficient in driving the avoidance behavior.

Here, we use FLIPSOTi and FLIPSOTa to evaluate the necessity and sufficiency of the HC PNs in warmth avoidance behavior, respectively. Behavioral controls are used to establish a threshold to use for dividing the FLIPSOT flies into groups (affected behavioral response vs null). *trans*-Tango is used to identify typical HC PN morphology. Finally, FLIPSOTi and FLIPSOTa flies are tested for behavioral response, and targeted neurons are examined to identify PNs necessary or sufficient for warmth avoidance behavior.

3.2 Establishing experimental controls

In order to determine which FLIPSOT flies are displaying optogenetically modified behaviors, a cutoff or threshold must be established for whether to designate a trial as

displaying modified behavior or as behaving “normally” (similarly to wild type). To do this, we ran several behavioral assays using either positive or negative control flies. Negative control flies included wild type, the *HC-GAL4* control, UAS controls, and *HC>GtACR2* or *HC>CsChrimson* without dietary ATR. These flies were expected to behave relatively similarly across the three experimental conditions. Positive control flies included *HC>GtACR2* and *HC>CsChrimson* with dietary ATR, which allowed for optogenetic activity; based on previous experiments, these flies were expected to fail to avoid warmth (*HC>GtACR2*) or avoid red light (*HC>CsChrimson*) respectively.

A warmth avoidance assay under ambient room light was used as a control condition to discern whether or not flies’ innate warmth avoidance behavior was still intact (Figure 11A). Flies of all genotypes avoided warmth with no significant difference between groups (Figure 11B), indicating that FLIPSOT flies should also have no issues avoiding warmth under regular light conditions. A similar warmth avoidance assay under blue light was carried out to set the threshold for FLIPSOTi flies (Figure 11A). All genotypes except the ATR+ *HC>GtACR2* avoided warmth, while *HC>GtACR2* neglected to avoid warmth and had a preference index close to zero (Figure 11C). It should be noted that the ATR+ *HC>CsChrimson* flies displayed a slightly lower preference to room temperature than expected; this disruption in behavior could be due genetic background or to blue light very weakly activating CsChrimson (and causing flies to try to avoid the blue light instead of the warmth). However, since this group was not significantly different from the wild type and was also significantly different from the ATR+ *HC>GtACR2* flies, we still counted this group as displaying proper avoidance. Finally, a red light assay with two opaque quarters of the fly arena was used to assess flies’ avoidance of red light (Figure 11A). All genotypes except ATR+ *HC>CsChrimson* displayed neither a preference to dark nor to red light; *HC>CsChrimson* flies highly preferred the dark (Figure 11D).

Figure 11: Single fly temperature/optogenetic avoidance behavior

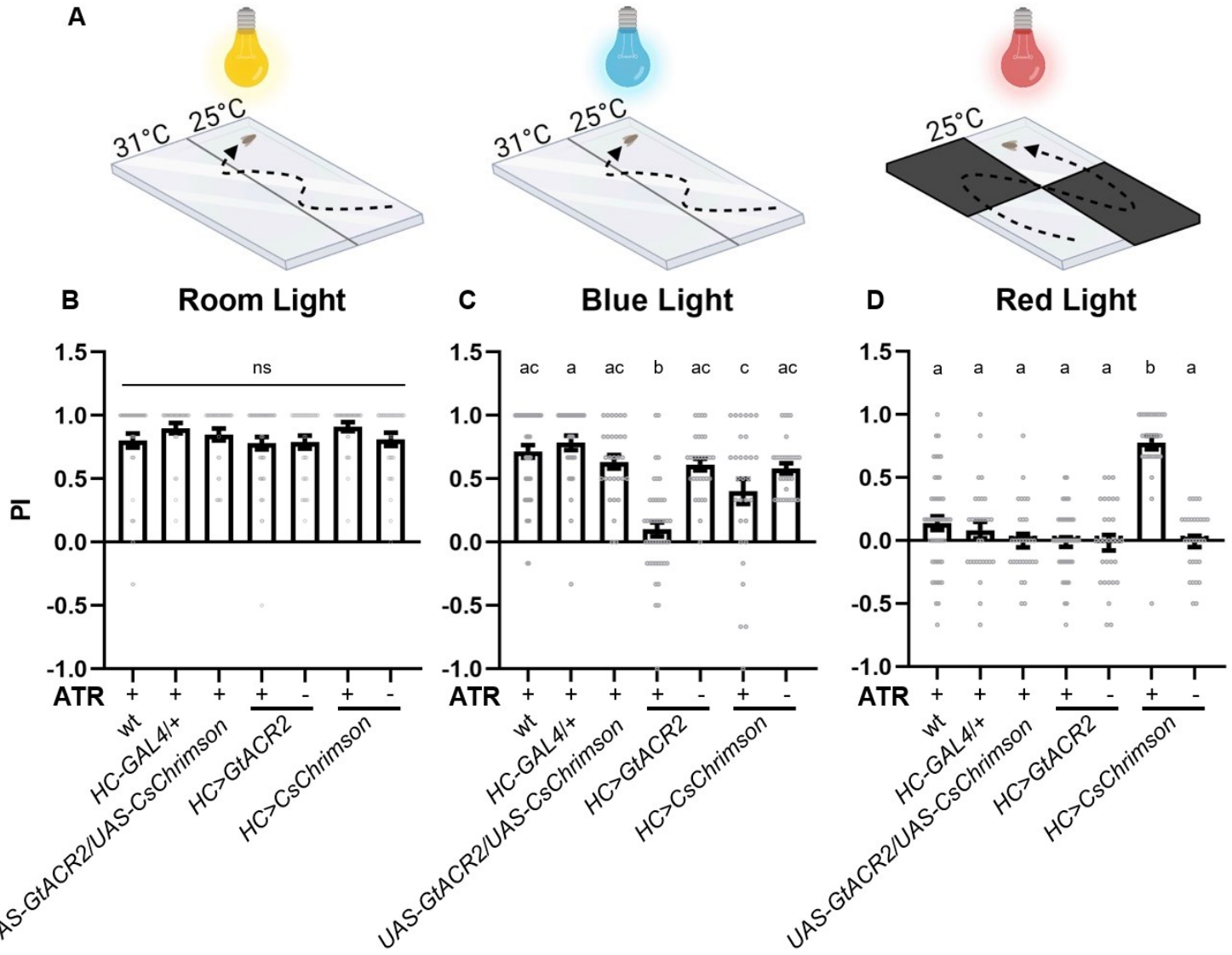

Figure 11. Flies of various genotypes (wild type, GAL4/UAS controls, *HC>GtACR2*, or *HC>CsChrimson*) were examined for behavioral response to warmth under ambient room or blue light, or to red light.

(A) Schematic of single fly behavioral preference assays. Flies were given one minute to choose between temperatures (room and blue light assays) or between darkness and red light. Traces shown are typical of wild type flies.

(B) Preference to room temperature (vs 31ºC) under ambient room light. All genotypes and ATR conditions were non-significant. n=30, data represent means ± SEM, Kruskal-Wallis followed by Dunn's multiple comparisons test.

(C) Preference to room temperature (vs 31ºC) under blue light. n=30, data represent means ± SEM, Kruskal-Wallis followed by Dunn's multiple comparisons test, letters denote statistically significant groups of $p<0.05$.

(D) Preference to dark (vs red light). n=30, data represent means ± SEM, Kruskal-Wallis followed by Dunn's multiple comparisons test, letters denote statistically significant groups of $p<0.0005$.

Thresholds for FLIPSOTi and FLIPSOTa experiments were set by pooling the data from flies whose genotypes failed to avoid warmth (ATR+ *HC>GtACR2* and ATR+ *HC>GtACR2/CsChrimson*) or from those who avoided red light (ATR+ *HC>CsChrimson* and ATR+ *HC>GtACR2/CsChrimson*), respectively (Figures 6B-C, 11C-D). We averaged the means and used ± 1 standard deviation in order to set a threshold that was permissive enough not to exclude too many positive flies but restrictive enough to omit most false positives.

We tested wild type flies in the ambient room light assay to examine whether or not there were behavioral differences between the sexes and found none (Figure 12A); therefore, for our future assays, we combined males and females together. To ensure our behavioral assays were not influenced by external cues, we tested a version of the ambient room light assay where the warm and room temperature sides were flipped from our typical assay, and we found no significant difference between the two (Figure 12B). We also tested our assay with both sides at room temperature and found that flies did not prefer either side (Figure 12B), indicating that our assay is not influenced by external cues. Finally, the FLIPSOT system requires a relatively quick turnaround between behavioral experiments and dissection in order to limit any interim changes due to aging, which greatly affects *trans*-Tango expression (Talay et al, 2017). This limits the amount of time available for behavioral data analysis between the two segments of the experiment, so all behavior was evaluated manually. We compared our manually analyzed *HC>CsChrimson* trials, which theoretically is more difficult to assess due to half of the arena being opaque, with that of a set of trials analyzed by computational software (TrackMate) and found that the preference indices were indistinguishable from those analyzed manually (Figure 12D; data reproduced with permission from Huda et al 2022 – see Appendix B).

Figure 12: Verification of behavioral assay conditions

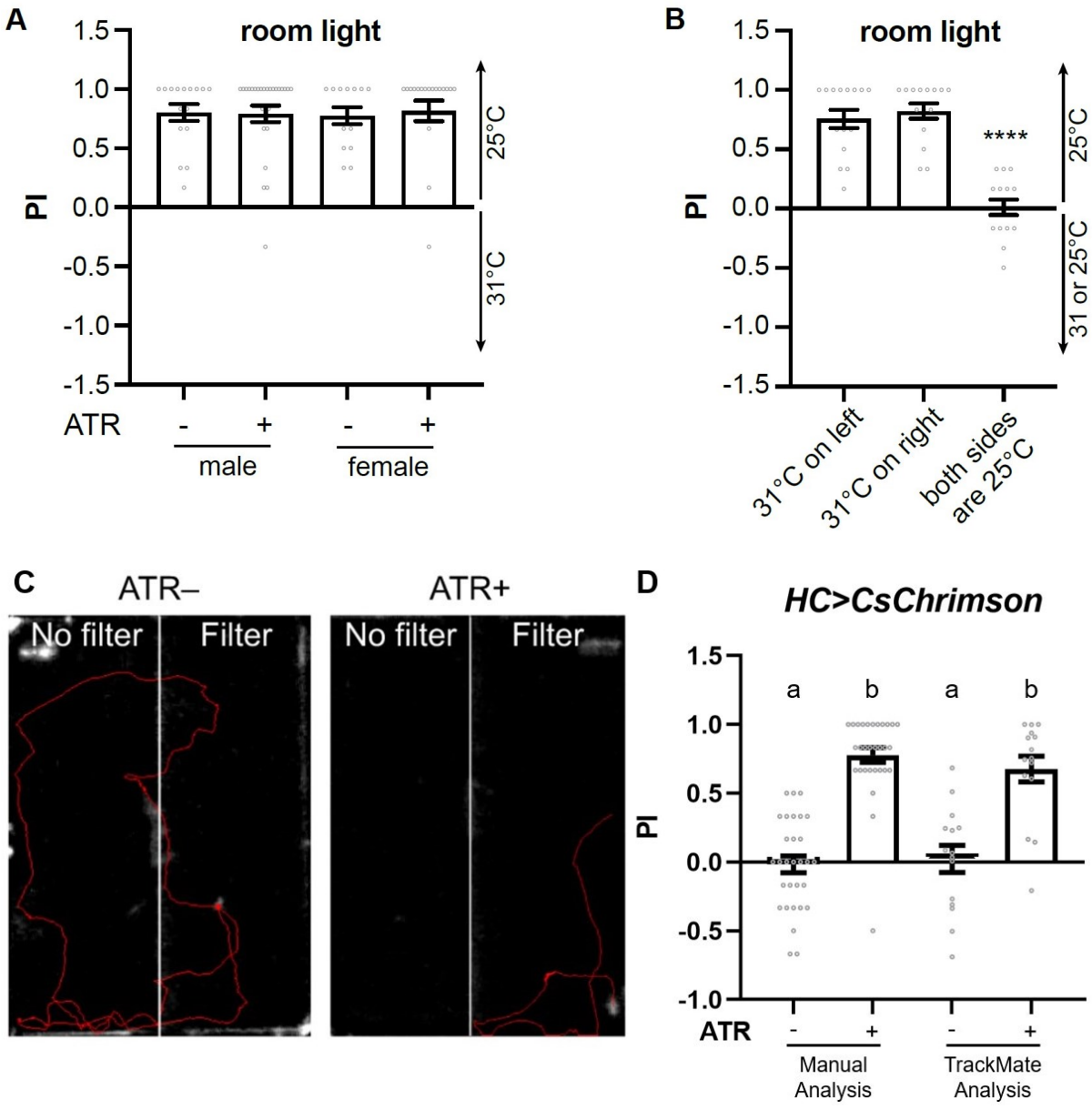

Figure 12. PI is not affected by fly gender, dietary retinal (ATR), whether 31°C is on the left or right, or analysis method.

(A) PI of the indicated genders that were raised with (+) or without (-) dietary retinal (ATR). *n* = 14-28; data represent means ± s.e.m; Kruskal-Wallis test followed by Dunn's multiple comparisons test.

(B) PI from tests that 31°C was on the left, on the right or both sides were 25°C. *n* = 15; data represent means ± s.e.m; Kruskal-Wallis test followed by Dunn's multiple comparisons test; **** $p < 0.0001$.

(C) TrackMate trajectories of *HC-Gal4;UAS-CsChrimson* (*HC>CsChrimson*) flies with or without dietary retinal (ATR) in the red light avoidance assay. Figure reproduced from Huda et al, 2022 – see Appendix B.

(D) Preference to dark vs red light of *HC>CsChrimson* flies with or without ATR, analyzed either manually or via TrackMate. *n*=15-30; data represent means ± SEM, Kruskal-Wallis followed by Dunns' multiple comparisons test, letters denote statistically significant groups of $p < 0.005$.

Next, we turned to the assessment of *trans*-Tango within our system. We used *HC-GAL4* to drive *trans*-Tango and discovered several similar PN tracts to those previously reported: a medial tract that curves upward and outward along the midline (mALT), reminiscent of the one described by Frank et al and several neurons identified by Marin et al; a lateral tract (lALT), which resembles both the one discovered by Frank et al as well as one from Liu et al; and a mediolateral tract (mlALT), which again was similar to one described by Frank et al. There was also a transverse mediolateral tract with a waving bend in it (tALT) that has only been described by Marin et al's electron microscopy findings, and thus has not yet been functionally analyzed (Frank et al, 2015; Liu et al, 2015; Marin et al, 2020). Using *Gr28b(D)-GAL4* to drive expression of *trans*-Tango revealed the same four tracts, validating the results of our *HC-GAL4* driver line. We will thus refer to the four tracts as mALT (medial antennal lobe tract), lALT (lateral), mlALT (mediolateral), and tALT (transverse).

Figure 13: Heating Cell projection neurons

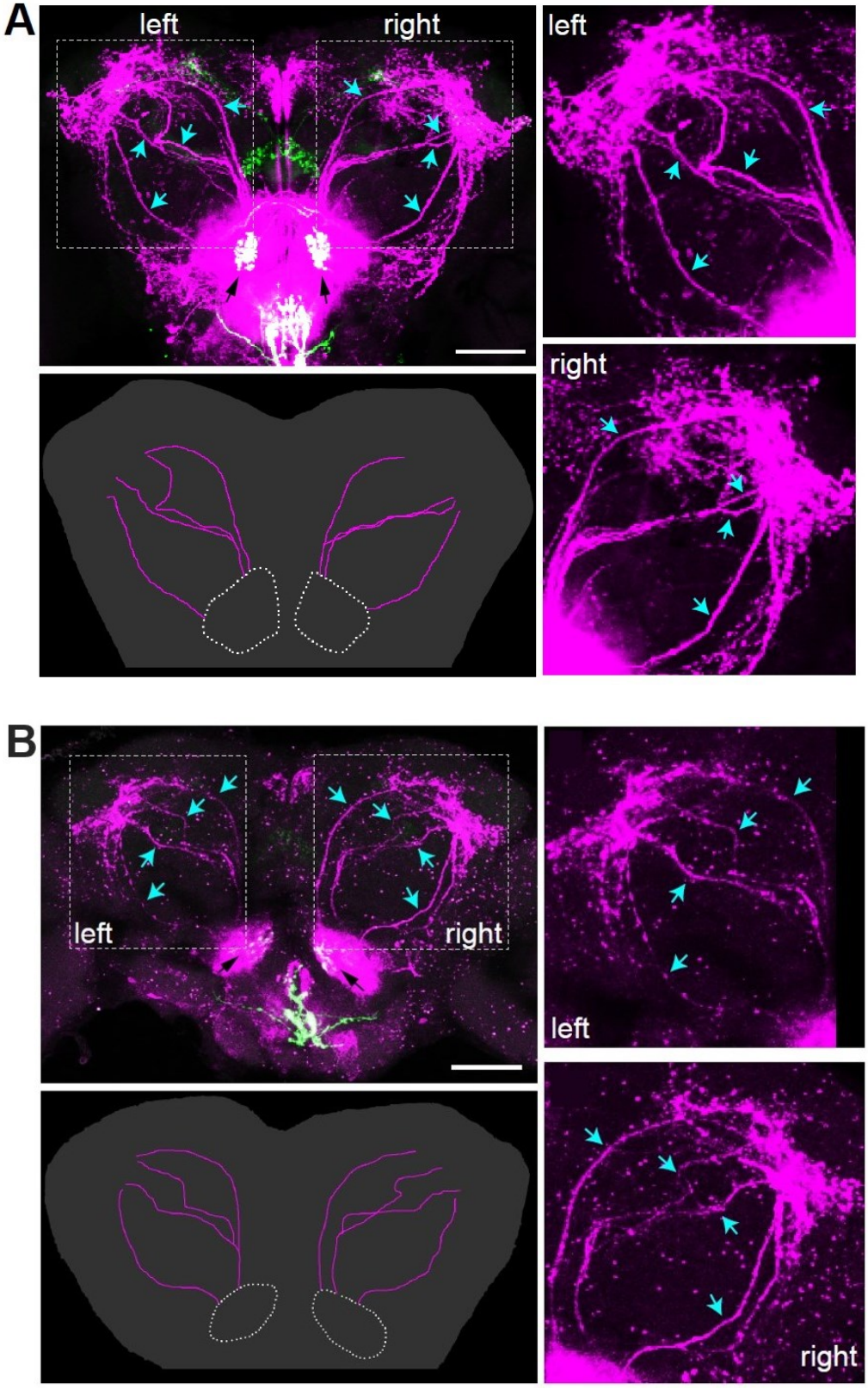

Figure 13. *HC>GAL4* and *Gr28b(D)-GAL4* were used to drive *trans*-Tango.

(A) Representative *HC>trans-Tango* images. Scale bar = 50μm. GFP (green) indicates pre-synaptic cells and RFP (magenta) indicates post-synaptic cells. Four main PN tracts are visible (blue arrows): a medial tract, a lateral tract, and two mediolateral tracts. One of the mediolateral tracts is typically wavier/bended in morphology and shares a similar brain depth as the lateral tract; the other mediolateral tract is in a similar slice as the medial tract and can vary in morphology (see right side compared to left).

(B) Representative *Gr28b(D)>trans-Tango* images. Scale bar = 50μm. GFP (green) indicates pre-synaptic cells and RFP (magenta) indicates post-synaptic cells. The four main tracts visible in *HC>trans-Tango* images are captured here as well (blue arrows).

Once there was adequate information gathered about the morphology of the neurons as well as for how to set the threshold for behavior, we next asked whether one arista alone was sufficient to drive warmth avoidance behavior. This is important as it changes the method of analysis for both FLIPSOTa and FLIPSOTi; it is necessary to know whether activation or inhibition is needed in both sides of a PN pair to affect behavior, or if one side alone is sufficient to cause changes. One or both aristae were removed from wild type flies before exposing them to the two-choice warmth avoidance assay; only double arista ablation significantly reduced avoidance, not singular (Figure 14A). We also removed single aristae from *HC>trans-Tango* flies and found singular arista removal was enough to eliminate PN reporter expression (Figure 14B). For FLIPSOTi, these data implied that both neurons in a pair of necessary PN tracts need to be inhibited in order to cause a defect in warmth avoidance. For FLIPSOTa, on the other hand, only one half of a pair of PNs need to be activated in order to drive warmth avoidance.

Figure 14: Effects of arista ablation on warmth avoidance and PNs

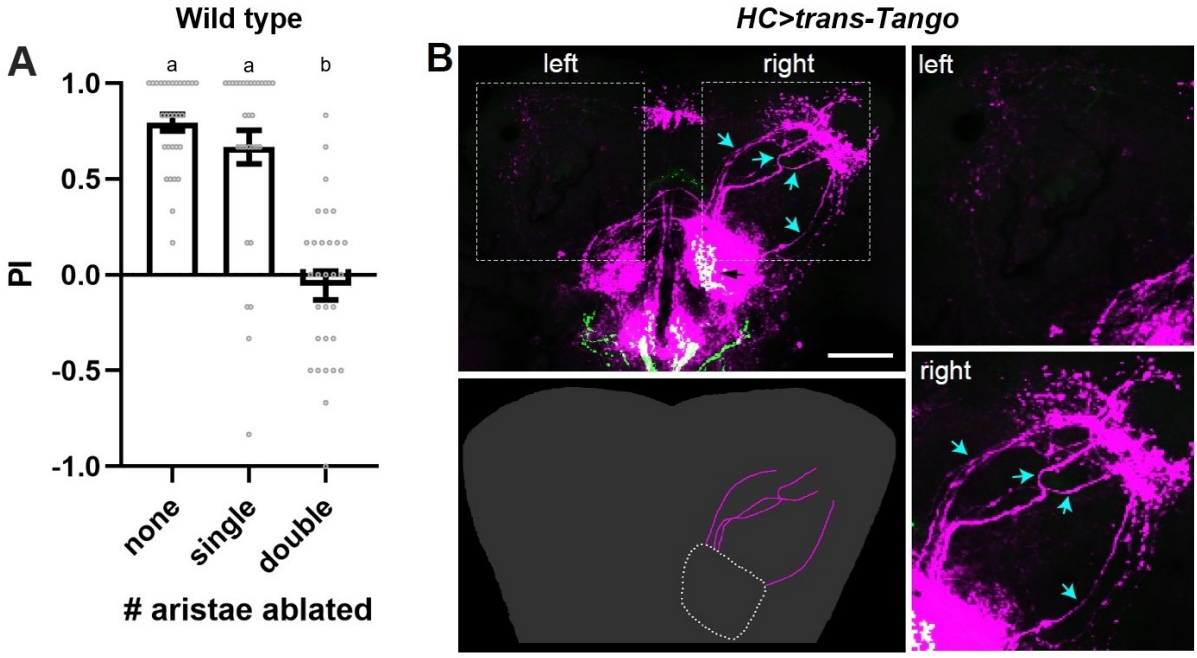

Figure 14. Aristae were removed from wild type or *HC>trans-Tango* flies.

(A) One, both, or neither arista were removed from wild type flies. Flies were then allowed to choose between room temperature and 31ºC in ambient room light. n=30, data represent means ± s.e.m; Kruskal-Wallis test followed by Dunn's multiple comparisons test; letters denote statistically significant groups of $p<0.0001$.

(B) Representative image; one arista was removed from *HC>trans-Tango* flies, which correlated with lack of signal in one half of PNs. Scale bar = 50µm. GFP - pre-synaptic; RFP (magenta) - post-synaptic.

We used flies of several genotypes to set the stage for usage of FLIPSOT in the HC neural circuit. We ensured that our behavioral assays were scientifically sound through multiple control experiments. A threshold for dividing FLIPSOT flies into behavioral groups was set based on optogenetic control data. The morphology of the HC PNs was confirmed using multiple driver lines. Finally, we confirmed that expression in the HC circuit on one side of the brain is sufficient to drive warmth avoidance, which has important implications for analyzing FLIPSOT data.

3.3 Using FLIPSOT to determine necessity and sufficiency

Once the necessary controls were established, it was finally possible to use FLIPSOT to assess necessity and sufficiency. We began with *HC>FLIPSOTi*, which would make use of *trans*-Tango to allow randomized inhibition in post-synaptic cells to the HCs, and started by developing an experimental workflow for the tool (Figure 15).

Figure 15: FLIPSOTi experimental workflow

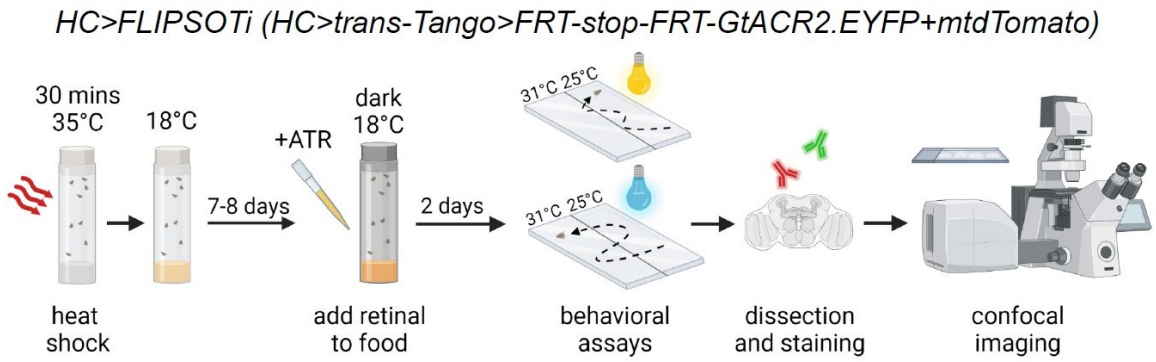

Figure 15. *HC>FLIPSOTi* flies were heat shocked post-eclosion at 35ºC for 30 minutes. After 7-8 days at 18ºC, dietary ATR was added to the food, and warmth avoidance assays in blue and room (control) light were run two days later. Finally, brains were dissected, stained, and imaged. Flies were allowed to age for about ten days total between eclosion and the final dissection.

When we first began running FLIPSOTi experiments, we started with the flies aged to three weeks at the time of dissection as recommended by Talay et al (2017). However, we quickly found out that for reasons unknown, our FLIPSOTi construct yielded extremely leaky expression at that time point (data not shown). We thus chose a shorter timepoint of about 10 days between eclosion and dissection with much cleaner results. Though leaky expression is an issue with both FLIPSOT and *trans*-Tango itself, steps such as moderation of fly age can be taken to minimize extraneous signal. We included an ambient room light assay as a control to assess warmth avoidance without GtACR2 inactivation; if flies failed to avoid warmth correctly in room light, they were discarded.

FLIPSOTi was then tested in the HC PNs. *hs>FLP, HC>trans-Tango>FRT-stop-FRT-GtACR.EYFP/mtdTomato* flies were first separated based on behavioral response;

those with a PI that fell within one standard deviation of other non-warmth avoiding genotypes (*HC>GtACR2 and HC>GtACR2/CsChrimson*) or had a negative preference to room temperature were counted as having a defect in warmth avoidance (Figure 16A). Brains were then dissected, stained, and analyzed to compare PNs between samples. Examples of expression variance between flies are shown in Figure 16B-C. Overall summary of PNs targeted by FLIPSOTi is shown in Figure 16D-E.

Figure 16. *HC>FLIPSOTi* indicates necessary PNs for warmth avoidance

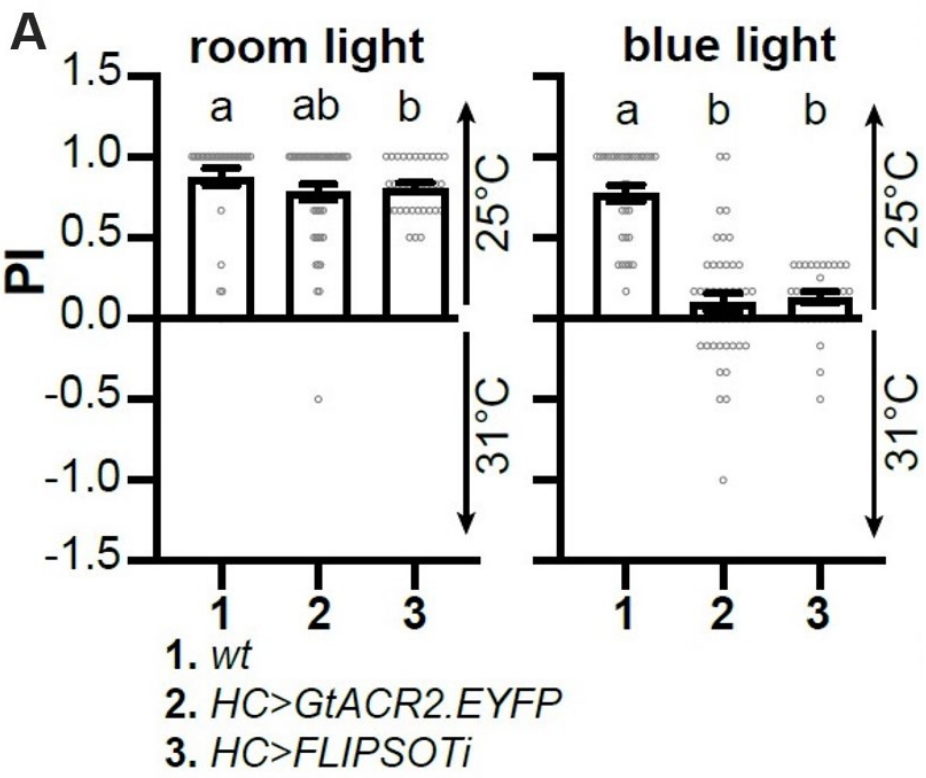

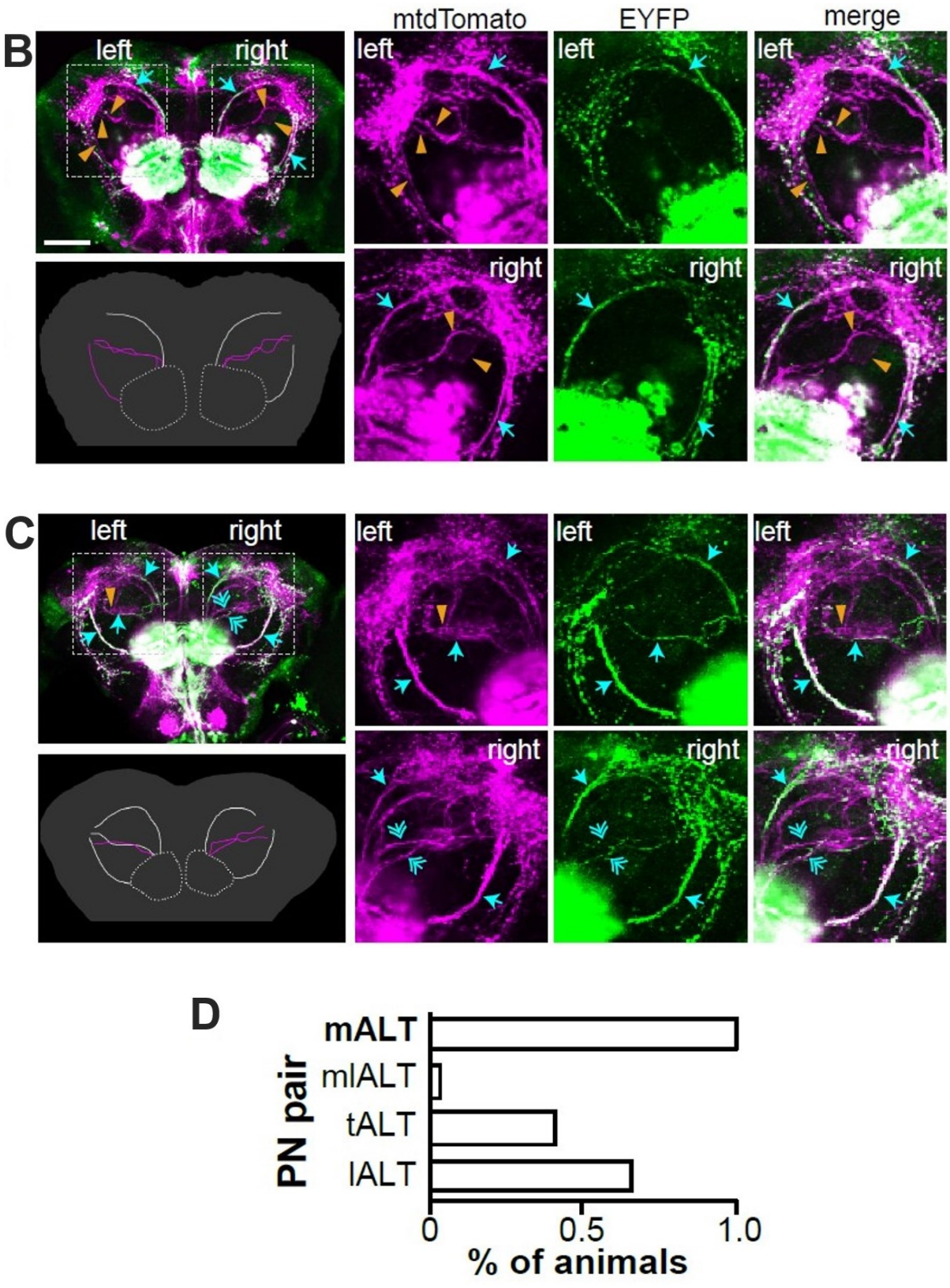
B
left
right
mtdTomato
EYFP
merge
left
right
C
D
mALT
mlALT
tALT
lALT
PN pair
0
0.5
1.0
% of animals

E

EYFP Projections								mtdTomato Projections							
l	t	ml	m	m	ml	t	l	l	t	ml	m	m	ml	t	l
	y		y	y	y	y	y	y	y		y	y	y	y	y
y	y		y	y			y	y	y	y	y	y	y	y	y
y		y	y	y	y	y	y	y	y	y	y	y	y	y	y
y		y	y	y			y	y	y	y	y	y	y	y	y
y		y	y	y			y	y	y	y	y	y	y	y	y
y			y	y			y	y	y	y	y	y	y	y	y
y	y		y	y		y	y	y	y	y	y	y	y	y	y
			y	y				y	y	y	y	y	y	y	y
y	y		y	y		y	y	y	y	y	y	y	y	y	y
			y	y	y		y	y	y	y	y	y	y	y	y
y	y		y	y		y	y	y	y	y	y	y	y	y	y
			y	y				y	y	y	y	y	y	y	y
			y	y			y	y	y	y	y	y	y	y	y
y			y	y				y	y	y	y	y	y	y	y
y	y	y	y	y		y		y	y	y	y	y	y	y	y
	y		y	y				y	y	y	y	y	y	y	y
y	y		y	y		y	y	y	y	y	y	y	y	y	y
y	y		y	y		y	y	y	y	y	y	y	y	y	y
y			y	y		y	y	y	y	y	y	y	y	y	y
y			y	y			y	y	y	y	y	y	y	y	y
y	y		y	y	y	y	y	y	y	y	y	y	y	y	y
y	y		y	y		y	y	y	y	y	y	y	y	y	y
y	y		y	y		y	y	y	y	y	y	y	y	y	y
y	y		y	y		y	y	y	y	y	y	y	y	y	y
	y		y	y			y	y	y	y	y	y	y	y	y
y	y		y	y	y	y	y	y	y	y	y	y	y	y	y
y			y	y	y	y	y	y	y	y	y	y	y	y	y
			y	y			y	y	y	y	y	y	y	y	y
			y	y		y	y	y	y	y	y	y	y	y	y
y			y	y			y	y	y	y	y	y	y	y	y

Figure 16. *hs>FLP, HC>trans-Tango>FRT-stop-FRT-GtACR.EYFP/mtdTomato* warmth-avoiding flies are used to determine necessary PNs for the behavior.

(A) ATR+ *HC>FLIPSOTi* flies (the above genotype) chose between 25ºC and 31ºC in ambient room or blue light. Flies were separated based on behavioral phenotype in blue light using the threshold established from control experiments (*HC>GtACR2*); *HC>FLIPSOTi* flies shown are those that fell within the designated threshold and thus were determined to

have a defect in warmth avoidance. n = 31; data represent means ± SEM; Kruskal-Wallis test followed by Dunn's multiple comparisons test; letters denote statistically distinct groups, $p < 0.05$.

(B-C) Representative images of GtACR2.EYFP-positive HC PNs in flies that failed to avoid 31ºC. HA-tagged mtdTomato (magenta) – control stain (all PNs); EYFP (green) – PNs with *FLIPSOTi* inhibition. Cyan arrows indicate GtACR2.EYFP-positive PNs; orange arrows indicate GtACR2.EYFP-negative PNs. Cyan double arrows indicate GtACR2.EYFP-weak PNs, or circumstances in which the EYFP staining is much weaker than the HA staining; these are considered GtACR2.EYFP-negative. Scale bars = 50μm. Left lower panels include illustrations of corresponding PNs. (B) Three PNs express GtACR2.EYFP (both mALTs and the right lALT). (C) Five PNs express GtACR2.EYFP (both mALTs and lALTs along with the left tALT).

(D-E) The mALTs are necessary to drive warmth avoidance behavior. GtACR2.EYFP-positive PNs were analyzed from 30 flies failing to avoid 31°C under blue light, all of which expressed EYFP in both mALT PNs. All other PN pairs lacked EYFP expression on both sides in at least one animal. (E) l, lALT; t, tALT; ml, mlALT; m, mALT.

All *HC>FLIPSOTi* flies with a defect in warmth avoidance showed expression in both mALTs (the most medial of the PN groups), indicating that the mALTs are necessary for warmth avoidance behavior. No other pair of PNs had expression present in all flies, and all other pairs lacked expression on both sides in at least one animal per pair. Additionally, there were multiple animals where the mALTs were the only complete PN pair showing expression. Since FLIPSOTi requires inhibition in both sides of the brain in order to cause a

defect in warmth avoidance, we concluded that the mALTs are the only VP2 PNs necessary for warmth avoidance of 31ºC.

HC>FLIPSOTa experiments required a similar process to *FLIPSOTi* with only a few small changes. We found that the three-week aging time recommended by Talay et al (2017) resulted in good signal without too much leaky expression; dissecting at earlier timepoints yielded samples that were too weak to see (data not shown), consistent with the original *trans*-Tango experiments. Though this experiment required red light avoidance instead of warmth avoidance, we still tested flies' innate warmth avoidance in room light as a control; flies that failed to avoid 31ºC were discarded.

Figure 17: FLIPSOTa experimental workflow

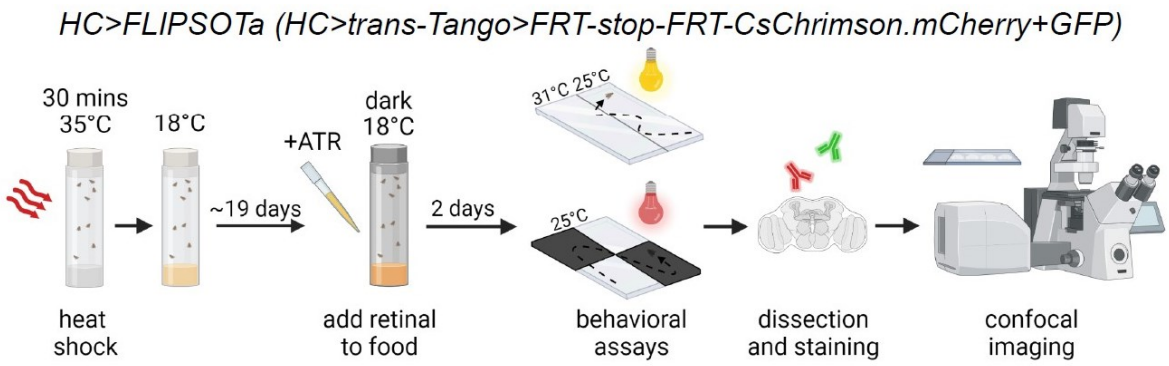

Figure 17. *HC>FLIPSOTa* flies were heat shocked post-eclosion at 35ºC for 30 minutes. After ~19 days at 18ºC, dietary ATR was added to the food, and red light avoidance assays plus warmth avoidance control assays were run two days later. Finally, brains were dissected, stained, and imaged. Flies were allowed to age for about three weeks total between eclosion and the final dissection.

FLIPSOTa was then tested in the HC PNs. *hs>FLP, HC>trans-Tango>FRT-stop-FRT-CsChrimson.mCherry/GFP* flies were first separated based on behavioral response; those with a PI that fell within one standard deviation of other red light avoiding genotypes (*HC>CsChrimson and HC>GtACR2/CsChrimson*) were counted as exhibiting red light avoidance (Figure 18A). Brains were then dissected, stained, and analyzed to compare PNs between samples. Examples of expression variance between flies are shown in Figure 18B-C. Overall summary of PNs targeted by FLIPSOTa is shown in Figure 18D-E.

Figure 18. *HC>FLIPSOTa* indicates sufficient PNs for warmth avoidance

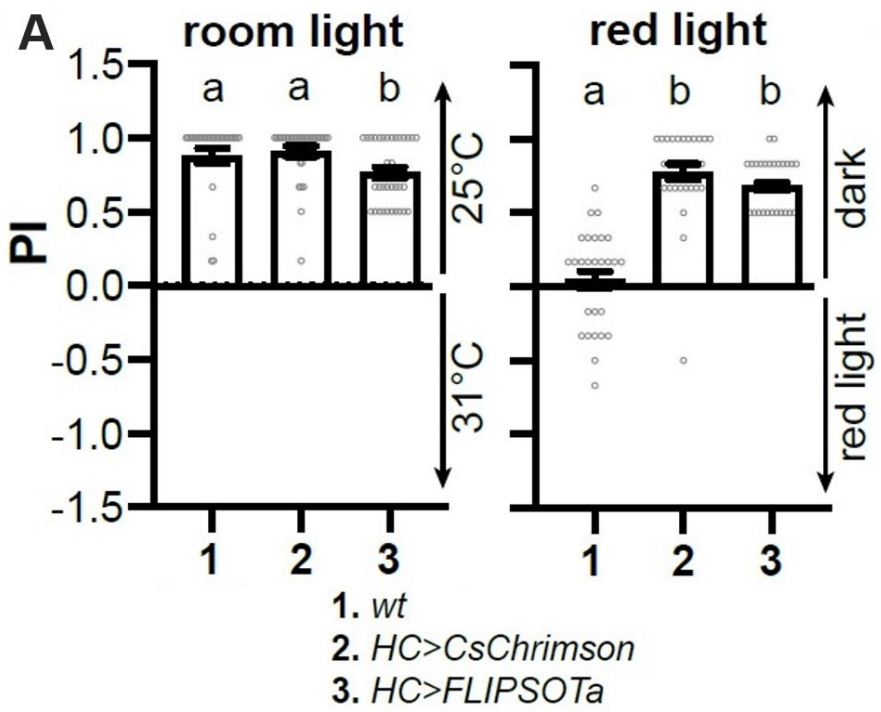

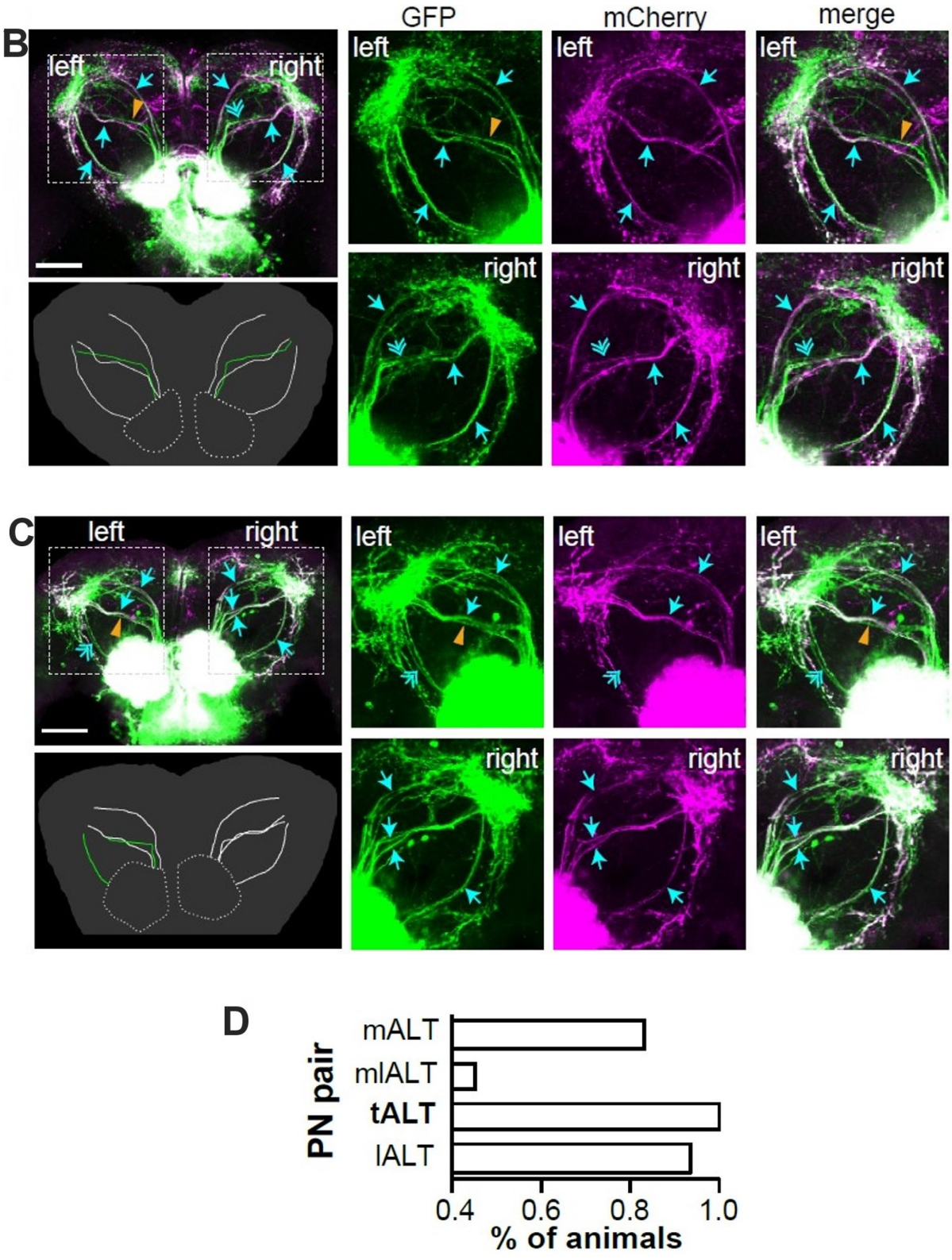
B
GFP
mCherry
merge
left
right
C
D
mALT
mlALT
tALT
lALT
PN pair
0.4
0.6
0.8
1.0
% of animals

E

GFP Projections								mCherry Projections							
l	t	ml	m	m	ml	t	l	l	t	ml	m	m	ml	t	l
y	y	y	y	y	y	y	y	y	y		y	y	y	y	
y	y	y	y	y	y	y	y		y		y	y		y	y
y	y	y	y	y	y	y	y		y	y	y	y	y	y	y
y	y	y	y	y	y	y	y	y	y	y	y		y	y	y
y	y	y	y	y	y	y	y	y			y			y	y
y	y	y	y	y	y	y	y	y	y		y	y		y	y
y	y	y	y	y	y	y	y	y	y	y				y	y
y	y	y	y	y	y	y	y	y	y		y	y	y	y	y
y	y	y	y	y	y	y	y	y	y					y	
y	y	y	y	y	y	y	y		y		y				
y	y	y	y	y	y	y	y	y	y	y					y
y	y	y	y	y	y	y	y	y	y		y			y	y
y	y	y	y	y	y	y	y		y					y	y
y	y	y	y	y	y	y	y	y	y			y		y	
y	y		y	y	y	y	y	y	y					y	y
y	y	y	y	y	y	y	y		y	y	y		y	y	y
y	y	y	y	y	y	y	y		y		y	y		y	y
y	y	y	y	y	y	y	y	y	y		y	y		y	y
y	y	y	y	y	y	y	y		y	y		y		y	
y	y	y	y	y	y	y	y	y	y		y	y		y	y
y	y			y	y	y	y	y	y			y		y	y
y	y	y	y	y	y	y	y		y	y	y	y		y	y
y	y	y	y	y	y	y	y	y	y			y		y	y
y	y	y	y	y	y	y	y	y	y		y	y		y	y
y	y	y	y	y	y	y	y	y	y		y	y		y	y
y	y	y	y	y	y	y	y	y	y	y	y	y		y	y
y	y	y	y	y	y	y	y	y	y	y	y	y		y	y
y	y	y	y	y	y	y	y		y		y	y	y	y	y
y	y	y	y	y	y	y	y		y		y	y		y	y

Figure 18. *hs>FLP, HC>trans-Tango>FRT-stop-FRT-CsChrimson.mCherry/GFP* red light-avoiding flies are used to determine sufficient PNs for warmth avoidance behavior.

(A) ATR+ *HC>FLIPSOTa* flies (the above genotype) chose between 25ºC and 31ºC in ambient room light, or between dark and red light. Flies were separated based on behavioral phenotype in red light using the threshold established from control experiments (*HC>CsChrimson*); *HC>FLIPSOTa* flies shown are those that fell above the designated threshold and thus had *CsChrimson* activation in cells sufficient for warmth avoidance.

n=29; data represent means ± SEM; Kruskal-Wallis test followed by Dunn's multiple comparisons test; letters denote statistically distinct groups, $p < 0.05$.

(B-C) Representative images of CsChrimson-positive HC PNs in flies that avoided red light. GFP (green) – control stain (all PNs); mCherry (magenta) – PNs with *FLIPSOTa* activation. Cyan arrows indicate CsChrimson.mCherry-positive PNs; orange arrows indicate CsChrimson.mCherry-negative PNs. Cyan double arrows indicate CsChrimson.mCherry-weak PNs, or circumstances in which the mCherry staining is much weaker than the GFP staining; these are considered CsChrimson.mCherry-negative. Scale bars = 50μm. Left lower panels include illustrations of corresponding PNs. (B) Six PNs express CsChrimson.mCherry (both lALTS, mlALTs, and tALTs). (C) Five PNs express CsChrimson.mCherry (both mlALTs and tALTs along with the right mALT).

(D-E) The tALTs are sufficient to drive warmth avoidance behavior. CsChrimson.mCherry-positive PNs were analyzed from 29 flies that avoided red light, all of which contained at least one mCherry-positive tALT PN. All other PN pairs lacked mCherry expression on both sides in at least one animal. (E) l, lALT; t, tALT; ml, mlALT; m, mALT.

All *HC>FLIPSOTa* flies that avoided red light showed expression in at least one tALT, or the mediolateral, bended/wavy PN group, indicating that the tALTs are sufficient for warmth avoidance behavior. No other pair of PNs had expression present in all flies, and all other pairs lacked expression on both sides at least once per pair. FLIPSOTa requires activation in one side of the HC circuit in order to drive avoidance of red light, and since the tALT was the only PN pair that consistently expressed mCherry on at least one side, we concluded that the tALTs are sufficient to drive warmth avoidance behavior.

We did notice a significant difference in the room light warmth avoidance between *HC>FLIPSOTa* flies and our controls (Figure 18A). We theorized that this was due to the older age of the *HC>FLIPSOTa* flies, since our control flies were run at 2-7 days post eclosion instead of three weeks. To test this, we ran wild type flies at both 10 days and 3 weeks in order to compare them with our FLIPSOTi and FLIPSOTa flies, respectively; we found that at the appropriate ages, there was no significant difference between FLIPSOTi/FLIPSOTa flies and the wild type (Figure 19).

Figure 19. Age of flies affects thermal preference

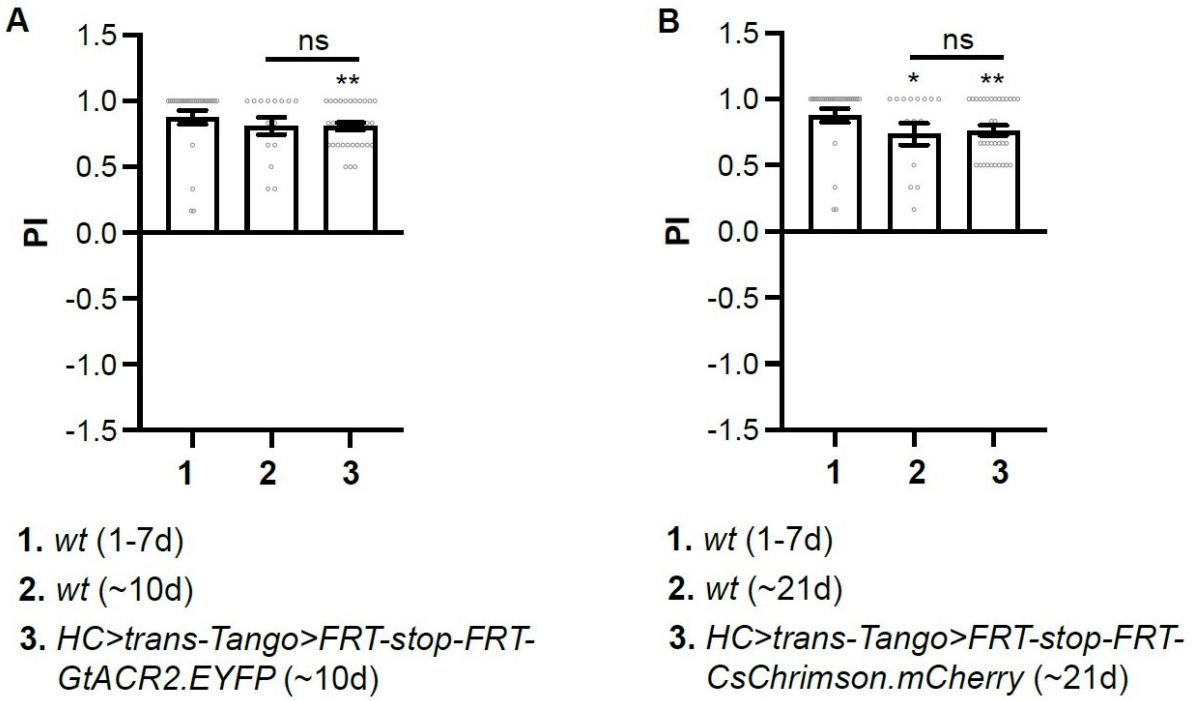

Figure 19. *HC>FLIPSOTi* (A) and *HC>FLIPSOTa* (B) flies were compared to wild type flies of 10 days and 21 days old, respectively. Flies were allowed to choose between room temperature and 31ºC. n=15-31; data represent means ± SEM; Mann-Whitney test compared to wild type. * $p < 0.05$; ** $p < 0.01$.

3.4 Methods

Drosophila strains

The wild-type control used for all behavioral assays was w^{1118}. *UAS-GtACR2* (Mauss et al, 2017) was previously described and was a kind gift from the Gaudry Lab. *HC-GAL4* (Gallio et al, 2011), *Gr28b.d-GAL4* (Thorne & Amrein, 2008), *UAS-CsChrimson* (BDSC 55135 & 55136, Klapoetke et al, 2014), *hs-FLP* (BDSC 6938, Golic et al, 1989), *QUAS-GFP* & *QUAS-RFP* (BDSC 30002 & 30004, Riabinina et al, 2016), and *UAS-trans-Tango* (BDSC 77123 & 77124, Talay et al, 2017) were previously described.

Heat shock

Heat shock was performed 1-3 days post-eclosure. Flies were placed in an empty vial with a flug pressed into the bottom for added protection. Vials were then submerged in a water bath set to 35ºC for 30 minutes, and flies were returned to regular food immediately post heat shock.

Single-fly two-choice behavior assays

All flies were maintained at about a 12:12 hour light:dark cycle and crossed at 23.5ºC. For flies containing hs-FLP, heat shock was performed. Flies were then placed at either 18ºC if involved in *trans*-Tango-containing experiments or at 23.5ºC if not. Two days before behavioral experiments, flies were placed on food containing 40 µM all-trans retinal (ATR, Sigma-Aldrich) and moved to 24-hour dark conditions until testing. Control experiment flies were tested at 2-10 days old. Flies containing *trans*-Tango were tested at 10 days to 3 weeks old, depending on the genotype.

Warmth avoidance assays were set up using a sheet protector taped over top of two contiguous metal plates, with one plate warmed on a heat source to 31ºC and the other at room temperature (25ºC). Flies were placed under a small plastic cover and allowed to acclimate for 15-25 seconds before starting the experiment; all experiments were started with flies on the 25ºC side of the assay. The position of the fly was recorded every 5 seconds for 1 minute. Flies that did not move for more than 30 seconds were discarded. For control experiments, a centered desk lamp (22lux) was used as ambient lighting. For blue light optogenetic experiments, a blue light source (20Klux) was built using similar specifications to a previously described red light source (Tyrrell et al, 2021), though modified to use a triple blue LED light instead (470nm, Luxeon Star LEDs SP-03-B3).

Preference index to room temperature was calculated using the formula:

$$\frac{\text{(\# of times in 25ºC - \# of times in 31ºC)}}{\text{total \# of times}}$$

Red light optogenetic assays were conducted at 25ºC, and the base of the experiment consisted of a sheet protector overlaid on a black background. Flies were placed on the sheet protector under a small plastic cover, with two quadrants of the cover blocked from light with opaque, black electrical tape. Flies were given 10 seconds to acclimate, and all experiments started with flies in one of the visible quadrants; flies that did not move for more than 30 seconds were discarded. The red light source (32Klux) was previously described (Tyrrell et al, 2021). Assessment and analysis using TrackMate was carried out as previously described (Huda et al, 2022).

Preference index to dark quadrants was calculated using the formula:

$$\frac{\text{(\# of times in dark - \# of times in red light)}}{\text{total \# of times}}$$

Dissection and Immunostaining

Brains were dissected using forceps (FST 11413-11) in 1X PBS with methodology similar to a tutorial video (映像 IMAGE, 2019), then transferred to PBS on ice immediately after dissection. Fixation, blocking, and immunostaining were carried out as previously described (Kang et al, 2012) with the following changes in timing: fixation was lengthened to 30 minutes; samples were placed in the primary antibody solution for 3 nights, washed overnight, placed in the secondary antibody solution overnight, and washed overnight once more. Samples were mounted using Vectashield Mounting Medium and imaged using a Nikon A1 Confocal Microscope. Primary antibodies used were rabbit anti-dsRed (1:200, Takara Bio), rabbit anti-GFP (1:500, Invitrogen), mouse anti-GFP (1:500, Sigma-Aldrich), and mouse anti-HA (1:200, Invitrogen)**.** Secondary antibodies were all diluted to 1:250 and included goat anti-rabbit Cy3 (Jackson Immuno), goat anti-rabbit Alexa Fluor 488 (Jackson Immuno), goat anti-mouse CF488A (Sigma-Aldrich), and goat anti-mouse TRITC (Invitrogen)**.**

For relevant experiments, aristae were removed with forceps, during which flies were anesthetized by CO_2. Flies were then allowed to reawaken and aged for either behavior or brain dissection, depending on the genotype. No antibodies were used in brains for the arista ablation experiments; samples were dissected, fixed, and mounted (arista ablation brains).

Statistical Analysis

Statistical analysis details of each experiment can be found in the figure legends. Statistical comparisons were performed by either the Mann-Whitney test (for two samples or comparison to wild type) or the Kruskal-Wallis test followed by Dunn’s multiple comparisons

test. Data were plotted using bar graphs representing mean ± SEM along with scatterplots representing individual data points. Analysis was performed using GraphPad Prism 9.

3.5 Discussion & Conclusions

FLIPSOT was used to investigate the necessity and sufficiency of HC PNs. Based on preliminary experiments, thresholds were set to identify optogenetically modified behavior, and HC PN morphology was described. *FLIPSOTi* was then used to inhibit randomized HC PNs, and analysis of visible PNs from flies that failed to avoid warmth suggested that the mALT was necessary for warmth avoidance behavior. This is consistent with findings from Frank et al (2015). Similarly, *FLIPSOTa* was used to activate randomized HC PNs, and analysis of visible PNs from flies that avoided red light suggested that the tALT was sufficient to drive warmth avoidance behavior.

The finding that the necessary and sufficient PNs for behavior differed was a surprising one, as necessity and sufficiency of neurons are generally expected to overlap. However, the *Drosophila* temperature sensation system has known mechanisms of feedback between neurons (Liu et al, 2015); it is feasible to suggest that the separation of necessity and sufficiency of these PNs is related to feedback mechanisms between the warm and cool sensing systems. This could help better attune the fly when experiencing different levels of thermoreceptor activation on either side of the brain.

It is possible that the results here were confounded by presence of indirect signal in the interneurons; interneurons are unfortunately very difficult to distinguish in FLIPSOT images in the antennal lobe due to overlap in signal. If FLIPSOT activation of interneurons were to activate another path that either drives or inhibits warmth sensation, that could contradict the results presented here. However, it is unlikely in this case that we would

achieve such high percentages of specific FLIPSOT-positive PNs. Most local interneurons are predicted to be weakly inhibitory due to the neurotransmitters used and the low number of synapses compared to sensory neurons (Horne et al, 2018; Wilson & Laurent, 2005). Thus, it is increasingly unlikely that local interneurons would be used to activate a pathway sufficient for avoidance. It cannot be discounted in this case that interneurons could be inhibiting the PNs necessary for avoidance during FLIPSOTi experiments. However, due to the randomization aspect of FLIPSOT, the probability of simultaneously targeting the same PNs (the mALTs) in every trial along with enough correct local interneurons to achieve strong inhibition is statistically unlikely.

FLIPSOTa requires expression in only one side of the organism to drive avoidance. Though we found that the tALTs were sufficient here due to their presence in one hundred percent of flies with avoidance behavior, there were other ALTs that were seen at high frequencies on at least one side (though not in all flies). Additional validation of the sufficiency of the tALTs, either through expansion of trials or alternative experimentation, would provide further support to these results.

Overall, this chapter demonstrates the choice and optimization of FLIPSOT components, the setup required in order to use FLIPSOT within the HC neural circuit system, and finally the usage of FLIPSOT to identify necessary and sufficient HC PNs for warmth avoidance.

CHAPTER 4: GENERAL DISCUSSION

4.1 General findings

FLIPSOT, or functional labeling of individualized post-synaptic neurons using optogenetics and *trans*-Tango, is a tool created to assess the necessity and sufficiency of post-synaptic neurons using a pre-synaptic driver. It accomplishes this through usage of 1) *trans*-Tango, which allows targeting of post-synaptic neurons; 2) heat shock driving FLP Out, which randomizes the post-synaptic neurons targeted, and 3) the optogenetic receptors GtACR2 and CsChrimson, which allow behavioral inhibition (FLIPSOTi) or activation (FLIPSOTa) in turn. Each of these tools were tested and optimized, both separately and in combination, in order to determine an optimal experimental design.

FLIPSOT was then tested within the HC neurons to examine necessary or sufficient PNs. Two experimental workflows were created: one for FLIPSOTi and one for FLIPSOTa. Additionally, preliminary experiments were done in order to set a threshold for dividing behavior into affected vs non-affected groups, as well as to determine that FLIPSOTa requires expression in one side while FLIPSOTi requires both. Finally, we determined that the medial tract (mALT) is necessary for warmth avoidance behavior, while the wavy/bended tract (tALT) is sufficient to drive warmth avoidance behavior.

4.2 Strengths and weaknesses of FLIPSOT

A key feature of FLIPSOT is that it is easily modified to work in any circuit that features an assessable behavioral output. This versatility is based on its reliance on the GAL4 driver system, for which most experiments in *Drosophila* already make heavy use of; implementation in a new system only requires crossing of the *FLIPSOTi* or *FLIPSOTa* QUAS lines with the right GAL4 line, along with *UAS-trans-Tango* and *hs>FLP*. It is

therefore inexpensive to generate the flies needed for many behavioral trials. Experimentally, FLIPSOT only requires a validated behavioral assay along with brain dissection and confocal imaging, all of which are common techniques in labs investigating neural circuits and thus should be relatively easy to execute. Finally, for experiments that require larval behavior, a new *trans*-Tango variant for larvae was recently established that could easily be switched in instead of the original *trans*-Tango (Sorkaç et al 2022).

Compared to other neural circuit analysis tools, FLIPSOT combines investigation of post-synaptic morphology with functional analysis, for which there are very few tools possible. FLIPSOT is a reliable indicator of synaptic connection due to its inclusion of *trans*-Tango, and its ability to test behavior helps reconfirm that connection. Using FLIPSOT also bypasses the need to screen multiple driver lines to find post-synaptic drivers, which often either don't express in all neurons of interest or express in extraneous neurons. Though methods such as GRASP can be used to confirm whether a driver line labels post-synaptic neurons of interest, it can be difficult to distinguish if all post-synaptic neurons are correctly labeled with absolute certainty due to morphological similarities between neurons of similar types (such as PNs) that have different functions. FLIPSOT solves this problem by providing a direct link to the pre-synaptic neuron while simultaneously assessing post-synaptic function.

Though FLIPSOT was originally designed to include both activation and inhibition in one tool, we eventually ended up with two variants, FLIPSOTi and FLIPSOTa. This turned out to have the unexpected benefit of separating necessity and sufficiency, which was not only relevant for our system but could also be important for other users. Though necessity and sufficiency could theoretically still be discerned separately within the combination FLIPSOT system, it may require many more trials due to overlap in PNs with FLIPSOT expression between animals. Separation of necessity and sufficiency may not be needed if

necessary and sufficient neurons are one and the same, but since users likely will not know whether or not this is the case pre-FLIPSOT experimentation, it may be best to use FLIPSOTi and FLIPSOTa separately in most situations.

Though FLIPSOT has many strengths as a tool, there are also some weaknesses and areas of potential improvement. The most prominent of these is the presence of false positives, or leaky expression. False positives have been associated with the original *trans*-Tango tool (Talay et al, 2017) and may also be correlated with leaky expression of FLP recombinase, or with the stop sequence used between FRT sites. Further testing and experimentation can be done to fine tune and reduce the leaky expression seen in FLIPSOT, including but not limited to adjusting heat shock parameters and reducing the rearing temperature further (which could reduce leakiness of *hs>FLP*).

FLIPSOT randomizes expression in all post-synaptic neurons of a pre-synaptic driver, which can potentially confound results through activation of unexpected or less visible pathways (i.e. local interneurons). Additionally, FLIPSOT requires a relatively clean pre-synaptic driver line; if the pre-synaptic driver line includes extraneous expression, the post-synaptic neuron morphology will be much harder to determine, and there may be difficulties in determining which of the neurons are necessary or sufficient for the behavior due to overlap in signal.

Finally, FLIPSOT requires robust behavior in order to establish a behavioral threshold, which may be limiting for experiments with more nuanced results. Similarly, because FLIPSOT relies on *trans*-Tango, it is likely that optimal imaging results will require aging flies for three weeks before testing behavior and dissecting them. This may have negative effects on behavioral phenotype due to reduced health as flies age; in certain assays this may cause issues such as reducing their locomotion. We found that ensuring flies were on fresh food (with ATR added) no longer than 2-3 days before behavioral assays

helped to maintain locomotor activity and allowed proper ability to choose between dark and light in our FLIPSOTa assay. If behavioral effects due to aging are severe, experimentation may be done to find the age that best balances behavioral assay viability with post-synaptic neuronal imaging. FLIPSOT flies must also be raised at 18ºC in order to provide the best imaging results, which could potentially affect behavior due to the slowing of physiological processes. However, raising flies at 23.5ºC until eclosion may help avoid negative effects of cooler temperature on early development and did not negatively impact our imaging results.

4.3 Future directions

There are many future directions that can be taken with FLIPSOT as a tool. Besides fine-tuning FLIPSOT to reduce its leaky expression, one of the easiest potential modifications is replacing *trans*-Tango with the newer, larval variant of *trans*-Tango (Sorkaç et al 2022) and testing a larval behavior with it. This would greatly expand the repertoire of available behavior. While the larval version in theory should work just as well as the adult FLIPSOT tool, as it only requires an alternate cross, compatibility has not yet been tested.

FLIPSOTa and FLIPSOTi have yet to be combined into one complete FLIPSOT tool capable of both activation and inhibition. While this separation has been useful, as discussed earlier in this chapter, there may still be circumstances where users require both activation and inhibition in the same animal. Further examination of our *QUAS-FRT-stop-FRT-GtACR2-T2A-CsChrimson.mCherry* line is needed to indicate how to proceed; it is possible that insertion into a different site in the genome may fix the issue.

Now that FLIPSOT has been used to successfully identify second order neurons, it is possible to add TRACT into the system to allow visualization and testing of third order neurons as well (see Chapter 2 discussion). This would represent a strong advance in

neural circuit analysis, as the third order neurons in many systems are still currently unknown. Another possible addition into the existing FLIPSOT system is the calcium indicator gCAMP, which would be placed after the channelrhodopsin and a *T2A* sequence in the QUAS line. This would allow an additional indication of neuronal activation or inhibition during optogenetic stimulation, which would assist in comparison of FLIPSOT-positive cells with non-positive ones as well as help to pinpoint cell bodies for further analysis.

With regards to temperature sensation, the HC circuit second order neurons have now been tested for function in behavior. This paves the way for experiments to discover third-order neurons and eventually to map the whole circuit, as well as for experiments using FLIPSOT in other temperature-sensing neurons.

Finally, FLIPSOT as a system opens up possibilities for use in other model organisms in the future. FLIPSOT could be used in mammalian models to help deduce functional parts of neural circuits involved in states such as thermal stress, addiction, or depression or anxiety-like behaviors. Deducing functional neurons in these circuits can provide important knowledge about how these circuits may work in human patients; identifying new functional neurons may also allow for investigation of molecules or receptors that could serve as potential therapeutic targets.

4.4 Conclusion

FLIPSOT is a tool that can aid in neural circuit tracing and analysis for circuits related to many behaviors. It uses a combination of genetic tools to allow individualized labelling as well as functional analysis of post-synaptic neurons. Though there are some drawbacks to the tool, there are many strengths, especially considering that it is the first tool to combine behavioral and morphological analysis without requiring usage of a post-synaptic driver line.

Implications for this study go beyond *Drosophila*, as many tools developed in *Drosophila* or other simpler models such as *C. elegans* have gone on to be used in mammalian or mosquito models. Studying simple neural circuits helps us to understand more complicated ones. Similarly, implementing tools in simpler animals helps users to eventually create versions for more complicated ones. Though *trans*-Tango has not yet been implemented in mammalian models such as mice, once it has been properly modified, FLIPSOT is a tool that could easily be replicated in other organisms soon after.

REFERENCES

Figures 1, 2, 3, 7, 10, 11A, 15, and 17 created with Biorender.com.

Aso, Y., Sitaraman, D., Ichinose, T., Kaun, K. R., Vogt, K., Belliart-Guérin, G., ... & Rubin, G. M. (2014). Mushroom body output neurons encode valence and guide memory-based action selection in Drosophila. *eLife*, *3*, e04580.

Barbagallo, B., & Garrity, P. A. (2015). Temperature sensation in Drosophila. *Current opinion in neurobiology*, *34*, 8-13.

Bear, M., Connors, B., & Paradiso, M. A. (2020). Neuroscience: exploring the brain, enhanced edition: exploring the brain. *Jones & Bartlett Learning*.

Boekhoff-Falk, G., & Eberl, D. F. (2014). The Drosophila auditory system. *Wiley Interdisciplinary Reviews: Developmental Biology*, *3*(2), 179-191.

Brankatschk, M., Gutmann, T., Knittelfelder, O., Palladini, A., Prince, E., Grzybek, M., ... & Eaton, S. (2018). A temperature-dependent switch in feeding preference improves Drosophila development and survival in the cold. *Developmental Cell*, *46*(6), 781-793.

Burraco, P., Orizaola, G., Monaghan, P., & Metcalfe, N. B. (2020). Climate change and ageing in ectotherms. *Global Change Biology*, *26*(10), 5371-5381.

Bykhovskaia, M., & Vasin, A. (2017). Electrophysiological analysis of synaptic transmission in Drosophila. *Wiley Interdisciplinary Reviews: Developmental Biology*, *6*(5), e277.

Cachero, S., Gkantia, M., Bates, A. S., Frechter, S., Blackie, L., McCarthy, A., ... & Jefferis, G. S. (2020). BAcTrace, a tool for retrograde tracing of neuronal circuits in Drosophila. *Nature methods*, *17*(12), 1254-1261.

Corfas, R. A., & Vosshall, L. B. (2015). The cation channel TRPA1 tunes mosquito thermotaxis to host temperatures. *eLife*, 4, e11750.

Couto, A., Alenius, M., & Dickson, B. J. (2005). Molecular, anatomical, and functional organization of the Drosophila olfactory system. *Current Biology*, *15*(17), 1535-1547.

del Valle Rodríguez, A., Didiano, D., & Desplan, C. (2012). Power tools for gene expression and clonal analysis in Drosophila. *Nature methods*, *9*(1), 47-55.

Deutsch, C. A., Tewksbury, J. J., Huey, R. B., Sheldon, K. S., Ghalambor, C. K., Haak, D. C., & Martin, P. R. (2008). Impacts of climate warming on terrestrial ectotherms across latitude. *Proceedings of the National Academy of Sciences*, *105*(18), 6668-6672.

Dillon, M. E., Wang, G., Garrity, P. A., & Huey, R. B. (2009). Thermal preference in Drosophila. *Journal of thermal biology*, *34*(3), 109-119.

Dunipace, L., Meister, S., McNealy, C., & Amrein, H. (2001). Spatially restricted expression of candidate taste receptors in the Drosophila gustatory system. Current Biology, 11(11), 822-835.

Dweck, H. K., & Carlson, J. R. (2020). Molecular logic and evolution of bitter taste in Drosophila. *Current Biology*, *30*(1), 17-30.

Frank, D. D., Jouandet, G. C., Kearney, P. J., Macpherson, L. J., & Gallio, M. (2015). Temperature representation in the Drosophila brain. *Nature*, *519*(7543), 358-361.

Feinberg, E. H., VanHoven, M. K., Bendesky, A., Wang, G., Fetter, R. D., Shen, K., & Bargmann, C. I. (2008). GFP Reconstitution Across Synaptic Partners (GRASP) defines cell contacts and synapses in living nervous systems. *Neuron*, *57*(3), 353-363.

Gallio, M., Ofstad, T. A., Macpherson, L. J., Wang, J. W., & Zuker, C. S. (2011). The coding of temperature in the Drosophila brain. *Cell*, 144(4), 614-624.

Garrity, P. A., Goodman, M. B., Samuel, A. D., & Sengupta, P. (2010). Running hot and cold: behavioral strategies, neural circuits, and the molecular machinery for thermotaxis in C. elegans and Drosophila. *Genes & development*, *24*(21), 2365-2382.

Golic, K. G., & Lindquist, S. (1989). The FLP recombinase of yeast catalyzes site-specific recombination in the Drosophila genome. *Cell*, 59(3), 499-509.

Guo, F., Holla, M., Díaz, M. M., & Rosbash, M. (2018). A circadian output circuit controls sleep-wake arousal in Drosophila. *Neuron*, *100*(3), 624-635.

Hamada, F. N., Rosenzweig, M., Kang, K., Pulver, S. R., Ghezzi, A., Jegla, T. J., & Garrity, P. A. (2008). An internal thermal sensor controlling temperature preference in Drosophila. *Nature*, *454*(7201), 217-220.

Hodge, J. J. (2009). Ion channels to inactivate neurons in Drosophila. *Frontiers in molecular neuroscience*, 13.

Hong, W., Zhu, H., Potter, C. J., Barsh, G., Kurusu, M., Zinn, K., & Luo, L. (2009). Leucine-rich repeat transmembrane proteins instruct discrete dendrite targeting in an olfactory map. *Nature neuroscience*, 12(12), 1542-1550.

Horne, J. A., Langille, C., McLin, S., Wiederman, M., Lu, Z., Xu, C. S., ... & Meinertzhagen, I. A. (2018). A resource for the Drosophila antennal lobe provided by the connectome of glomerulus VA1v. Elife, 7, e37550.

Huang, T. H., Niesman, P., Arasu, D., Lee, D., De La Cruz, A. L., Callejas, A., ... & Lois, C. (2017). Tracing neuronal circuits in transgenic animals by transneuronal control of transcription (TRACT). *eLife*, 6, e32027.

Huda, A., Omelchenko, A. A., Vaden, T. J., Castaneda, A. N., & Ni, L. (2022). Responses of different Drosophila species to temperature changes. *Journal of Experimental Biology*, *225*(11), jeb243708. https://journals.biologists.com/jeb/article/225/11/jeb243708/275567/Responses-of-different-Drosophila-species-to

Hunter, I., Coulson, B., Zarin, A. A., & Baines, R. A. (2021). The Drosophila larval locomotor circuit provides a model to understand neural circuit development and function. *Frontiers in Neural Circuits*, 62.

Inada, K., Kohsaka, H., Takasu, E., Matsunaga, T., & Nose, A. (2011). Optical dissection of neural circuits responsible for Drosophila larval locomotion with halorhodopsin. *PloS one*, *6*(12), e29019.

Jeibmann, A., & Paulus, W. (2009). Drosophila melanogaster as a model organism of brain diseases. *International journal of molecular sciences*, *10*(2), 407-440.

Jørgensen, L. B., Ørsted, M., Malte, H., Wang, T., & Overgaard, J. (2022). Extreme escalation of heat failure rates in ectotherms with global warming. *Nature*, 1-6.

Kang, K., Panzano, V. C., Chang, E. C., Ni, L., Dainis, A. M., Jenkins, A. M., ... & Garrity, P. A. (2012). Modulation of TRPA1 thermal sensitivity enables sensory discrimination in Drosophila. *Nature*, *481*(7379), 76-80.

Keene, A. C., & Waddell, S. (2007). Drosophila olfactory memory: single genes to complex neural circuits. *Nature Reviews Neuroscience*, *8*(5), 341-354.

Kim, H., Kirkhart, C., & Scott, K. (2017). Long-range projection neurons in the taste circuit of Drosophila. *Elife*, *6*, e23386.

King, A. N., & Sehgal, A. (2020). Molecular and circuit mechanisms mediating circadian clock output in the Drosophila brain. *European Journal of Neuroscience*, *51*(1), 268-281.

Klapoetke, N. C., Murata, Y., Kim, S. S., Pulver, S. R., Birdsey-Benson, A., Cho, Y. K., ... & Boyden, E. S. (2014). Independent optical excitation of distinct neural populations. *Nature methods*, 11(3), 338-346.

Klepsatel, P., Gáliková, M., Xu, Y., & Kühnlein, R. P. (2016). Thermal stress depletes energy reserves in Drosophila. *Scientific reports*, 6(1), 33667.

Lacetera, N. (2019). Impact of climate change on animal health and welfare. *Animal Frontiers*, *9*(1), 26-31.

Larderet, I., Fritsch, P. M., Gendre, N., Neagu-Maier, G. L., Fetter, R. D., Schneider-Mizell, C. M., ... & Sprecher, S. G. (2017). Organization of the Drosophila larval visual circuit. *Elife*, *6*, e28387.

Lee, P. T., Zirin, J., Kanca, O., Lin, W. W., Schulze, K. L., Li-Kroeger, D., ... & Bellen, H. J. (2018). A gene-specific T2A-GAL4 library for Drosophila. *eLife*, *7*, e35574.

Lehmann, F. O., & Bartussek, J. (2017). Neural control and precision of flight muscle activation in Drosophila. *Journal of Comparative Physiology A*, *203*, 1-14.

Li, K., & Gong, Z. (2017). Feeling hot and cold: thermal sensation in Drosophila. *Neuroscience bulletin*, *33*, 317-322.

Liu, W. W., Mazor, O., & Wilson, R. I. (2015). Thermosensory processing in the Drosophila brain. *Nature*, *519*(7543), 353-357.

Mauss, A. S., Busch, C., & Borst, A. (2017). Optogenetic neuronal silencing in Drosophila during visual processing. *Scientific reports*, 7(1), 13823.

Marin, E. C., Jefferis, G. S., Komiyama, T., Zhu, H., & Luo, L. (2002). Representation of the glomerular olfactory map in the Drosophila brain. *Cell*, *109*(2), 243-255.

Marin, E. C., Büld, L., Theiss, M., Sarkissian, T., Roberts, R. J., Turnbull, R., ... & Jefferis, G. S. (2020). Connectomics analysis reveals first-, second-, and third-order thermosensory and hygrosensory neurons in the adult Drosophila brain. *Current Biology*, *30*(16), 3167-3182.

McTeague, L. M., Huemer, J., Carreon, D. M., Jiang, Y., Eickhoff, S. B., & Etkin, A. (2017). Identification of common neural circuit disruptions in cognitive control across psychiatric disorders. *American Journal of Psychiatry*, *174*(7), 676-685.

Meloni, I., Sachidanandan, D., Thum, A. S., Kittel, R. J., & Murawski, C. (2020). Controlling the behaviour of Drosophila melanogaster via smartphone optogenetics. *Scientific Reports*, *10*(1), 1-11.

Miller, D. E., Cook, K. R., & Hawley, R. S. (2019). The joy of balancers. *PLoS genetics*, *15*(11), e1008421.

Mishra, A., Salari, A., Berigan, B. R., Miguel, K. C., Amirshenava, M., Robinson, A., ... & Zars, T. (2018). The Drosophila Gr28bD product is a non-specific cation channel that can be used as a novel thermogenetic tool. *Scientific reports*, *8*(1), 901.

Miwa, Y., Koganezawa, M., & Yamamoto, D. (2018). Antennae sense heat stress to inhibit mating and promote escaping in Drosophila females. *Journal of neurogenetics*, *32*(4), 353-363.

Mohammad, F., Stewart, J. C., Ott, S., Chlebikova, K., Chua, J. Y., Koh, T. W., ... & Claridge-Chang, A. (2017). Optogenetic inhibition of behavior with anion channelrhodopsins. *Nature methods*, *14*(3), 271-274.

Moulin, T. C., Covill, L. E., Itskov, P. M., Williams, M. J., & Schiöth, H. B. (2021). Rodent and fly models in behavioral neuroscience: An evaluation of methodological advances, comparative research, and future perspectives. *Neuroscience & Biobehavioral Reviews*, *120*, 1-12.

Ni, L., Bronk, P., Chang, E. C., Lowell, A. M., Flam, J. O., Panzano, V. C., ... & Garrity, P. A. (2013). A gustatory receptor paralogue controls rapid warmth avoidance in Drosophila. *Nature*, *500*(7464), 580-584.

Ni, L., Klein, M., Svec, K. V., Budelli, G., Chang, E. C., Ferrer, A. J., ... & Garrity, P. A. (2016). The ionotropic receptors IR21a and IR25a mediate cool sensing in Drosophila. *eLife*, *5*, e13254.

Ni, L. (2021). Genetic Transsynaptic Techniques for Mapping Neural Circuits in Drosophila. *Frontiers in Neural Circuits*, 104.

Neely, G. G., Keene, A. C., Duchek, P., Chang, E. C., Wang, Q. P., Aksoy, Y. A., ... & Penninger, J. M. (2011). TrpA1 regulates thermal nociception in Drosophila. *PloS one*, *6*(8), e24343.

Olsen, S. R., & Wilson, R. I. (2008). Cracking neural circuits in a tiny brain: new approaches for understanding the neural circuitry of Drosophila. *Trends in neurosciences*, *31*(10), 512-520.

Patterson, G. H., & Lippincott-Schwartz, J. (2002). A photoactivatable GFP for selective photolabeling of proteins and cells. *Science*, *297*(5588), 1873-1877.

Peter, M., Bathellier, B., Fontinha, B., Pliota, P., Haubensak, W., & Rumpel, S. (2013). Transgenic mouse models enabling photolabeling of individual neurons in vivo. *PloS one*, *8*(4), e62132.

Putz, G., & Heisenberg, M. (2002). Memories in Drosophila heat-box learning. *Learning & memory*, *9*(5), 349-359.

Riabinina, O., & Potter, C. J. (2016). The Q-system: a versatile expression system for Drosophila. *Drosophila: Methods and Protocols*, 53-78.

Sahin, M., & Sur, M. (2015). Genes, circuits, and precision therapies for autism and related neurodevelopmental disorders. *Science*, *350*(6263), aab3897.

Sarnat, H. B., & Netsky, M. G. (1985). The brain of the planarian as the ancestor of the human brain. *Canadian Journal of Neurological Sciences*, 12(4), 296-302.

Scheffer, L. K., Xu, C. S., Januszewski, M., Lu, Z., Takemura, S. Y., Hayworth, K. J., ... & Plaza, S. M. (2020). A connectome and analysis of the adult Drosophila central brain. *Elife*, *9*, e57443.

Seltenrich, N. (2015). Between extremes: health effects of heat and cold. *Environmental Health Perspectives,* 123(11), A275–A280.

Shearin, H. K., Quinn, C. D., Mackin, R. D., Macdonald, I. S., & Stowers, R. S. (2018). t-GRASP, a targeted GRASP for assessing neuronal connectivity. *Journal of Neuroscience Methods*, *306*, 94-102.

Snell, N. J., Fisher, J. D., Hartmann, G. G., Zolyomi, B., Talay, M., & Barnea, G. (2022). Complex representation of taste quality by second-order gustatory neurons in Drosophila. *Current Biology*, *32*(17), 3758-3772.

Sorkaç, A., Savva, Y. A., Savaş, D., Talay, M., & Barnea, G. (2022). Circuit analysis reveals a neural pathway for light avoidance in Drosophila larvae. *Nature Communications*, *13*(1), 5274.

Takayanagi-Kiya, S., & Kiya, T. (2019). Activity-dependent visualization and control of neural circuits for courtship behavior in the fly Drosophila melanogaster. *Proceedings of the National Academy of Sciences*, *116*(12), 5715-5720.

Talay, M., Richman, E. B., Snell, N. J., Hartmann, G. G., Fisher, J. D., Sorkaç, A., ... & Barnea, G. (2017). Transsynaptic mapping of second-order taste neurons in flies by trans-Tango. *Neuron*, 96(4), 783-795.

Thau, L., Reddy, V., & Singh, P. (2019). Anatomy, Central Nervous System.

Tuthill, J. C., & Wilson, R. I. (2016). Parallel transformation of tactile signals in central circuits of Drosophila. *Cell*, *164*(5), 1046-1059.

Vajente, N., Norante, R., Pizzo, P., & Pendin, D. (2020). Calcium imaging in drosophila melanogaster. *Calcium Signaling*, 881-900.

Venken, K. J., Simpson, J. H., & Bellen, H. J. (2011). Genetic manipulation of genes and cells in the nervous system of the fruit fly. *Neuron*, *72*(2), 202-230.

Wang, G., Qiu, Y. T., Lu, T., Kwon, H. W., Jason Pitts, R., Van Loon, J. J., ... & Zwiebel, L. J. (2009). Anopheles gambiae TRPA1 is a heat-activated channel expressed in

thermosensitive sensilla of female antennae. *European Journal of Neuroscience*, 30(6), 967-974.

Werner, C. T., Williams, C. J., Fermelia, M. R., Lin, D. T., & Li, Y. (2019). Circuit mechanisms of neurodegenerative diseases: a new frontier with miniature fluorescence microscopy. *Frontiers in neuroscience*, *13*, 1174.

White, B. H. (2016). What genetic model organisms offer the study of behavior and neural circuits. *Journal of neurogenetics*, *30*(2), 54-61.

Wilson, R. I., & Laurent, G. (2005). Role of GABAergic inhibition in shaping odor-evoked spatiotemporal patterns in the Drosophila antennal lobe. *Journal of Neuroscience*, *25*(40), 9069-9079.

Yamagata, M., & Sanes, J. R. (2012). Transgenic strategy for identifying synaptic connections in mice by fluorescence complementation (GRASP). *Frontiers in molecular neuroscience*, 5, 18.

Zheng, Z., Lauritzen, J. S., Perlman, E., Robinson, C. G., Nichols, M., Milkie, D., ... & Bock, D. D. (2018). A complete electron microscopy volume of the brain of adult Drosophila melanogaster. *Cell*, *174*(3), 730-743.

APPENDIX A

Below is the manuscript in submission for the paper detailing the creation and investigation of FLIPSOT.

Functional labeling of individualized postsynaptic neurons using optogenetics and *trans*-Tango

Allison N. Castaneda, Ainul Huda, Iona B.M. Whitaker, Julianne E. Reilly, Grace S. Shelby, Hua Bai, Lina Ni

Title

Functional labeling of individualized postsynaptic neurons using optogenetics and *trans*-Tango

Summary

A population of neurons interconnected by synapses constitutes a neural circuit, which performs specific functions upon activation. It is essential to identify both anatomical and functional entities of neural circuits to comprehend the components and processes necessary for healthy brain function and the changes that characterize brain disorders. To date, few methods are available to study these two aspects of a neural circuit simultaneously. In this study, we developed FLIPSOT, or functional labeling of individualized postsynaptic neurons using optogenetics and *trans*-Tango. FLIPSOT uses (1) *trans*-Tango accessing postsynaptic neurons genetically, (2) optogenetic approaches activating (FLIPSOTa) or inhibiting (FLIPSOTi) postsynaptic neurons in a random and sparse manner, and (3) fluorescence markers tagged with optogenetic genes visualizing these neurons. Therefore, FLIPSOT allows using a presynaptic driver to identify the behavioral function of individual postsynaptic neurons. It is readily applied to identify functions of individual postsynaptic neurons in many other fruit fly neural circuits and has the potential to be adapted for use in mammalian circuits.

Keywords

FLIPSOT, optogenetics, GtACR, CsChrimson, FLP/FRT, *trans*-Tango, *Drosophila,* thermotaxis, heating cells, projection neurons

Introduction

A population of neurons that are interconnected by synapses constitutes a neural circuit, which performs specific functions upon activation[1]. Neural circuits are the fundamental framework for all brain activities, such as processing perception and cognition and coordinating behavior. Impairments in neural circuits can lead to a wide range of neurodegenerative and psychiatric disorders[2-4]. Therefore, it is essential to identify both anatomical and functional entities of neural circuits to comprehend the components and processes necessary for healthy brain function and the changes that characterize brain disorders.

Drosophila melanogaster is an attractive model to study the circuit basis of animal behavior because of its relatively small nervous system, sophisticated and robust behaviors, and extensive collections of genetic reagents to label and manipulate various classes of neurons[5]. Multiple techniques have been developed to investigate *Drosophila* neural circuits, including serial-section electron microscopy (EM)[6-8], paired-recording[9,10], photoactivatable GFP (PA-GFP)[11-17], and calcium imaging[6,18]. Each method has its own advantage. EM and PA-GFP can indicate synaptic connections and identify the morphology of potential postsynaptic neurons. Calcium imaging and paired recording provide information on functional connections between neurons. However, none of these techniques simultaneously track the synaptic connections and evaluate the functional relevance of individual neurons in a circuit.

GFP Reconstitution Across Synaptic Partners (GRASP) is a well-established genetic transsynaptic tool labeling synapses based on the proximity of pre- and postsynaptic plasma membranes. GRASP allows for visualization of synaptic connection and activity between two neurons by light microscopy but requires driver lines of both pre- and postsynaptic neurons[19-27]. Recently, new genetic transsynaptic tools, including *trans*-Tango[28], TRACT (TRAnsneuronal Control of Transcription)[29], and BAcTrace (Botulinum-Activated Tracer)[30], have been developed. Unlike GRASP, these methods rely on only one driver to label and provide genetic access to synaptic partners. Among them, *trans*-Tango is the most widely used tool for labeling synaptic partners in various *Drosophila* neural circuits[31]. The design of *trans*-Tango is based on the Tango assay, which converts transient interaction between G protein-coupled receptors (GPCRs) and their ligands to a more stable readout[28,32]. The GAL4 drives the expression of the *trans*-Tango ligand in presynaptic neurons, which binds to and activates the *trans*-Tango receptor (a GPCR) on postsynaptic membranes. The activated *trans*-Tango receptor, in turn, recruits β-arrestin2 linked to a protease. The protease releases QF from the *trans*-Tango receptor. QF then translocates to nuclei and expresses a reporter to visualize postsynaptic neurons. While optogenetic and calcium imaging techniques have been combined with *trans*-Tango to investigate the functional connectivity between pre- and

postsynaptic neurons[33-36], these approaches cannot determine the behavioral importance of individual postsynaptic neurons.

Heating cells (HCs) are peripheral warm receptors located in the arista and are activated at about 25°C[37,38]. They guide animals to avoid warm temperature rapidly when exposed to a steep gradient[37,39,40]. HCs project their axonal termini to VP2, a glomerulus of the antennal lobe (AL) in the brain[41,42]. The postsynaptic neurons of HCs consist of projection neurons (PNs) and local interneurons (LNs). PNs are the output cells of the AL. EM tracing has identified four tracts of projection neurons (PNs) from VP2: a medial AL tract (mALT), a mediolateral AL tract (mlALT), a transversal AL tract (tALT), and a lateral AL tract (lALT)[43]. The mALT comprises at least 14 PNs, while lALT includes five PNs, and mlALT and tALT each contains one PN[43]. Based on the similarity in morphology between the EM data and studies using PA-GFP, driver lines, or dye injected by the electrophysiological pipettes, the function of some PNs has been identified. One or more mALT PNs respond to warm and cool temperatures and are necessary for rapid warm and cool avoidance behavior[17,43]. A single mlALT PN also responds to both warm and cold, while one lALT PN responds exclusively to warm[43,44]. The tALT is a novel tract with unknown functions[43]. Due to the lack of direct genetic access to postsynaptic neurons by a presynaptic driver, it is challenging to comprehensively understand the behavioral importance of each PN in response to temperature changes.

In this study, the HC-controlled circuit was used as a model to develop this tool. Single-fly thermotactic and optogenetic assays were set up to define the behavioral function of HCs and their circuit. Optogenetic genes tagged with fluorescence markers were inserted downstream of an FRT-stop-FRT cassette to modulate neuronal activity in a random and sparse manner. Then, we combined *UAS-trans-Tango*, *hs-FLP*, *QUAS-mtdTomato-HA,* and *QUAS-FRT-stop-FRT-GtACR2.EYFP* (*FLIPSOTi*) to identify HC PNs necessary for rapid warm avoidance. Similarly, *UAS-trans-Tango*, *hs-FLP*, *QUAS-mCD8-GFP,* and *QUAS-FRT-stop-FRT-CsChrimson.mCherry* were combined to create *FLIPSOTa* to determine HC PNs sufficient for avoidance. FLIPSOT is readily applied to identify functions of individual postsynaptic neurons in many other fruit fly neural circuits and has the potential to be adapted for use in mammalian circuits.

Results

The design of FLIPSOT

To generate a genetic tool that uses a presynaptic driver to label and manipulate postsynaptic neurons randomly and sparsely, we incorporate the following genetic components in FLIPSOT (Figure 1A). The *trans*-Tango allows for the genetic access of postsynaptic neurons by a

presynaptic driver[28]. The *QUAS-reporter*, controlled by *trans*-Tango, enables the visualization of postsynaptic neurons (Figure 1B). Optogenetic tools were used to manipulate the activity of postsynaptic neurons. Two versions of FLIPSOT have been created: FLIPSOTa, which activates postsynaptic neurons and contains *QUAS-FRT-stop-FRT-CsChrimson.mCherry,* and FLIPSOTi, which inhibits the activation of postsynaptic neurons and has *QUAS-FRT-stop-FRT-GtACR2.EYFP.* Both CsChrimson[45] and GtACR2[46-48] are channelrhodopsins (ChRs). CsChrimson is activated by red light to depolarize cells. GtACR2 is activated by blue light to hyperpolarize cells. Fluorescence markers (mCherry and EYFP) are tagged to ChRs to visualize postsynaptic neurons expressing ChRs. ChRs are downstream of a QUAS sequence to enable *trans*-Tango to control the expression of postsynaptic ChRs. An FRT-stop-FRT cassette is inserted between QUAS and ChRs[49]. The stop sequence blocks ChR expression without a FLP recombinase[50]. When heat shock is applied, FLP removes the stop sequence in some, but not all, postsynaptic neurons, allowing random and sparse postsynaptic neurons to express ChRs and the tagged fluorescence markers (Figure 1C).

Single-fly thermotactic and optogenetic assays

Single-fly behavioral assays are required to use FLIPSOT to analyze the behavioral roles of individual postsynaptic neurons. In this study, we used rapid warm avoidance as a model to test FLIPSOT[51] (Figure 2A). Briefly, a single fly was acclimated under a transparent cover (2 mm (height) X 58 mm (width) X 83 mm (length)) for 15-25 seconds. Then, it was allowed to choose between 25°C and 31°C for one minute. The preference index (PI) was calculated. All tested genotypes with intact aristae avoided 31°C (Figure 2B). Neither fly genders nor the exchange of temperature sides affected warm avoidance (Figure S1). Importantly, *wild-type* flies with both aristae ablated did not exhibit a preference between 25 and 31°C, while flies with single aristae ablated avoided 31°C, indicating one arista is sufficient to drive warm avoidance (Figure 2B).

Then, we set up single-fly optogenetic assays to test whether GtACR2 and CsChrimson could suppress and activate the neural circuit controlling rapid warm avoidance, respectively. Either GtACR2 or CsChrimson was expressed in HCs by *HC-Gal4*. A blue light was used to replace the regular ambient room light to activate GtACR2 (Figure 2C). Similarly, a single fly was acclimated for 15-25 seconds before being given a choice between 25 and 31°C for one minute under blue light. Flies expressing GtACR2 in HCs failed to avoid 31°C, suggesting HCs are necessary for rapid warm avoidance (Figure 2D).

A red light was used to activate CsChrimson (Figure 2E). In this assay, flies were not exposed to different temperatures. The cover was created with two opposing transparent quadrants and two light-impermeable quadrants. The red light illuminated the cover from

above. When flies passed the transparent quadrants, CsChrimson was activated by red light. The fly was given one min to choose between dark and red-light quadrants. Control flies did not show a preference between dark and red-light quadrants. However, flies expressing CsChrimson in HCs significantly preferred dark quadrants, demonstrating that activation of HCs is sufficient to drive avoidance of red light (Figure 2F).

HCs connect to four tracts of PNs

Next, we used *HC-Gal4* to drive *trans*-Tango and label postsynaptic neurons of HCs. Projections of *HC-Gal4*-positive neurons in the brain were observed in the VP2 glomerulus of the antennal lobe (AL), the subesophageal zone (SEZ), and the fan-shaped body (FB) (Figure 3A). Besides local interneurons (LNs) in the AL and SEZ, four tracts of PNs from the AL were observed: mALT, mlALT, tALT, and lALT. These PNs were arborated in the mushroom body (MB), lateral horn (LH), and posterior lateral protocerebrum (PLP). Postsynaptic neurons were also observed in the superior medial protocerebrum (SMP). GR28B(D) is the warm sensor in HCs[37]. Flies using *Gr28b.d-Gal4* to drive *trans*-Tango exhibited similar patterns of pre- and postsynaptic neurons (Figure S2).

The ablation of one arista diminished the projections of *HC-Gal4* positive neurons in VP2 but did not affect those in the SEZ and FB (Figure 3B). In the AL, the mtdTomato expression was decreased significantly on the side the arista was removed, and PNs were not detectable. However, the postsynaptic labeling in the SEZ and SMP was not affected. These findings suggested that HCs project to VP2 and synaptically connect to PNs and LNs in the AL. Since PNs send information to higher-level brain regions, along with the behavioral analysis of flies with one arista ablated (Figure 2B), we concluded that single-side PNs are sufficient for guiding warm avoidance behavior.

Random and sparse labeling

We created two transgenic fly lines: *QUAS-FRT-stop-FRT-GtACR2.EYFP* for FLIPSOTi and *QUAS-FRT-stop-FRT-CsChrimson.mCherry* for FLIPSOTa to modulate the activity of individual postsynaptic neurons. GtACR2 and CsChrimson were cloned downstream of QUAS to allow *trans*-Tango to control their expression. To achieve the modulation in a random and sparse fashion, we inserted an FRT-stop-FRT cassette between QUAS and optogenetic genes. Fluorescence tags, EYFP and mCherry, were added at the C termini of optogenetic genes to enable the visualization of the neurons expressing GtACR2 and CsChrimson, respectively.

We used *Ir21a-QF2w* to drive *QUAS-FRT-stop-FRT-GtACR2.EYFP* and *QUAS-FRT-stop-FRT-CsChrimson.mCherry* and expressed FLP using a heat shock promoter. *Ir21a-QF2w* labels three neurons in each dorsal organ ganglion in fly larvae (Figure S3). Heat shock allowed for FLP expression. In *Ir21a-QF2w* positive cells, the stop sequence was removed, and GtACR2.EYFP or CsChrimson.mCherry was expressed (Figure 4A, C). Since FLP was inadequate to trigger recombination in all cells, each dorsal organ ganglion (DOG) might have zero, one, two, or three cells expressing EYFP or mCherry (Figure 4A, C). The expression ratio of fluorescence markers and heat shock duration were correlated. Elongation of heat shock increased the expression ratio (Figure 4B, D). Heat shock also randomly removed the stop sequence between two FRT sites in adult HCs (Figure S4). These results suggested that managing heat shock duration enables the random and sparse expression of GtACR2.EYFP or CsChrimson.mCherry. In the following experiments, we applied 30 min heat shock to achieve the sparse expression of GtACR2.EYFP and CsChrimson.mCherry.

Necessary and sufficient PNs for rapid warm avoidance

Finally, we combined *UAS-trans-Tango*, *hs-FLP*, *QUAS-mtdTomato-HA,* and *QUAS-FRT-stop-FRT-GtACR2.EYFP* to generate *FLIPSOTi*. Similarly, *UAS-trans-Tango*, *hs-FLP*, *QUAS-mCD8-GFP,* and *QUAS-FRT-stop-FRT-GtACR2.EYFP* were combined to create *FLIPSOTa*. *FLIPSOTi* and *FLIPSOTa* were designed to determine individual postsynaptic neurons that were necessary and sufficient, respectively, to transduce information for the behaviors controlled by presynaptic neurons.

HCs are necessary and sufficient to guide rapid warm avoidance[37,40,51]. We first used *HC-Gal4* to express *FLIPSOTi* to identify individual PNs necessary for rapid warm avoidance (Figure 5A). Newly eclosed flies were exposed to 35°C for 30 min and then kept at 18°C for about ten days. ATR was supplemented with food two days before behavioral tests. Single-fly rapid warm avoidance assays were conducted under regular ambient room light and blue light. Flies that had normal avoidance in room light and diminished avoidance in blue light were collected (Figure 5B and S5A). Fly brains were dissected, and PNs expressing GtACR2.EYFP were identified. In *FLIPSOTi, QUAS-mtdTomato-HA* was used as a control to visualize postsynaptic neurons. Four tracts of PNs were observed on each side (magenta). In Figure 5C, the mALT was the only tract expressing GtACR2.EYFP (green) in the left brain, while both mALT and lALT expressed GtACR2.EYFP in the right brain. In Figure 5D, the left mlALT did not express GtACR2.EYFP. In the right brain, all four tracts were visible by EYFP. However, EYFP signals in the mlALT and tALT were faint compared to mtdTomato, and thus the mlALT and tALT were considered to lack GtACR2.EYFP. We analyzed 29 brains, all of

which expressed the mALT on both sides (Figure 5E), suggesting mALT from VP2 is necessary to transduce information for rapid warm avoidance.

Then, we crossed *HC-Gal4* with *FLIPSOTa* to identify the individual PNs sufficient for rapid warm avoidance (Figure 6A). In this case, we gave flies 21 days to develop *trans*-Tango. The single-fly rapid warm avoidance assay was conducted to select flies with normal warm avoidance. A slight but significant decrease preference observed in *HC>FLIPSOTa* was due to the fly age (Figure S5B). Then, the red light avoidance assay was performed, and flies with strong red light avoidance were collected (Figure 6B). In *FLIPSOTa, QUAS-mCD8-GFP* served as a control to visualize postsynaptic neurons. Four tracts of PNs were observed on each side (green). In Figure 6C, the left mlALT did not express CsChrimson.mCherry (magenta), while the right mlALT only showed faint CsChrimson.mCherry. In Figure 6D, the left mlALT was absent of CsChrimson.mCherry, and the lALT had faint CsChrimson.mCherry. In the right brain, all four tracts expressed CsChrimson.mCherry. We analyzed 29 brains of *HC>FLIPSOTa*, all of which had at least one tALT expressing CsChrimson.mCherry (Figure 6E), indicating that the tALT is sufficient for driving rapid warm avoidance.

Discussion

FLIPSOT relies on a presynaptic driver to identify the behavioral function of individual postsynaptic neurons. FLIPSOT uses (1) *trans*-Tango accessing postsynaptic neurons genetically, (2) optogenetic approaches activating (FLIPSOTa) or inhibiting (FLIPSOTi) postsynaptic neurons in a random and sparse manner, and (3) fluorescence markers tagged with optogenetic genes visualizing these neurons. As long as a single-fly behavioral assay is available to reflect the function of presynaptic neurons, FLIPSOT is readily applied to identify functions of individual postsynaptic neurons in many other fruit fly neural circuits. It also has the potential to be adapted for use in mammalian circuits.

Many methods depend on the similarity in morphology to identify postsynaptic drivers[40,43,44]. However, the same neuron may have different morphologies in different flies, even between two sides of a single brain. For example, two mlALTs in Figure 3A exhibit different morphologies. Moreover, when the neurons are packed heavily, and multiple neurons have similar morphologies, relying on morphology to determine postsynaptic drivers becomes impracticable, and validation of direct synaptic interaction is not trivial. Therefore, this approach is challenging to investigate the function of postsynaptic neurons comprehensively. FLIPSOT adopts *trans*-Tango, which provides genetic access to postsynaptic neurons using a presynaptic driver. Importantly, *HC>trans-Tango* labels all four tracts of HCs postsynaptic neurons identified by EM tracing[43] (Figure 3A). Among these four tracts, FLIPSOTi demonstrates that the mALT is necessary to drive rapid warm avoidance (Figure 5), consistent

with a previous report[17]. The tALT is a novel PN with unknown functions[43]. FLIPSOTa suggests that activation of the tALT is sufficient to drive avoidance (Figure 6). Easy and comprehensive access to postsynaptic neurons makes it possible to use FLIPSOT investigating the function of individual postsynaptic neurons.

In FLIPSOT, *trans*-Tango controls an optogenetic tool and a reporter. This reporter labels all postsynaptic neurons and thus serves as an internal control to determine the neurons expressing optogenetic genes. Even though both reporters and fluorescence markers can be observed under confocal microscopy, we suggest using immunohistochemistry to enhance their signals and limit some false-positive noise.

FLIPSOT causes leaky expression of optogenetic genes and their tagged fluorescence markers. Even without heat shock, the AL is strongly fluorescent. In some brains, PNs also have fluorescence signals. This leaky expression makes FLIPSOT unable to differentiate LNs. Moreover, the strong expression of optogenetic genes in the AL may have indirect impacts on behavior and weaken the argument of the behavioral function of PNs. Since the arboration of PNs in the AL and their target regions is a critical criterion for identifying different PNs in the same tract, the leaky expression limits our ability to distinguish different PNs.

The leaky expression can be from *trans*-Tango[28]. A new version of *trans*-Tango with less background noise is needed, and adoption of this new version in FLIPSOT might reduce the leaky expression. The second source of leaky expression is trace amounts of FLP. Although the leaky expression is not observed in larval *Ir21a-QF2w* positive cells (Figure 4A, C), the long period for developing *trans*-Tango (10-21 days) may accumulate FLP, resulting in its expression sufficient to remove the stop sequence from the FRT-stop-FRT cassette in some cells. Raising flies in lower temperatures may limit the FLP amount. Moreover, the leaky expression may be because the stop sequence from the FRT-stop-FRT cassette is skipped, and thus downstream optogenetic tools and their tagged fluorescence markers are transcribed, which can be resolved using an alternative or additional stop sequence.

In the future, besides solving the leaky problem, we will generate a new FLIPSOT variant expressing both inhibitory and activatable optogenetic tools to test necessity and sufficiency in the same flies. Expression of both GtACR2 and CsChrimson in HCs leads to inhibition of HCs by blue light and activation of HCs in red light (Figure S6). Moreover, the combination of a genetic calcium indicator and optogenetic tools may help understand the physiological responses of the individual postsynaptic neurons in response to environmental stimuli.

Materials and Methods:

***Drosophila* strains**

The *wild-type* control used for all behavioral assays was *w*^{1118}. *UAS-GtACR2*[47], *HC-Gal4*[40], *Gr28b.d-Gal4*[52], *UAS-CsChrimson*[45] (RRID:BDSC_55135 and 55136), *hs-FLP*[53] (RRID:BDSC_6938), *UAS-FRT-stop-FRT-GFP*[54] (RRID:BDSC_30032), *QUAS-mCD8-GFP*[55] (RRID:BDSC_30002), *QUAS-mtdTomato-HA*[55] (RRID:BDSC_30004), *QUAS-GCaMP3* (RRID:BDSC_65684), and *UAS-trans-Tango*[28] (RRID:BDSC_77123 and 77124) were previously described.

To create the *QUAS-FRT-stop-FRT-CsChrimson.mCherry* and *QUAS-FRT-stop-FRT-GtACR2.EYFP* lines, the *FRT-stop-FRT* sequence[49] (Addgene plasmid #64716) was cloned into the *pQUAST-attB* (RRID:DGRC_1438) vector. Then, either the *CsChrimson.mCherry*[45] (Addgene plasmid #111547) sequence or the *GtACR2.EYFP*[48] (Addgene plasmid #67877) sequence was cloned into the vector. The final constructs were integrated into attP2[56] (RRID:DGRC_8622).

Ir21a-QF2w was created by removing the *synaptobrevin* promoter and subcloning the *Ir21a* promoter region into *pattB-synaptobrevin-QF2w-hsp70*[57,58] (Addgene plasmid #46116). The construct was also integrated into attP40[56] (RRID:DGRC_8622).

Single-fly rapid warm avoidance assay and optogenetic assay

Flies were maintained at about a 12:12 hour light:dark cycle at 22°C (or 18°C for *trans*-Tango development). All behavioral experiments were performed between 2 pm to 10 pm. Two days before behavioral experiments, flies were placed in the dark on food supplemented 40 μM ATR (Sigma-Aldrich).

The rapid warm avoidance assay was performed in a behavioral room, in which the temperature was set at 25°C. Two steel plates were used to set up the temperature gradience. One steel plate was placed on top of a hot plate, and the other one was lifted up to align with the first steel plate. A sheet protector was taped on top. The hot plate temperature was adjusted so that the surface of the steel plate was about 31°C. A single fly was placed under a plastic cover (2 mm (height) X 58 mm (width) X 83 mm (length)) and allowed to acclimate for 15-25 seconds. Flies were moved to 25°C to start the behavior. The position of the fly was recorded every five seconds for one minute. Flies that did not move for over 30 seconds were discarded. A desk lamp (room light) (~22 lux) was used to illuminate the rapid warm avoidance

assay. A blue light source (~20 klux) was built[59] to activate GtACR2. The preference index (PI) was calculated using the following formula:

$$\mathrm{PI} = \frac{(\text{time point number in } 25°\mathrm{C}) - (\text{time point number in } 31°\mathrm{C})}{\text{total time point number}}$$

Red light optogenetic assays were conducted at 25ºC. The base of the experiment was a sheet protector overlaid on a black background. Flies were placed on the sheet protector under a plastic cover with two opposing transparent quadrants and two light-impermeable quadrants. The red light illuminated the cover from the top. Flies were given ten seconds to acclimate, and all experiments started with flies in one of the visible quadrants. Flies that did not move for more than 30 seconds were discarded. The red light source (32 klux) was previously described[59]. The preference index (PI) was calculated using the following formula:

$$\mathrm{PI} = \frac{(\text{time point number in the "dark"}) - (\text{time point number in red light})}{\text{total time point number}}$$

Brain dissection and immunostaining

Brains were dissected using forceps (FST 11413-11) in 1X PBS and then transferred to PBS on ice. Immunohistochemistry was performed as previously described with some modifications[59]. Brains were fixed in 1XPBS with 4% paraformaldehyde for 30 min. After washing three times (5 min each) in PBST (1XPBS with 0.5% Triton-100), antigen retrieval was performed by incubating brains in 1XPBS with 0.1% SDS and 20% H_2O_2 for 30 min. Next, brains were washed three times in PBST (5 min each), blocked in 10% NGS for one hour, and incubated in the primary antibody solution for three days. After washing overnight in PBST, brains were transferred to the secondary antibody solution overnight and then washed in PBST overnight. Samples were mounted using Vectashield Mounting Medium (VECTASHIELD) and imaged using a Nikon A1 Confocal Microscope. Primary antibodies used were rabbit anti-dsRed (1:200, Takara Bio), rabbit anti-GFP (1:500, Invitrogen), mouse anti-GFP (1:500, Sigma-Aldrich), and mouse anti-HA (1:200, Invitrogen)**.** Secondary antibodies included goat anti-rabbit Cy3 (1:250, Jackson Immuno), goat anti-rabbit Alexa Fluor 488 (1:250, Jackson Immuno), goat anti-mouse CF488A (1:250, Sigma-Aldrich), and goat anti-mouse TRITC (1:250, Invitrogen)**.**

Statistical Analysis

Statistical details of experiments were mentioned in the figure legends. The normality of distributions was assessed by the Shapiro-Wilk W test ($p \leq 0.05$ rejected normal distribution).

Statistical comparisons were performed by the Mann-Whitney test or Kruskal-Wallis test. Data analysis was conducted using GraphPad Prism 9.

Acknowledgments

This work was supported by the National Institutes of Health (R21MH122987 to L.N. and R01GM140130 to L.N.).

Author contributions

Conceptualization, A.N.C. and L.N.; Methodology, A.N.C. and L.N.; Investigation, A.N.C., A.H., I.B.M.W., J.E.R., G.S.S., H.B., and L.N.; Writing – Original Draft, A.N.C. and L.N.; Writing – Review & Editing, A.N.C., A.H., I.B.M.W., J.E.R., G.S.S., and L.N.; Funding Acquisition, L.N.; Resources, L.N.; Supervision, L.N..

Declaration of interests

The authors declare no competing interests.

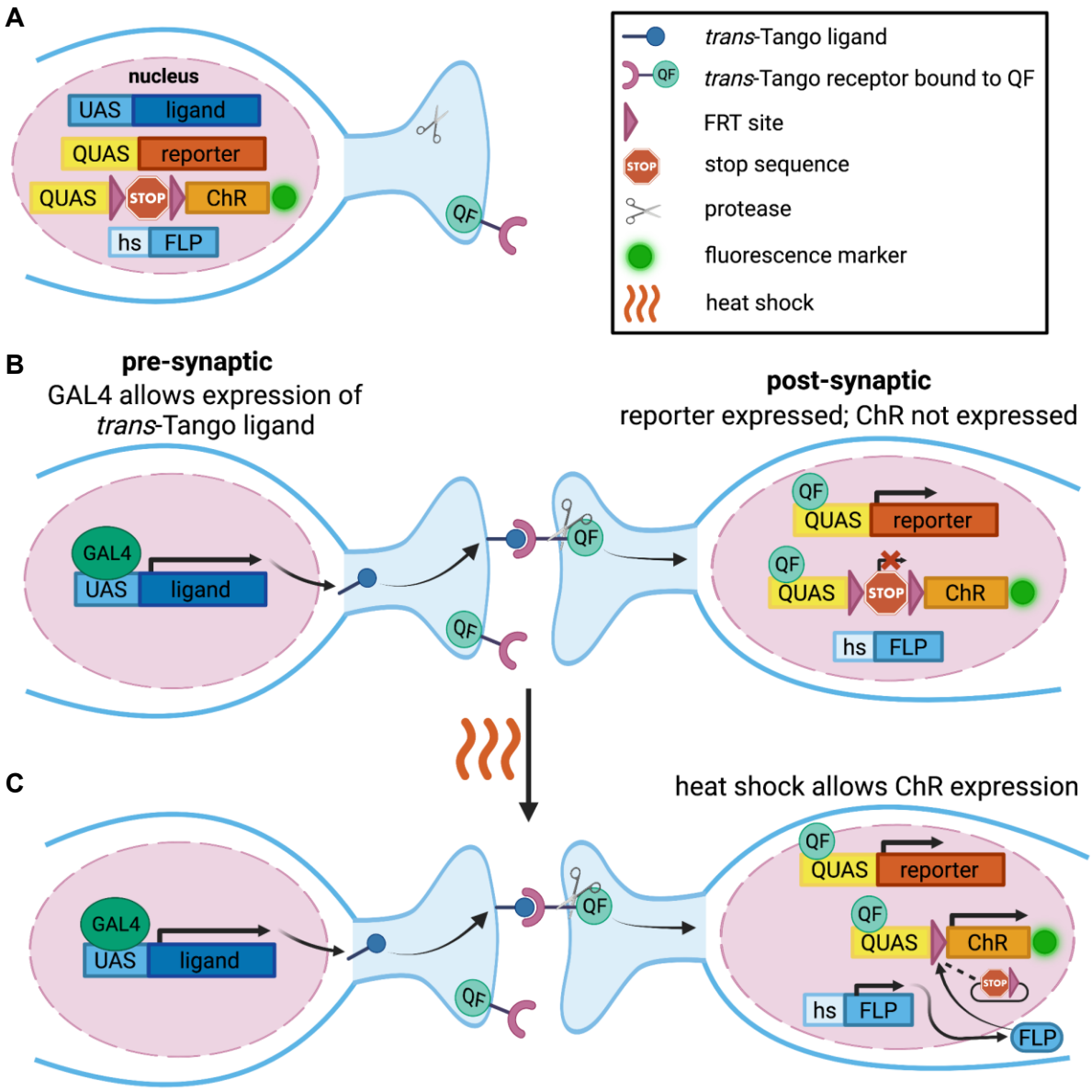

Figure 1. Schematic design of FLIPSOT.

(A) Genetic components in FLIPSOT include a *trans*-Tango ligand, *trans*-Tango receptor bound to QF, protease, FLP, fluorescence reporter, and optogenetic tool (ChR) tagged with a fluorescence marker. The *trans*-Tango ligand is downstream of a UAS sequence, a binding site of the transcription activator GAL4. Both the *trans*-Tango receptor and protease are pan-neuronally expressed. When the ligand binds to the receptor on synaptically connected neurons, the protease is recruited to release the transcription activator QF from the *trans*-Tango receptor in postsynaptic neurons. The reporter is downstream of a QUAS sequence, a binding site of QF. Heat shock permits the expression of FLP. The optogenetic gene is under the control of QUAS and an FRT-stop-FRT cassette, so both QF and FLP must translocate to nuclei to allow its expression, which is visualized by a tagged

fluorescence protein.
(B,C) A presynaptic GAL4 drives the expression of the *trans*-Tango ligand in presynaptic neurons. The ligand binds to *the trans*-Tango receptor on synaptically connected neurons and releases QF. QF translocates to nuclei to express the reporter. Although QF binds to the QUAS sequence upstream of the optogenetic gene, the optogenetic gene will not be expressed (B) until heat shock allows the expression of FLP, which removes the stop sequence from the FRT-stop-FRT cassette randomly to permit its expression (C).
This figure was created with BioRender.com

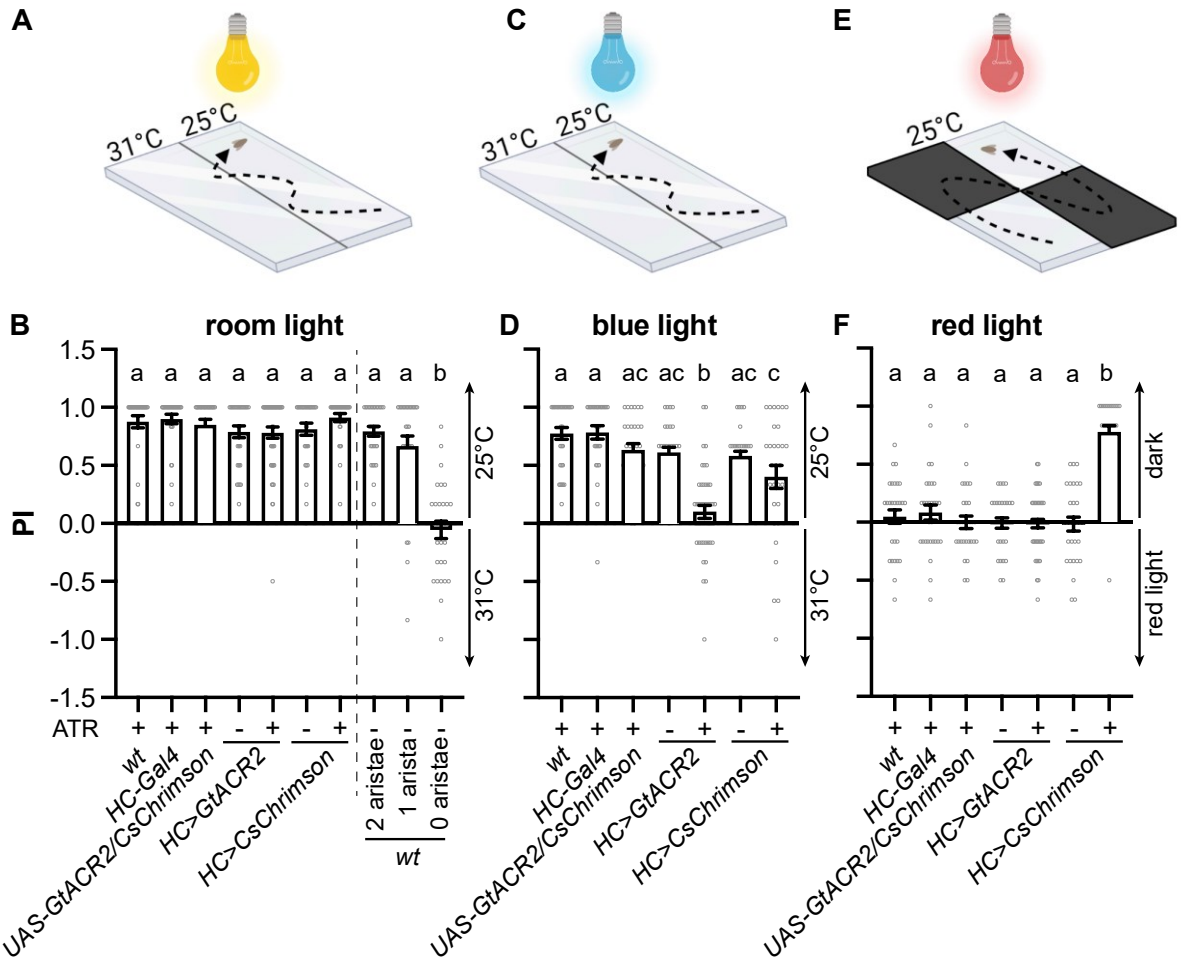

Figure 2. Single-fly thermotactic and optogenetic assays.
(A) Setup for the single-fly two-choice thermotactic assay under ambient light condition. Flies were given one minute to choose between 25 and 31°C (created with BioRender.com).
(B) PI of the indicated genotypes that were raised with (+) or without (-) dietary retinal (ATR).

n = 30-45; data represent means ± SEM; Kruskal-Wallis test followed by Dunn's multiple comparisons test; letters denote statistically distinct groups, $p < 0.05$. Genotypes: *HC>GtACR2* is *HC-Gal4;UAS-GtACR.EYFP; HC>CsChrimson* is *HC-Gal4;UAS-CsChrimson.mCherry*.

(C) Setup for the single-fly two-choice thermotactic assay under blue light condition. Flies were given one minute to choose between 25 and 31°C (created with BioRender.com).

(D) PI of the indicated genotypes that were raised with (+) or without (-) dietary retinal (ATR). *n* = 30-45; data represent means ± SEM; Kruskal-Wallis test followed by Dunn's multiple comparisons test; letters denote statistically distinct groups, $p < 0.05$.

(E) Setup for the single-fly optogenetic assay under red light condition. Flies were given one minute to choose between the dark and light environment (created with BioRender.com).

(F) PI of the indicated genotypes that were raised with (+) or without (-) dietary retinal (ATR). *n* = 30-45; data represent means ± SEM; Kruskal-Wallis test followed by Dunn's multiple comparisons test; letters denote statistically distinct groups, $p < 0.05$.

See also Figure S1.

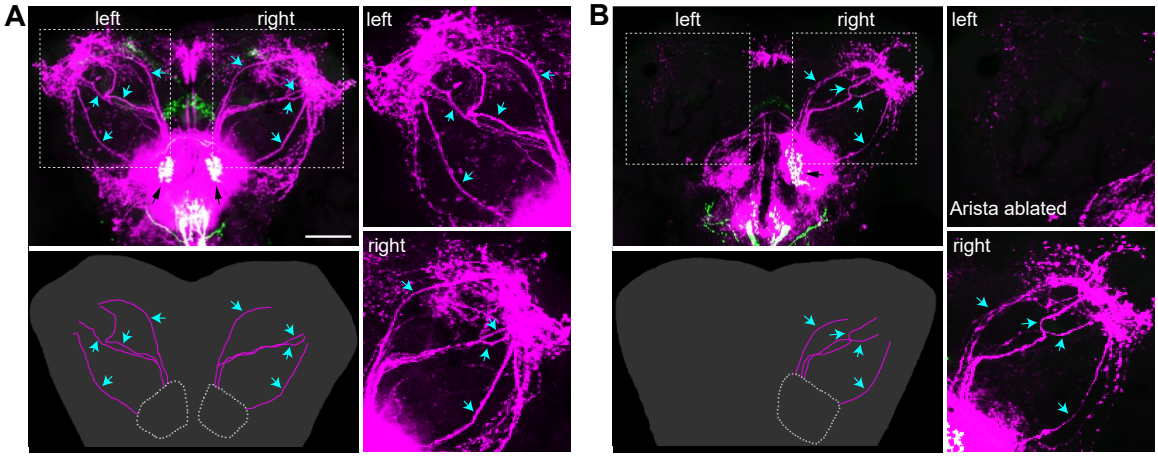

Figure 3. HCs connect to four tracts of PNs.

(A) In flies bearing *trans*-Tango components, driving ligands and GFP expressing in VP2 (black arrows) of the AL by *HC-Gal4* results in mtdTomato expression (magenta) in postsynaptic LNs and PNs (cyan arrows). Scale bar: 50 μm. Left lower panel: illustration of PNs; right upper panel: left PNs; right lower panel: right PNs.

(B) The ablation of the left arista results in the absence of the left PNs while leaving the right PNs (cyan arrows) unaffected. Left lower panel: illustration of PNs; right upper panel: left PNs; right lower panel: right PNs.

See also Figure S2.

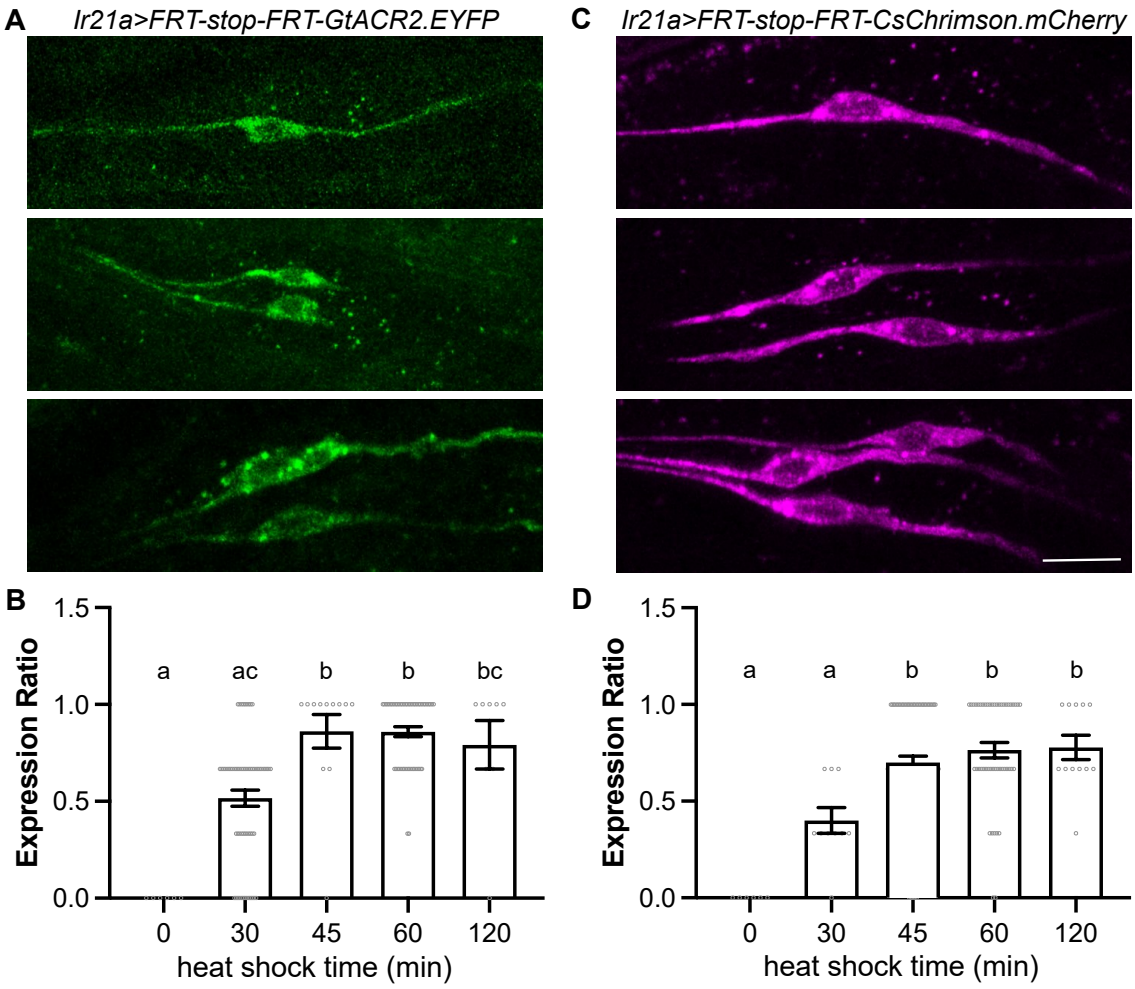

Figure 4. Heat shock removes the stop sequence from the FRT-stop-FRT cassette randomly.

(A) After heat shock, each DOG may contain zero, one (upper), two (middle), or three (lower) GtACR2.YFP-positive *Ir21a-QF2w*-labeled neurons. *Ir21a>FRT-stop-FRT-GtACR2.EYFP* is *Ir21a-QF2w,QUAS-FRT-stop-FRT-GtACR2.EYFP.* Scale bar: 10 μm.

(B) The percentage of GtACR2.YFP-positive *Ir21a-QF2w*-labeled neurons in each DOG after incubating larvae at 35°C for the indicated periods. n = 6-62; data represent means ± SEM; Kruskal-Wallis test followed by Dunn's multiple comparisons test; letters denote statistically distinct groups, $p < 0.05$.

(C) After heat shock, each DOG may contain zero, one (upper), two (middle), or three (lower) CsChrimson.mCherry-positive *Ir21a-QF2w*-labeled neurons. *Ir21a>FRT-stop-FRT-CsChrimson.mCherry* is *Ir21a-QF2w,QUAS-FRT-stop-FRT-CsChrimson.mCherry.* Scale bar: 10 μm.

(D) The percentage of CsChrimson.mCherry-positive *Ir21a-QF2w*-labeled neurons in each DOG after incubating larvae at 35°C for the indicated periods. n = 6-80; data represent

means ± SEM; Kruskal-Wallis test followed by Dunn's multiple comparisons test; letters denote statistically distinct groups, $p < 0.05$.
See also Figures S3 and S4.

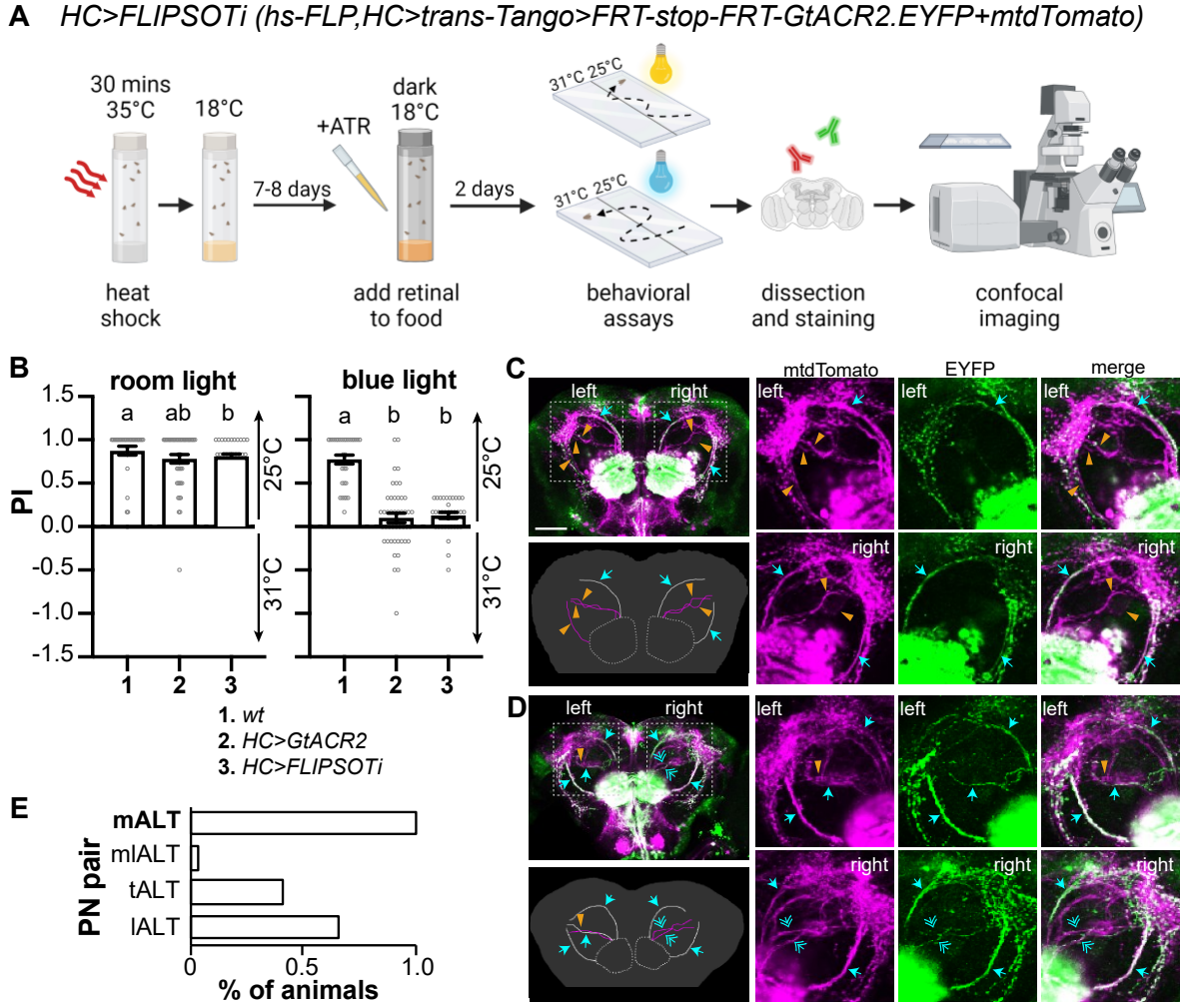

Figure 5. Identify PNs necessary to drive rapid warm avoidance.
(A) Schematic representation of identifying PNs necessary for the avoidance behavior. *FLISOTi* is *hs-FLP,UAS-trans-Tango,QUAS-FRT-stop-FRT-GtACR2.EYFP,QUAS-mtdTomato*. The pre-synaptic driver is *HC-Gal4* (created with BioRender.com).
(B) PI of the indicated genotypes to avoid 31°C under ambient room (left) or blue (right) light. Flies were raised with dietary retinal (ATR) in the dark for two days before experiments. n = 31-45; data represent means ± SEM; Kruskal-Wallis test followed by Dunn's multiple comparisons test; letters denote statistically distinct groups, $p < 0.05$.

(C,D) GtACR2.EYFP-positive HC PNs in flies not avoiding 31°C under blue light. Left upper panels: immunohistochemistry. Magenta: HA antibody to show all postsynaptic neurons of HCs, green: YFP antibody to indicate GtACR2.EYFP-positive postsynaptic neurons of HCs; cyan arrow: GtACR2.EYFP-positive PN, orange arrowhead: GtACR2.EYFP-negative PN; cyan double arrow: GtACR2.EYFP-weak PN; if the EYFP staining is much weaker than the HA staining, the PN is considered to lack GtACR2.EYFP. Scale bar: 50 µm. Left lower panels: illustration of PNs. White: GtACR2.EYFP-positive PN, magenta: GtACR2.EYFP-negative PN. Right three upper panels: left PNs; right three lower panels: right PNs. (C) Three PN tracts express GtACR2.EYFP (both mALTs and the right lALT). (D) Five PNs express GtACR2.EYFP (left: mALT, tALT, and lALT; right: mALT and lALT).
(E) The mALT PNs are necessary for rapid warm avoidance. We analyzed 29 brains, all of which expressed GtACR2.EYFP-positive mALT at both sides.
See also Figure S5.

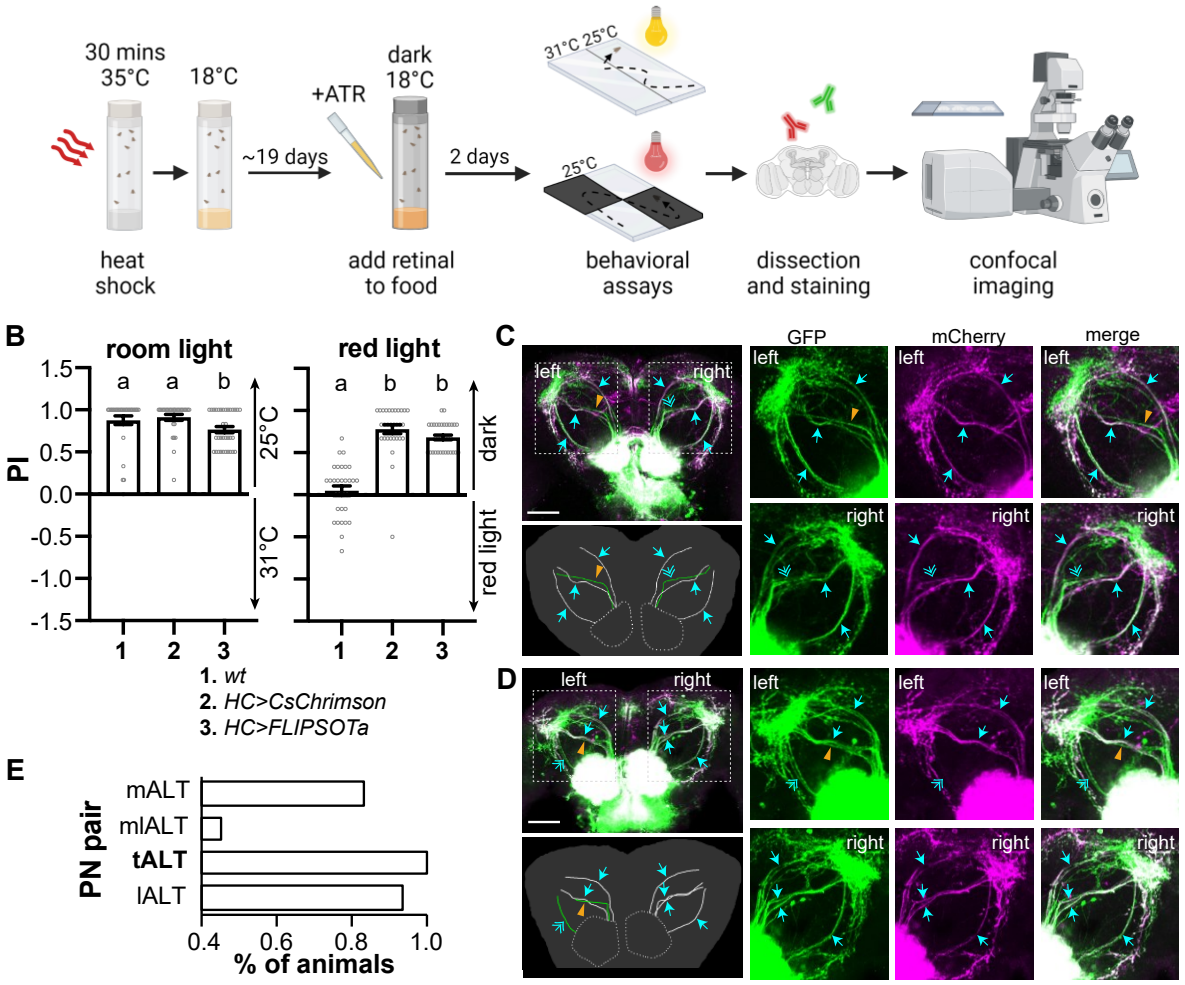

Figure 6. Identify PNs sufficient to drive avoidance.

(A) Schematic representation of identifying PNs sufficient for the avoidance behavior. FLISOTa is *hs-FLP,UAS-trans-Tango, QUAS-FRT-stop-FRT-CsChrimson.mCherry, QUAS-mCD8-GFP*. The pre-synaptic driver is *HC-Gal4* (created with BioRender.com).

(B) PI of the indicated genotypes to avoid 31°C (left) or red light (right). Flies were raised with dietary retinal (ATR) in the dark for two days before experiments. *n* = 29-45; data represent means ± SEM; Kruskal-Wallis test followed by Dunn's multiple comparisons test; letters denote statistically distinct groups, $p < 0.05$.

(C,D) CsChrimson.mCherry-positive HC PNs in flies avoiding red light. Left upper panels: immunohistochemistry. Green: GFP antibody to show all postsynaptic neurons of HCs, magenta: mCherry antibody to indicate CsChrimson.mCherry-positive postsynaptic neurons of HCs; cyan arrow: CsChrimson.mCherry-positive PN, orange arrowhead: CsChrimson.mCherry-negative PN, cyan double arrow: CsChrimson.mCherry-weak PN; if the mCherry staining is much weaker than the GFP staining, the PN is considered to lack CsChrimson.mCherry. Scale bar: 50 μm. Left lower panels: illustration of PNs. White:

CsChrimson.mCherry-positive PN, green: CsChrimson.mCherry-negative PN. Right three upper panels: left PNs; right three lower panels: right PNs. (C) Six PNs express CsChrimson.mCherry (both mALTs, tALTs, and lALT). (D) Six PNs express CsChrimson.mCherry (left: mALT and tALT; right: mALT, mlALT, tALT, and lALT). (E) The tALT is sufficient for the avoidance behavior. We analyzed 29 brains of *HC>FLIPSOTa*, all of which had at least one tALT expressing CsChrimson.mCherry. See also Figure S5.

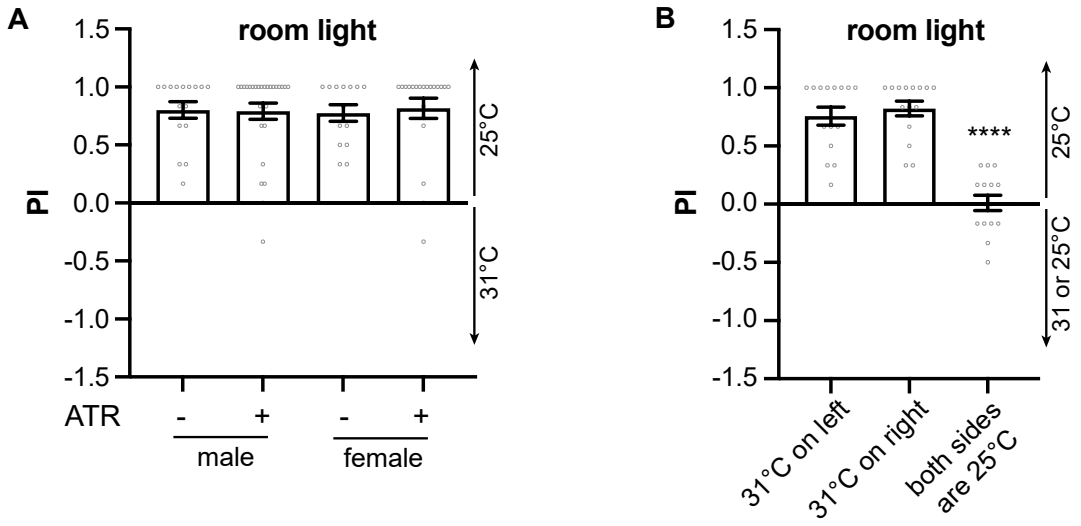

Figure S1. PI is not affected by fly gender, dietary retinal (ATR), or whether 31°C is on the left or right.

(A) PI of the indicated genders that were raised with (+) or without (-) dietary retinal (ATR). *n* = 14-28; data represent means ± SEM; Kruskal-Wallis test followed by Dunn's multiple comparisons test.

(B) PI from tests that 31°C was on the left, on the right or both sides were 25°C. *n* = 15; data represent means ± SEM; Kruskal-Wallis test followed by Dunn's multiple comparisons test; ****, $p < 0.0001$.

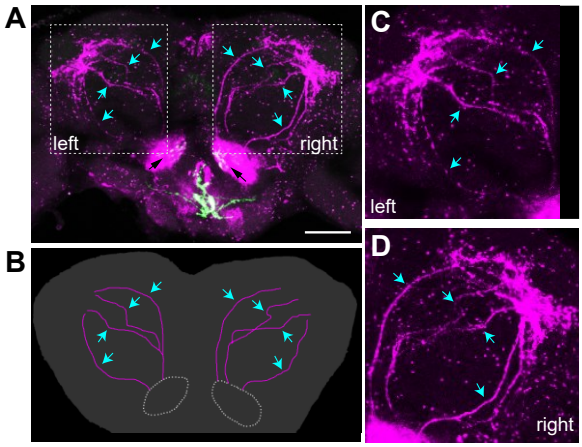

Figure S2. *Gr28b.d-Gal4* drives *trans*-Tango to label postsynaptic neurons of HCs.
(A) In flies bearing *trans*-Tango components, driving ligands and GFP expressing in VP2 (black arrow) of the AL by *Gr28b.d-Gal4* results in mtdTomato expression (magenta) in postsynaptic LNs and PNs (cyan arrow). Scale bar: 50 μm.
(B) Illustration of PNs.
(C) Left PNs.
(D) Right PNs.

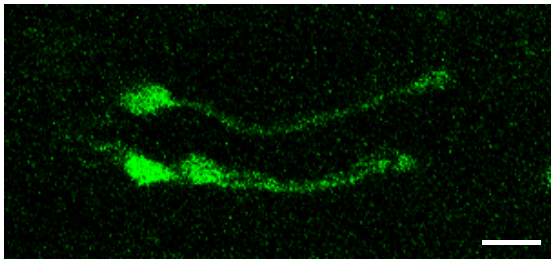

Figure S3. *Ir21a-QF2w* labels three neurons in each DOG. Genotype: *Ir21a-QF2w/QUAS-GCaMP3*. Scale bar: 10 μm.

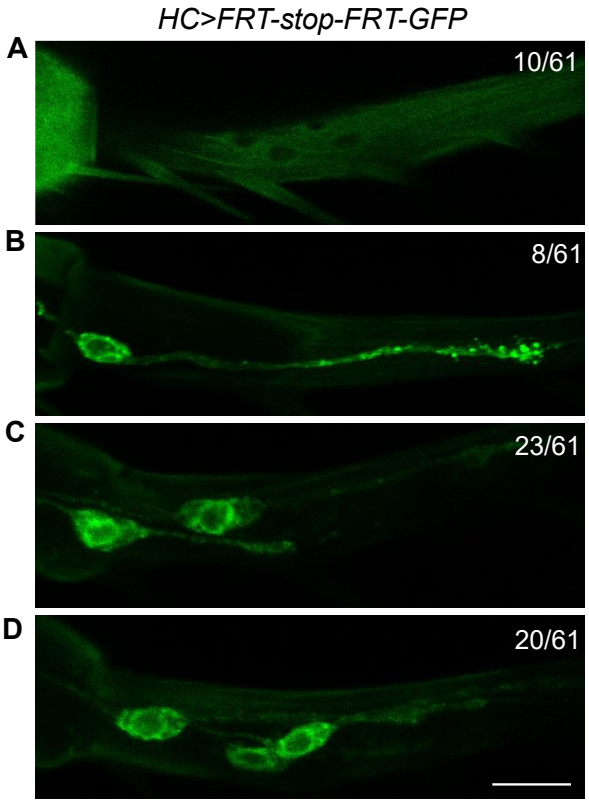

Figure S4. Heat shock removes the stop sequence from the FRT-stop-FRT cassette in HCs randomly. Among 61 aristae observed, ten had zero HCs (A), eight had one HC (B), 23 had two HCs (C), and 20 had three HCs (D). Scale bar: 10 μm.

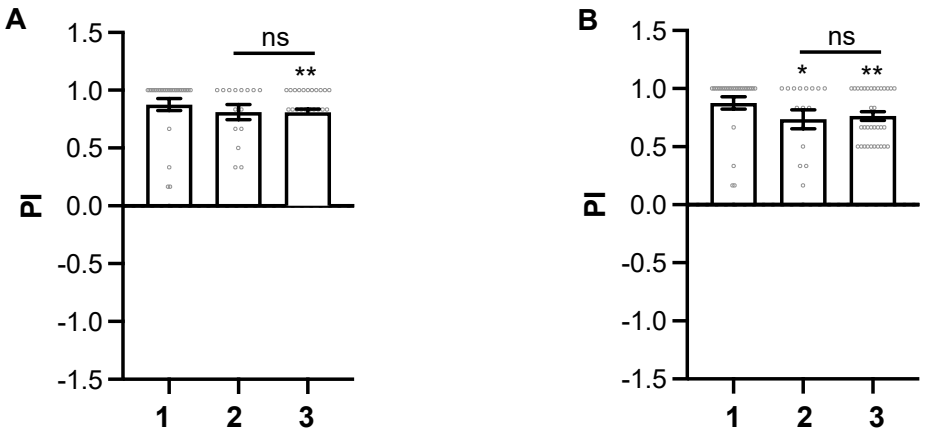

1. *wt* (2-7d)
2. *wt* (~10d)
3. *HC>FLIPSOTi* (~10d)

1. *wt* (2-7d)
2. *wt* (~21d)
3. *HC>FLIPSOTa* (~21d)

Figure S5. The rapid warm avoidance of old flies.
(A) PI of the indicated genotypes and ages. *n* = 15-34; data represent means ± SEM; Mann-Whitney test comparing to *wt* (2-7d) or the indicated group; **, $p < 0.01$; ns, not significant.
(B) PI of the indicated genotypes and ages. *n* = 17-34; data represent means ± SEM; Mann-Whitney test comparing to *wt* (2-7d) or the indicated group; *, $p < 0.05$; **, $p < 0.01$; ns, not significant.

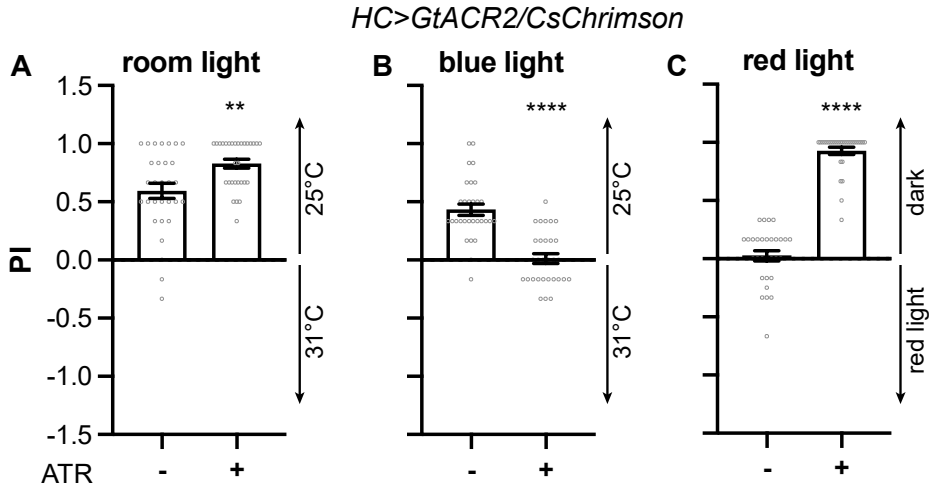

Figure S6. Single-fly thermotactic and optogenetic assays of *HC>GtACR2/CsChrimson*.
(A) PI of *HC>GtACR2/CsChrimson* that were raised with (+) or without (-) dietary retinal (ATR) under ambient room light condition. *n* = 30; data represent means ± SEM; Mann-Whitney test; **, $p < 0.01$. *HC>GtACR2/CsChrimson* is *HC-Gal4;UAS-GtACR2.EYFP/UAS-CsChrimson.mVenus.*
(B) PI of *HC>GtACR2/CsChrimson* that were raised with (+) or without (-) dietary retinal

(ATR) under blue light condition. *n* = 30; data represent means ± SEM; Mann-Whitney test; ****, $p < 0.0001$.

(C) PI of *HC>GtACR2/CsChrimson* that were raised with (+) or without (-) dietary retinal (ATR) under red light condition. *n* = 30; data represent means ± SEM; Mann-Whitney test; ****, $p < 0.0001$.

Reference:

1. Dale Purves, G.J.A., David Fitzpatrick, William C. Hall, Anthony-Samuel LaMantia, and Leonard E. White (2011). Neuroscience. 5th Edition.
2. Rubenstein, J.L., and Merzenich, M.M. (2003). Model of autism: increased ratio of excitation/inhibition in key neural systems. Genes Brain Behav *2*, 255-267.
3. Belmonte, M.K., Allen, G., Beckel-Mitchener, A., Boulanger, L.M., Carper, R.A., and Webb, S.J. (2004). Autism and abnormal development of brain connectivity. J Neurosci *24*, 9228-9231. 10.1523/jneurosci.3340-04.2004.
4. Lynall, M.-E., Bassett, D.S., Kerwin, R., McKenna, P.J., Kitzbichler, M., Muller, U., and Bullmore, E. (2010). Functional Connectivity and Brain Networks in Schizophrenia. The Journal of Neuroscience *30*, 9477-9487. 10.1523/jneurosci.0333-10.2010.
5. Venken, K.J., Simpson, J.H., and Bellen, H.J. (2011). Genetic manipulation of genes and cells in the nervous system of the fruit fly. Neuron *72*, 202-230. 10.1016/j.neuron.2011.09.021.
6. Luo, L., Callaway, E.M., and Svoboda, K. (2018). Genetic Dissection of Neural Circuits: A Decade of Progress. Neuron *98*, 256-281. 10.1016/j.neuron.2018.03.040.
7. Takemura, S.Y., Bharioke, A., Lu, Z., Nern, A., Vitaladevuni, S., Rivlin, P.K., Katz, W.T., Olbris, D.J., Plaza, S.M., Winston, P., et al. (2013). A visual motion detection circuit suggested by Drosophila connectomics. Nature *500*, 175-181. 10.1038/nature12450.
8. Zheng, Z., Lauritzen, J.S., Perlman, E., Robinson, C.G., Nichols, M., Milkie, D., Torrens, O., Price, J., Fisher, C.B., Sharifi, N., et al. (2018). A Complete Electron Microscopy Volume of the Brain of Adult Drosophila melanogaster. Cell *174*, 730-743.e722. 10.1016/j.cell.2018.06.019.
9. Miles, R., and Poncer, J.C. (1996). Paired recordings from neurones. Current opinion in neurobiology *6*, 387-394.
10. Wilson, R.I., Turner, G.C., and Laurent, G. (2004). Transformation of olfactory representations in the Drosophila antennal lobe. Science (New York, N.Y.) *303*, 366-370. 10.1126/science.1090782.
11. Patterson, G.H., and Lippincott-Schwartz, J. (2002). A photoactivatable GFP for selective photolabeling of proteins and cells. Science (New York, N.Y.) *297*, 1873-1877. 10.1126/science.1074952.
12. Datta, S.R., Vasconcelos, M.L., Ruta, V., Luo, S., Wong, A., Demir, E., Flores, J., Balonze, K., Dickson, B.J., and Axel, R. (2008). The Drosophila pheromone cVA activates a sexually dimorphic neural circuit. Nature *452*, 473-477. 10.1038/nature06808.

13. Ruta, V., Datta, S.R., Vasconcelos, M.L., Freeland, J., Looger, L.L., and Axel, R. (2010). A dimorphic pheromone circuit in Drosophila from sensory input to descending output. Nature *468*, 686-690. 10.1038/nature09554.
14. Clowney, E.J., Iguchi, S., Bussell, J.J., Scheer, E., and Ruta, V. (2015). Multimodal Chemosensory Circuits Controlling Male Courtship in Drosophila. Neuron *87*, 1036-1049. 10.1016/j.neuron.2015.07.025.
15. Lai, J.S., Lo, S.J., Dickson, B.J., and Chiang, A.S. (2012). Auditory circuit in the Drosophila brain. Proceedings of the National Academy of Sciences of the United States of America *109*, 2607-2612. 10.1073/pnas.1117307109.
16. Fisek, M., and Wilson, R.I. (2014). Stereotyped connectivity and computations in higher-order olfactory neurons. Nature neuroscience *17*, 280-288. 10.1038/nn.3613.
17. Frank, D.D., Jouandet, G.C., Kearney, P.J., Macpherson, L.J., and Gallio, M. (2015). Temperature representation in the Drosophila brain. Nature *519*, 358-361. 10.1038/nature14284.
18. Hong, E.J., and Wilson, R.I. (2015). Simultaneous encoding of odors by channels with diverse sensitivity to inhibition. Neuron *85*, 573-589. 10.1016/j.neuron.2014.12.040.
19. Feinberg, E.H., Vanhoven, M.K., Bendesky, A., Wang, G., Fetter, R.D., Shen, K., and Bargmann, C.I. (2008). GFP Reconstitution Across Synaptic Partners (GRASP) defines cell contacts and synapses in living nervous systems. Neuron *57*, 353-363. 10.1016/j.neuron.2007.11.030.
20. Gordon, M.D., and Scott, K. (2009). Motor control in a Drosophila taste circuit. Neuron *61*, 373-384. 10.1016/j.neuron.2008.12.033.
21. Masuda-Nakagawa, L.M., Ito, K., Awasaki, T., and O'Kane, C.J. (2014). A single GABAergic neuron mediates feedback of odor-evoked signals in the mushroom body of larval Drosophila. Front Neural Circuits *8*, 35. 10.3389/fncir.2014.00035.
22. Lin, T.Y., Luo, J., Shinomiya, K., Ting, C.Y., Lu, Z., Meinertzhagen, I.A., and Lee, C.H. (2016). Mapping chromatic pathways in the Drosophila visual system. The Journal of comparative neurology *524*, 213-227. 10.1002/cne.23857.
23. Gorostiza, E.A., Depetris-Chauvin, A., Frenkel, L., Pirez, N., and Ceriani, M.F. (2014). Circadian pacemaker neurons change synaptic contacts across the day. Current biology : CB *24*, 2161-2167. 10.1016/j.cub.2014.07.063.
24. Cavanaugh, D.J., Geratowski, J.D., Wooltorton, J.R., Spaethling, J.M., Hector, C.E., Zheng, X., Johnson, E.C., Eberwine, J.H., and Sehgal, A. (2014). Identification of a circadian output circuit for rest:activity rhythms in Drosophila. Cell *157*, 689-701. 10.1016/j.cell.2014.02.024.
25. Fan, P., Manoli, D.S., Ahmed, O.M., Chen, Y., Agarwal, N., Kwong, S., Cai, A.G., Neitz, J., Renslo, A., Baker, B.S., and Shah, N.M. (2013). Genetic and neural mechanisms that inhibit Drosophila from mating with other species. Cell *154*, 89-102. 10.1016/j.cell.2013.06.008.
26. Shearin, H.K., Quinn, C.D., Mackin, R.D., Macdonald, I.S., and Stowers, R.S. (2018). t-GRASP, a targeted GRASP for assessing neuronal connectivity. J Neurosci Methods *306*, 94-102. 10.1016/j.jneumeth.2018.05.014.
27. Macpherson, L.J., Zaharieva, E.E., Kearney, P.J., Alpert, M.H., Lin, T.Y., Turan, Z., Lee, C.H., and Gallio, M. (2015). Dynamic labelling of neural connections in multiple colours by trans-synaptic fluorescence complementation. Nature communications *6*, 10024. 10.1038/ncomms10024.
28. Talay, M., Richman, E.B., Snell, N.J., Hartmann, G.G., Fisher, J.D., Sorkac, A., Santoyo, J.F., Chou-Freed, C., Nair, N., Johnson, M., et al. (2017). Transsynaptic Mapping of Second-Order Taste Neurons in Flies by trans-Tango. Neuron *96*, 783-795.e784. 10.1016/j.neuron.2017.10.011.

29. Huang, T.H., Niesman, P., Arasu, D., Lee, D., De La Cruz, A.L., Callejas, A., Hong, E.J., and Lois, C. (2017). Tracing neuronal circuits in transgenic animals by transneuronal control of transcription (TRACT). eLife *6*. 10.7554/eLife.32027.
30. Cachero, S., Gkantia, M., Bates, A.S., Frechter, S., Blackie, L., McCarthy, A., Sutcliffe, B., Strano, A., Aso, Y., and Jefferis, G. (2020). BAcTrace, a tool for retrograde tracing of neuronal circuits in Drosophila. Nat Methods *17*, 1254-1261. 10.1038/s41592-020-00989-1.
31. Ni, L. (2021). Genetic Transsynaptic Techniques for Mapping Neural Circuits in Drosophila. Front Neural Circuits *15*, 749586. 10.3389/fncir.2021.749586.
32. Barnea, G., Strapps, W., Herrada, G., Berman, Y., Ong, J., Kloss, B., Axel, R., and Lee, K.J. (2008). The genetic design of signaling cascades to record receptor activation. Proceedings of the National Academy of Sciences of the United States of America *105*, 64-69. 10.1073/pnas.0710487105.
33. He, Z., Luo, Y., Shang, X., Sun, J.S., and Carlson, J.R. (2019). Chemosensory sensilla of the Drosophila wing express a candidate ionotropic pheromone receptor. PLoS biology *17*, e2006619. 10.1371/journal.pbio.2006619.
34. Feng, K., Sen, R., Minegishi, R., Dübbert, M., Bockemühl, T., Büschges, A., and Dickson, B.J. (2020). Distributed control of motor circuits for backward walking in Drosophila. Nature communications *11*, 6166. 10.1038/s41467-020-19936-x.
35. Guo, F., Holla, M., Díaz, M.M., and Rosbash, M. (2018). A Circadian Output Circuit Controls Sleep-Wake Arousal in Drosophila. Neuron *100*, 624-635.e624. 10.1016/j.neuron.2018.09.002.
36. Snell, N.J., Fisher, J.D., Hartmann, G.G., Zolyomi, B., Talay, M., and Barnea, G. (2022). Complex representation of taste quality by second-order gustatory neurons in Drosophila. Current biology : CB *32*, 3758-3772.e3754. 10.1016/j.cub.2022.07.048.
37. Ni, L., Bronk, P., Chang, E.C., Lowell, A.M., Flam, J.O., Panzano, V.C., Theobald, D.L., Griffith, L.C., and Garrity, P.A. (2013). A gustatory receptor paralogue controls rapid warmth avoidance in Drosophila. Nature *500*, 580-584. 10.1038/nature12390.
38. Mishra, A., Salari, A., Berigan, B.R., Miguel, K.C., Amirshenava, M., Robinson, A., Zars, B.C., Lin, J.L., Milescu, L.S., Milescu, M., and Zars, T. (2018). The Drosophila Gr28bD product is a non-specific cation channel that can be used as a novel thermogenetic tool. Scientific reports *8*, 901. 10.1038/s41598-017-19065-4.
39. Budelli, G., Ni, L., Berciu, C., van Giesen, L., Knecht, Z.A., Chang, E.C., Kaminski, B., Silbering, A.F., Samuel, A., Klein, M., et al. (2019). Ionotropic Receptors Specify the Morphogenesis of Phasic Sensors Controlling Rapid Thermal Preference in Drosophila. Neuron. 10.1016/j.neuron.2018.12.022.
40. Gallio, M., Ofstad, T.A., Macpherson, L.J., Wang, J.W., and Zuker, C.S. (2011). The coding of temperature in the Drosophila brain. Cell *144*, 614-624. 10.1016/j.cell.2011.01.028.
41. Silbering, A.F., Rytz, R., Grosjean, Y., Abuin, L., Ramdya, P., Jefferis, G.S., and Benton, R. (2011). Complementary function and integrated wiring of the evolutionarily distinct Drosophila olfactory subsystems. The Journal of neuroscience : the official journal of the Society for Neuroscience *31*, 13357-13375. 10.1523/jneurosci.2360-11.2011.
42. Stocker, R.F., Singh, R.N., Schorderet, M., and Siddiqi, O. (1983). Projection patterns of different types of antennal sensilla in the antennal glomeruli of Drosophila melanogaster. Cell and tissue research *232*, 237-248.
43. Marin, E.C., Büld, L., Theiss, M., Sarkissian, T., Roberts, R.J.V., Turnbull, R., Tamimi, I.F.M., Pleijzier, M.W., Laursen, W.J., Drummond, N., et al. (2020). Connectomics Analysis Reveals First-, Second-, and Third-Order Thermosensory

and Hygrosensory Neurons in the Adult Drosophila Brain. Current biology : CB *30*, 3167-3182.e3164. 10.1016/j.cub.2020.06.028.
44. Liu, W.W., Mazor, O., and Wilson, R.I. (2015). Thermosensory processing in the Drosophila brain. Nature *519*, 353-357. 10.1038/nature14170.
45. Klapoetke, N.C., Murata, Y., Kim, S.S., Pulver, S.R., Birdsey-Benson, A., Cho, Y.K., Morimoto, T.K., Chuong, A.S., Carpenter, E.J., Tian, Z., et al. (2014). Independent optical excitation of distinct neural populations. Nat Methods *11*, 338-346. 10.1038/nmeth.2836.
46. Mohammad, F., Stewart, J.C., Ott, S., Chlebikova, K., Chua, J.Y., Koh, T.-W., Ho, J., and Claridge-Chang, A. (2017). Optogenetic inhibition of behavior with anion channelrhodopsins. Nature Methods *14*, 271. 10.1038/nmeth.4148.
47. Mauss, A.S., Busch, C., and Borst, A. (2017). Optogenetic Neuronal Silencing in Drosophila during Visual Processing. Scientific reports *7*, 13823. 10.1038/s41598-017-14076-7.
48. Govorunova, E.G., Sineshchekov, O.A., Janz, R., Liu, X., and Spudich, J.L. (2015). NEUROSCIENCE. Natural light-gated anion channels: A family of microbial rhodopsins for advanced optogenetics. Science (New York, N.Y.) *349*, 647-650. 10.1126/science.aaa7484.
49. Gao, X.J., Riabinina, O., Li, J., Potter, C.J., Clandinin, T.R., and Luo, L. (2015). A transcriptional reporter of intracellular Ca(2+) in Drosophila. Nature neuroscience *18*, 917-925. 10.1038/nn.4016.
50. Golic, K.G., and Golic, M.M. (1996). Engineering the Drosophila genome: chromosome rearrangements by design. Genetics *144*, 1693-1711.
51. Huda, A., Omelchenko, A.A., Vaden, T.J., Castaneda, A.N., and Ni, L. (2022). Responses of different Drosophila species to temperature changes. The Journal of experimental biology *225.* 10.1242/jeb.243708.
52. Thorne, N., and Amrein, H. (2008). Atypical expression of Drosophila gustatory receptor genes in sensory and central neurons. The Journal of comparative neurology *506*, 548-568. 10.1002/cne.21547.
53. Golic, K.G., and Lindquist, S. (1989). The FLP recombinase of yeast catalyzes site-specific recombination in the Drosophila genome. Cell *59*, 499-509. 10.1016/0092-8674(89)90033-0.
54. Hong, W., Zhu, H., Potter, C.J., Barsh, G., Kurusu, M., Zinn, K., and Luo, L. (2009). Leucine-rich repeat transmembrane proteins instruct discrete dendrite targeting in an olfactory map. Nature neuroscience *12*, 1542-1550. 10.1038/nn.2442.
55. Riabinina, O., and Potter, C.J. (2016). The Q-System: A Versatile Expression System for Drosophila. Methods in molecular biology (Clifton, N.J.) *1478*, 53-78. 10.1007/978-1-4939-6371-3_3.
56. Markstein, M., Pitsouli, C., Villalta, C., Celniker, S.E., and Perrimon, N. (2008). Exploiting position effects and the gypsy retrovirus insulator to engineer precisely expressed transgenes. Nat Genet *40*, 476-483. 10.1038/ng.101.
57. Riabinina, O., Luginbuhl, D., Marr, E., Liu, S., Wu, M.N., Luo, L., and Potter, C.J. (2015). Improved and expanded Q-system reagents for genetic manipulations. Nat Methods *12*, 219-222, 215 p following 222. 10.1038/nmeth.3250.
58. Ni, L., Klein, M., Svec, K.V., Budelli, G., Chang, E.C., Ferrer, A.J., Benton, R., Samuel, A.D., and Garrity, P.A. (2016). The Ionotropic Receptors IR21a and IR25a mediate cool sensing in Drosophila. eLife *5*. 10.7554/eLife.13254.
59. Tyrrell, J.J., Wilbourne, J.T., Omelchenko, A.A., Yoon, J., and Ni, L. (2021). Ionotropic Receptor-dependent cool cells control the transition of temperature preference in Drosophila larvae. PLoS genetics *17*, e1009499. 10.1371/journal.pgen.1009499.

APPENDIX B

Below is the article “Responses of different Drosophila species to temperature changes”, reproduced from https://journals.biologists.com/jeb/article/225/11/jeb243708/275567/Responses-of-different-Drosophila-species-to. Data relevant to this dissertation can be found in Fig. 2I-J.

Responses of different Drosophila species to temperature changes

Ainul Huda, Alisa A. Omelchenko, Thomas J. Vaden, Allison N. Castaneda, Lina Ni

ABSTRACT

Temperature is a critical environmental variable that affects the distribution, survival and reproduction of most animals. Although temperature receptors have been identified in many animals, how these receptors respond to temperature is still unclear. Here, we describe an automated tracking method for studying the thermotactic behaviors of *Drosophila* larvae and adults. We built optimal experimental setups to capture behavioral recordings and analyzed them using free software, Fiji and TrackMate, which do not require programming knowledge. Then, we applied the adult thermotactic two-choice assay to examine the movement and temperature preferences of nine *Drosophila* species. The ability or inclination to move varied among these species and at different temperatures. Distinct species preferred various ranges of temperatures. Wild-type *D. melanogaster* flies avoided the warmer temperature in the warm avoidance assay and the cooler temperature in the cool avoidance assay. Conversely, *D. bipectinata* and *D. yakuba* did not avoid warm or cool temperatures in the respective assays, and *D. biarmipes* and *D. mojavensis* did not avoid the warm temperature in the warm avoidance assay. These results demonstrate that *Drosophila* species have different mobilities and temperature preferences, which will benefit further research in exploring molecular mechanisms of temperature responsiveness.

Keywords:

Drosophila, Thermosensation, Thermotaxis, Two-choice assay, Optogenetics, TrackMate

INTRODUCTION

Temperature affects all aspects of physiology, from the rate of chemical reactions and the activity of biomolecules to the distribution of living organisms (Dell et al., 2011; Sengupta and Garrity, 2013; Franks and Hoffmann, 2012). Temperature variation is particularly influential for small animals, such as insects, which depend on ambient temperatures to set their body temperatures (Garrity et al., 2010; Dillon et al., 2010). Many insect vectors of disease, including mosquitoes, respond to the temperature of their warm-blooded hosts and use it to guide blood-feeding behaviors (Brown, 1951; Howlett, 1910; Corfas and Vosshall, 2015; Greppi et al., 2015, 2020).

Fruit flies are an excellent insect model system for studying thermosensation. In many *Drosophila melanogaster* thermosensory systems, a small number of thermosensory neurons control robust behaviors (Ni et al., 2013; Hamada et al., 2008; Klein et al.,

2015; Budelli et al., 2019; Gallio et al., 2011). These sensory neurons contain evolutionarily conserved thermal molecules across *Drosophila* species and insect vectors of disease, including mosquitoes (Corfas and Vosshall, 2015; Greppi et al., 2020). Adult *D. melanogaster* flies possess several thermosensory systems to control innocuous thermotactic behaviors (Barbagallo and Garrity, 2015). TRPA1, a transient receptor potential cation channel, acts as an internal warm sensor in the brain, guiding flies to slowly avoid warm temperatures when they are exposed to a shallow temperature gradient (Hamada et al., 2008). Aristal heating and cooling neurons guide rapid warm and cool avoidance on steep temperature gradients. A gustatory receptor GR28B(D) is the warm receptor in aristal heating cells (HCs), and three members of the ionotropic receptor (IR) family (IR25a, IR93a and IR21a) form the cool receptor in aristal cooling cells (CCs) (Ni et al., 2013; Budelli et al., 2019). However, the molecular mechanisms underlying how these thermoreceptors respond to temperature are still unclear.

The genomes of more than 20 *Drosophila* species, besides *D. melanogaster*, have been sequenced (Celniker et al., 2002; Hoskins et al., 2007; Hu et al., 2013; Clark et al., 2007; Stark et al., 2007; Chen et al., 2014). These sequenced species span a wide range of global distributions with diverse temperatures (Powell, 1997). To adapt to their specific ecosystems, they may possess thermoreceptors that have evolved distinct temperature responsiveness through amino acid changes at a few residues. Thus, we expect that these *Drosophila* species offer opportunities to understand how thermoreceptors respond to temperature changes.

This study used thermotactic behaviors to understand the thermal preference of various *Drosophila* species. *Drosophila* thermotactic behaviors depend on locomotion – the ability of an animal to move. Therefore, we first describe an automated tracking method that utilizes an open-source Fiji plugin, TrackMate, to track the movement of larvae and adult flies. We built optimal experimental setups that allow for easy processing and reproducible analysis of the behavioral recordings. We also provide examples of how to analyze non-optimal recordings. TrackMate extracts the *X* and *Y* positions of an animal on each frame. This information allows the generation of animal trajectories, calculation of moving speeds and distances, and determination of preference indices in two-choice assays. This method can be used to analyze free-motion behaviors, two-choice thermotaxis and optogenetic assays in larvae and adult flies. Then, we used the adult thermotactic two-choice assay to examine the temperature preferences of different *Drosophila* species. We tested 801 flies, including four genotypes of *D. melanogaster* and eight other *Drosophila* species. We find that starting temperature and sex affect preference indices, and several species exhibit preferences similar to those of *D. melanogaster* thermoreceptor mutants. In summary, this study provides an automated tracking method to analyze *Drosophila* larval and adult movement. Results from various species can benefit the research pertaining to molecular mechanisms of temperature responsiveness.

MATERIALS AND METHODS

Drosophila strains

y^{1},*w** was used as the wild-type control for the larval behavioral assays in Fig. 1D–G. w^{1118} was used as the wild-type control for the adult behavioral assays in Figs 2–5. *Canton-S* (*CS*) and *D. mojavensis* were kind gifts from Dr Michael Dickinson. Other fly species were obtained from the National *Drosophila* Species Stock Center: *D. ananassae* (14024-0371.11), *D. biarmipes* (14023-0361.03), *D. bipectinata* (14024-0381.21), *D. erecta* (14021-0224.05), *D. ficusphila* (14025-0441.01), *D. simulans* (14021-0251.011) and *D. yakuba* (14021-0261.48). The following flies were previously

described: *UAS-CsChrimson* (Klapoetke et al., 2014), *Ir93a*^{MI} (Knecht et al., 2016), *Ir93a-Gal4* (Sánchez-Alcañiz et al., 2018), *Gr28b*^{MB} (Ni et al., 2013) and *HC-Gal4* (Gallio et al., 2011).

Fig. 1.

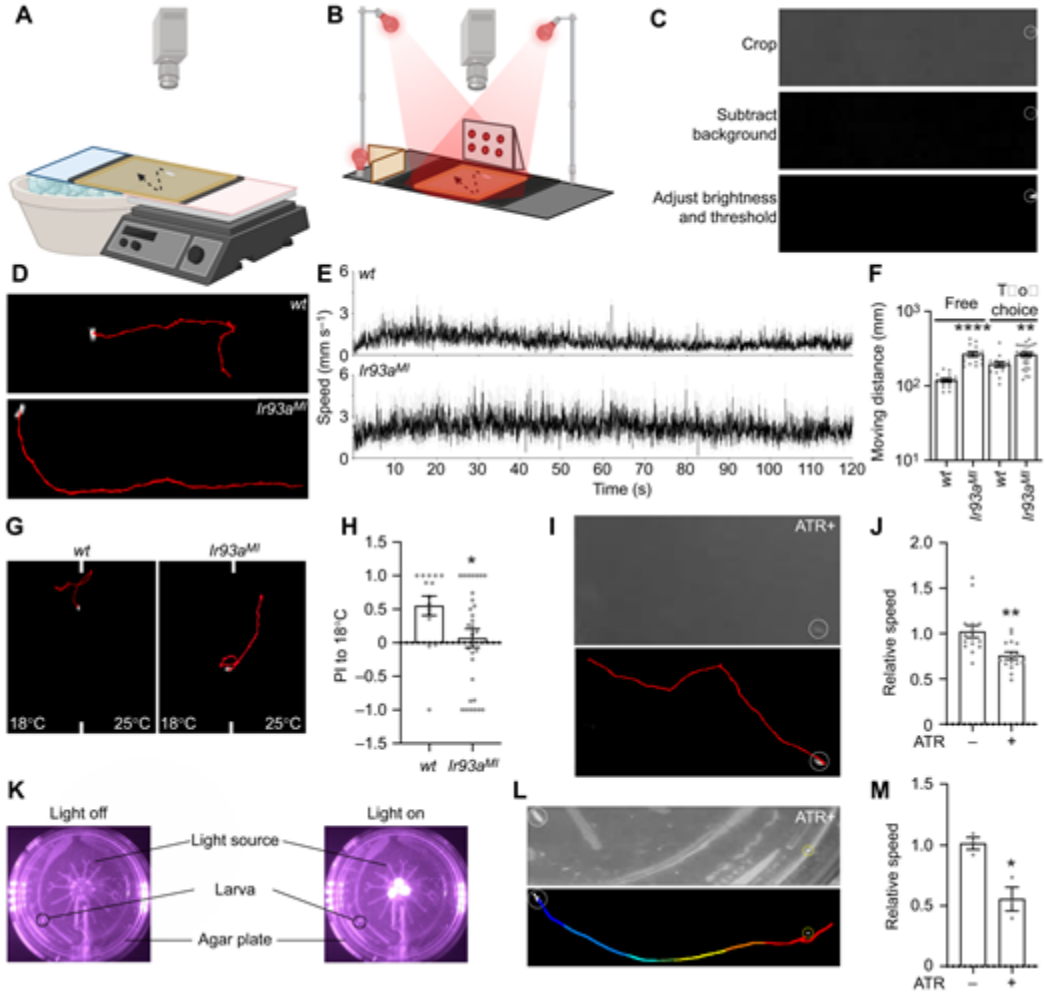

Using TrackMate to analyze larval behaviors. (A,B) Setup for the single-larva two-choice thermotactic (A) and optogenetic assay (B). The setup for the free-motion assay is similar to that for the optogenetic assay but performed in ambient light. (C) Preprocessing of images of the single-larva behavioral assay. Top: the image sequence was imported into Fiji and cropped. Middle: the background was subtracted. Bottom: brightness and threshold were adjusted. White circles show the larva. (D) *wt* (*y*^{1},*w**) and *Ir93a*^{MI} trajectories in the free-motion assay. (E) *wt* (*y*^{1},*w**) and *Ir93a*^{MI} moving speed in the free-motion assay. *n*=15; data represent means (black) ±s.e.m. (light gray). (F) Moving distances of indicated genotypes and conditions. *n*=15–30; data represent means±s.e.m; ***P*<0.01, *****P*<0.0001, Welch's test for the free-motion assay and Mann–Whitney test for the two-choice assay. (G) *wt* (*y*^{1},*w**) and *Ir93a*^{MI} trajectories in the two-choice assay. (H) Preference indices (PI) of the indicated genotypes. *n*=30; data represent means±s.e.m; **P*<0.05, Mann–Whitney test. (I) The locomotion of an *Ir21a-Gal4;UAS-CsChrimson* (*Ir21a>CsChrimson*) larva with all-trans retinal (ATR, dietary retinal) in the optogenetic assay. Top: the video was converted to grayscale and cropped by Fiji. Bottom: the recording was preprocessed by Fiji and analyzed

by TrackMate. White circles show the larva. (J) The relative speed of *Ir21a>CsChrimson* larvae with or without ATR. Relative speed is defined as the moving speed during red light on divided by the moving speed during red light off. *n*=15; data represent means±s.e.m; ***P*<0.01, Mann–Whitney test. (K–M) Using TrackMate to analyze non-optimal recordings. (K) A previous setup of the single-larva optogenetic assay, in which light glare and other background noise signals are detected. (L) Locomotion of an *Ir21a>CsChrimson* larva with ATR. Top: the video was converted to grayscale and cropped by Fiji. Bottom: the recording was preprocessed by Fiji and analyzed by TrackMate. White circles show the larva. Yellow circles show an unavoidable background noise signal. The trajectory is shown in rainbow colors. (M) The relative speed of *Ir21a>CsChrimson* larvae with or without ATR. *n*=3; data represent means±s.e.m; **P*<0.05, Welch's test.

Fig. 2.

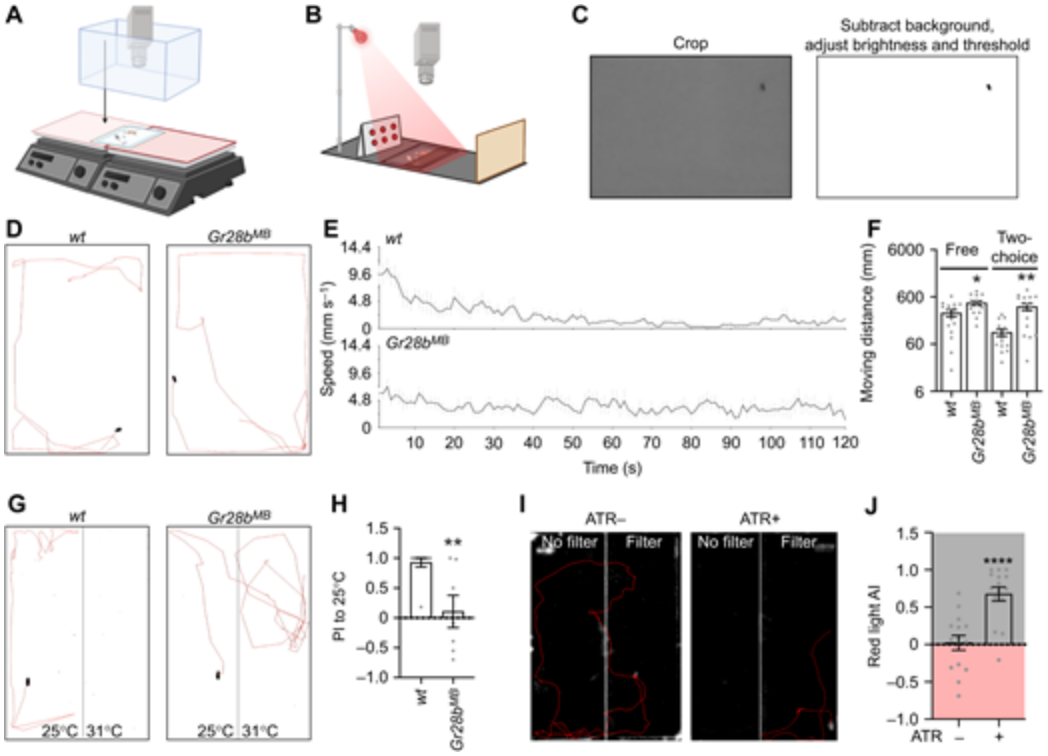

Using TrackMate to analyze adult behaviors. (A,B) Setup for the single-fly two-choice thermotactic (A) and optogenetic assay (B). The setup for the free-motion assay is similar to that for the two-choice assay but is performed on a single plate with a unique temperature (25°C). (C) Preprocessing of images of the single-fly behavioral assay. Left: the image sequence was imported into Fiji and cropped. Right: the background was subtracted, and brightness and threshold were adjusted. (D) *wt* (w^{1118}) and $Gr28b^{MB}$ trajectories in the free-motion assay. (E) *wt* (w^{1118}) and $Gr28b^{MB}$ moving speed in the free-motion assay. *n*=15; data represent means (black) ±s.e.m (light gray). (F) Moving distances of the indicated genotypes and conditions. *n*=15; data represent means±s.e.m; **P*<0.05, ***P*<0.01, Welch's test for the free-motion assay and Mann–Whitney test for the two-choice assay. (G) *wt* (w^{1118}) and $Gr28b^{MB}$ trajectories in the two-choice assay. (H) PI of the indicated genotypes. *n*=7–11; data represent means±s.e.m; ***P*<0.01, Mann–Whitney test. (I) Trajectories of *HC-Gal4;UAS-CsChrimson* (*HC>CsChrimson*) flies with or without dietary retinal (ATR) in the

optogenetic assay. (J) Avoidance indices (AI) of *HC>CsChrimson* flies with or without ATR. *n*=15; data represent means±s.e.m; ****P<0.0001, Mann–Whitney test.

Fig. 3.

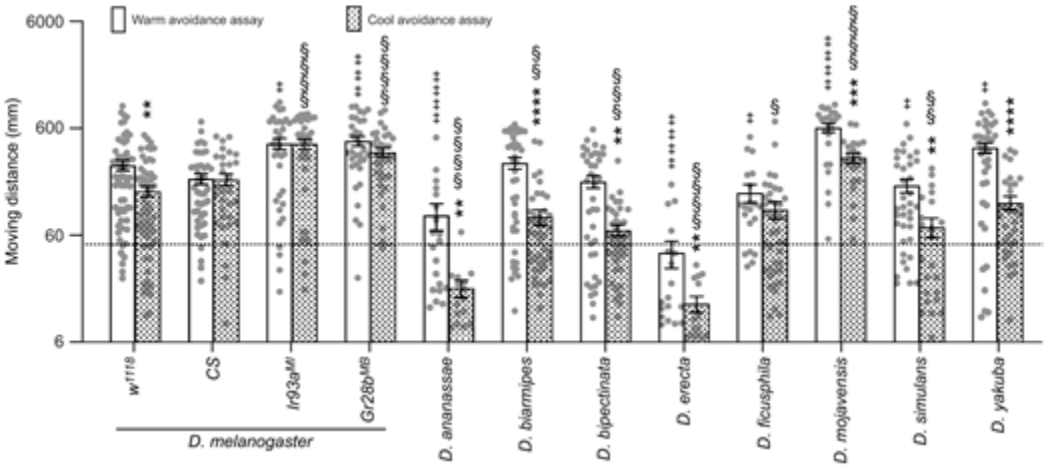

***Drosophila* species have diverse mobilities.** Four genotypes (w^{1118}, *CS*, $Ir93a^{MI}$ and $Gr28b^{MB}$) of *D. melanogaster*, as well as *D. ananassae*, *D. biarmipes*, *D. bipectinata*, *D. erecta*, *D. ficusphila*, *D. mojavensis*, *D. simulans* and *D. yakuba* were tested. The dashed line shows the threshold moving distance, 47.95 mm. Data represent means±s.e.m. **P<0.01, ***P<0.001 and ****P<0.0001, comparing moving distances of the corresponding genotype/species in the warm avoidance assay, Mann–Whitney test, except Welch's test for $Gr28b^{MB}$. ‡P<0.05, ‡‡‡P<0.001 and ‡‡‡‡P<0.0001, comparing moving distances of w^{1118} in the warm avoidance assay, Mann–Whitney test. §P<0.05, §§P<0.01, §§§P<0.001 and §§§§P<0.0001, comparing moving distances of w^{1118} in the cool avoidance assay, Mann–Whitney test.

Fig. 4.

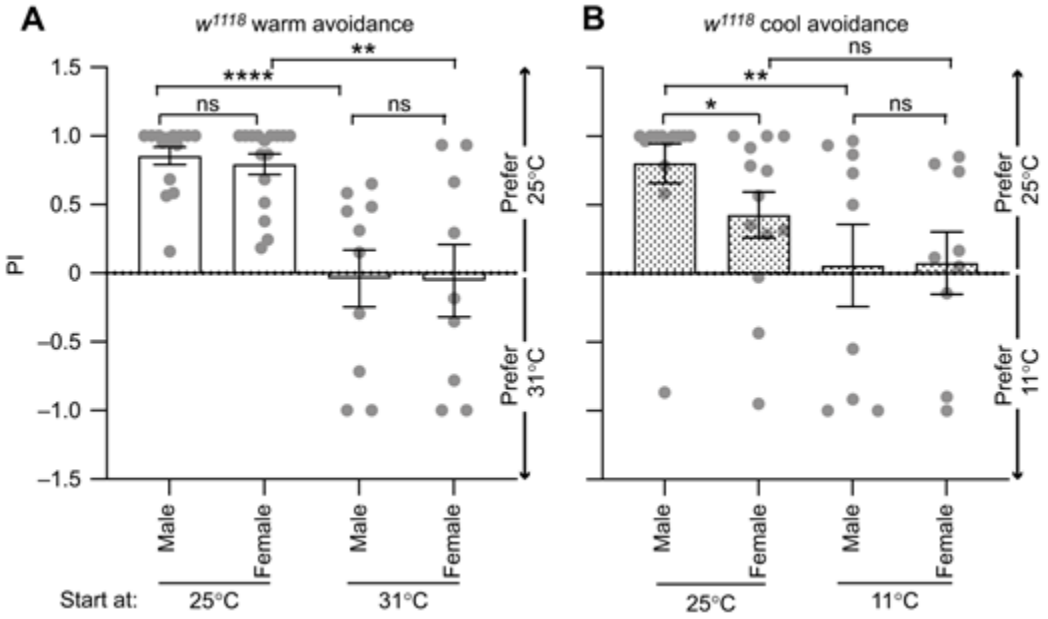

Both starting temperature and sex affect w^{1118} PI. PIs of indicated groups in warm (A) and cool (B) avoidance assays. Data represent means±s.e.m. *P<0.05, **P<0.01 and ****P<0.0001, Mann–Whitney test, except Welch's test for the comparison of males starting at 31°C and females starting at 31°C in A and the comparison of females starting at 25°C and females starting at 11°C in B.

Fig. 5.

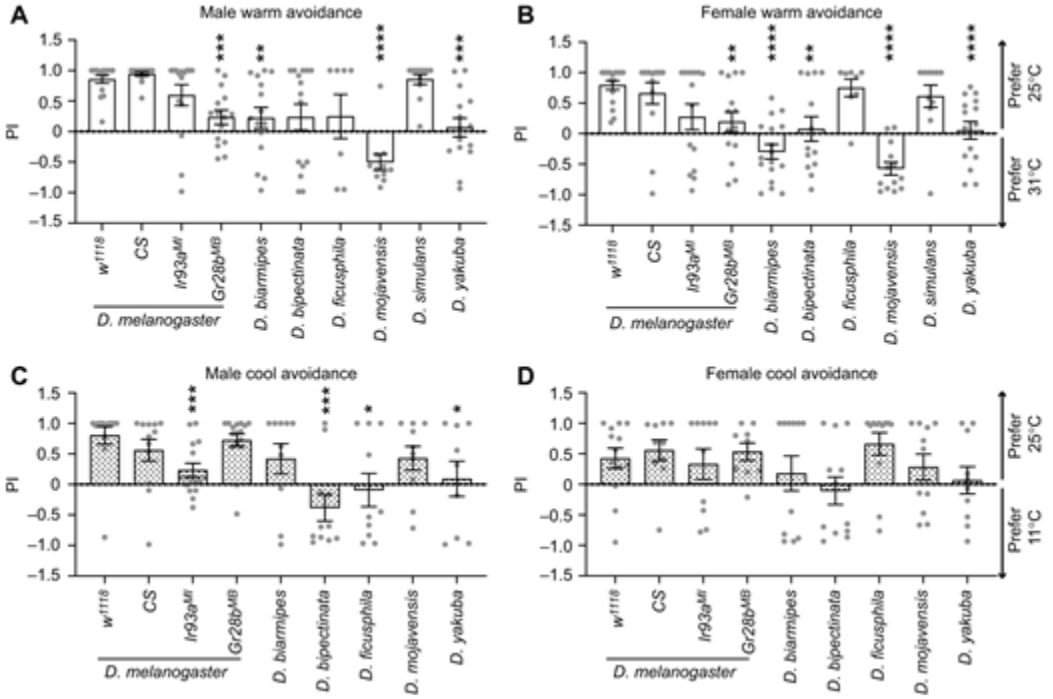

***Drosophila* species have distinct temperature preferences.** (A,B) PI of males (A) and females (B) of the indicated *D. melanogaster* genotypes and *Drosophila* species in the warm avoidance assay. (C,D) PI of males (C) and females (D) of the indicated *D. melanogaster* genotypes and *Drosophila* species in the cool avoidance assay. Data represent means±s.e.m. *P<0.05, **P<0.01, ***P<0.01 and ****P<0.0001, comparing PI with the corresponding w^{1118}, Mann–Whitney test, except Welch's test for the comparison of w^{1118} and $Gr28b^{MB}$ and w^{1118} and *D. yakuba* in B.

Larval behavioral assays

Flies were maintained at 25°C under a 12 h:12 h light:dark cycle. All larval experiments were performed between 15:00 h and 18:00 h. Larvae were collected as described previously, with some modifications (Tyrrell et al., 2021). Vials containing 20–45 males and females were allowed 4–8 h to lay eggs and larvae were collected on day 4 using 10 ml of a 20% w/v sucrose solution. Male and female larvae were not separated. Larvae were thoroughly washed 3 times with distilled water, plated on a 60 mm tissue culture dish (Corning) with about 13 ml of 3% room temperature (about 20°C) agar gel, and given 5–10 min to recover from the washing process and acclimate to the agar.

For the free-motion assay, a steel plate was placed on a hot plate and its surface temperature was adjusted to 18±1°C. A sheet of matte black poster paper was placed on top of the steel plates. A plastic sheet protector was placed on the poster paper to prevent warping from moisture. A 3% agar gel (~254×241 mm) was placed on the plastic sheet and

evenly positioned in the release zone. For the two-choice assay, two steel plates on different hot plates were separated by ~1.6 mm (the release zone). The surface temperature was 18±1°C on one side of the gel and 25±1°C on the other. The release zone was labeled at the top and bottom of the gel. The temperature was monitored before each trial using a surface temperature probe (80PK-3A, Fluke) and a thermometer (Fisherbrand Traceable Big-Digit Type K Thermometer). A wild-type control was run at the beginning of the daily experiments. Water was gently sprayed between trials to moisten the agar surface. A larva was placed at the release zone and given 2 min to wander. The experiment was conducted in dim ambient light (<10 lx) and a HERO8 GoPro camera was hung above the gel (~267 mm) to record the motion of the larva for each trial.

Larval optogenetic assays were recorded by a Sony HDR-CX405 camcorder with the internal infrared filter removed and an 830 nm long-pass filter (FSQ-RG830, Newport) installed. A 3% agar gel was cut to a ~76×127 mm size and a sheet of matte black poster paper was placed under the gel to reduce background noise signals. An infrared light (4331910725, Univivi) was used to visualize the larvae. Two red-light sources (Tyrrell et al., 2021) were attached 254 mm above the gel at a 45 deg angle on both sides of the gel such that the light intensity was even throughout the gel (~3 klx) and no glare was created. A third red-light source was placed in a box outside the experimental setup but within view of the camera to serve as an indicator to record when red lights were on or off. Larvae were collected and prepared for the assay as detailed above except that they were kept on food containing 40 µmol l^{-1} all-trans retinal (ATR, Sigma-Aldrich) in the dark for 72 h before testing. An individual larva was placed on the agar gel and given 30 s to acclimate. For the recording, the larva was given 30 s to wander followed by three cycles of 5 s red light on and 15 s red light off.

Adult behavioral assays

Flies were raised at 25°C under a 12 h:12 h light:dark cycle and were 2–7 days old when tested. All experiments were performed between 08:00 h and 12:00 h. Fly species for which sex was difficult to distinguish via the naked eye were placed on a cold plate and viewed under a microscope to observe and assign their sex 24 h before the experiments. The two-choice thermotactic assays included the warm avoidance assay and the cool avoidance assay. For the warm avoidance assay, two steel plates on different hot plates were aligned so that the steel plate boundaries were brought together. Hot plate temperatures were adjusted allowing the surface of the steel plates to be 25±1 and 31±1°C, respectively. For the cool avoidance assay, the right-side hot plate was replaced with a glass dish filled with ice. To hold the temperature, more ice was placed on top of the steel plate. The left plate temperature was set to 25±1°C and the right plate to 11±1°C. For the free-motion assay, a steel plate was placed on a hot plate, and its surface temperature was adjusted to 25±1°C. The plates were sprayed with distilled water, and a plastic sheet protector was placed on top. Excess moisture was removed via a Kimwipe. A piece of white paper was placed on top of the plastic sheet protector to reduce background noise signals. A clear plastic cover was coated with SigmaCote to prevent the fly from walking on the plastic cover; it was placed on top of the white paper. The cover was positioned so that it was divided evenly by the steel plate boundary, creating the experimental chamber. Temperature was monitored before each trial using a surface temperature probe (80PK-3A, Fluke) and a thermometer (Fisherbrand Traceable Big-Digit Type K Thermometer). A wild-type control test was run at the beginning of every data collection session. For the experiment, a fly of known sex was placed under the plastic cover and a Styrofoam box was placed above the plastic cover to shield the experimental area and allow the experiment to be conducted in dim ambient light (<10 lx). The flies were given 2 min to acclimate on the 25±1°C side under the clear plastic

cover. The cover was then moved towards the 31±1 or 11±1°C side so that the experimental area was divided evenly by the steel plate boundary. If the fly remained on the 25±1°C side during this process, the starting temperature was 25°C; if the fly moved to the 31±1°C or 11±1°C side, the starting temperature was 31 or 11°C, respectively. A HERO8 GoPro was positioned at the top of the box (~203 mm in height). The motion of the fly was recorded by taking a time-lapse photo every second for 120 s.

For the adult optogenetic assays, half of the clear plastic cover was covered with an infrared filter (LEE Filters 100×100 mm Infra Red #87 Infrared Polyester Filter). A sheet of matte black poster paper was put under the cover to reduce noise from the background. An infrared light (4331910725, Univivi) was used to visualize the flies. A red-light source (Tyrrell et al., 2021) was attached ~457 mm above the experimental surface with a light intensity of about 2.5 klx. Assays were recorded by a Sony HDR-CX405 camcorder with the internal infrared filter removed and an 830 nm long-pass filter (FSQ-RG830, Newport) installed. Flies of 1–3 days old were collected and kept in the dark for 40–48 h on food supplemented with 40 μmol l^{-1} ATR (Sigma-Aldrich). A single fly of known sex was pipetted under the plastic cover and given 30 s to acclimate. The light source was turned on and the motion of the fly was recorded for 60 s.

Preprocessing photos for adult behavioral assays

The individual photos for each trial were combined into a single file using Fiji and converted to 8-bit grayscale images (File>Import>Image Sequence function; boxes of Convert to 8-bit Grayscale and Sort names were numerically selected) (Schindelin et al., 2012). For the two-choice and optogenetic assays, the Rotate feature (Image>Transform>Rotate) was used to rotate images until the steel plate dividing line was vertical. A black line was drawn along the steel plate boundary using the draw function (Edit>Draw) and applied to all images. Then, for all assays (including free-motion behaviors and two-choice thermotaxis), the Crop feature (Image>Crop) was used to cut away all areas except the experimental area. Next, backgrounds were subtracted from all images (Process>Subtract Background; set rolling ball radius to 20.0 pixels; the light background box was selected). The brightness/contrast was adjusted to enhance the difference between the dark fly and the white background (Image>Adjust>Brightness/Contrast). Finally, the threshold was set to the automatically suggested setting (Image>Adjust>Threshold; Default and B&W settings were chosen, and the Don't reset range box was selected). In the Convert Stack to Binary box, the method was set to default, background was set to light, and the box corresponding to calculate threshold for each image was selected. The preprocessed image was then saved as a TIFF file (File>Save as>TIFF) for analysis.

Preprocessing videos for larval behavioral assays

Videos were converted to .avi and the resolution was decreased to 760×480 pixels by Any Video Converter 9 (AnvSoft). They were then uncompressed by Adobe Media Encoder or FFmpeg (ffmpeg -i input_file_name.avi -an -vcodec rawvideo -y output_file_name.avi).

Videos were imported to Fiji and converted to 8-bit grayscale (File>Import>AVI; the Convert to Grayscale box was selected). For the two-choice assays, the Rotate feature (Image>Transform>Rotate) was used to rotate images to make the marker line (release zone) vertical. Along the release zone, white lines were drawn at the top and bottom of the larval motion zone; these lines must not pass the larval moving path and should be applied to the first image only (Edit>Draw). Then, an area that was slightly larger than the larval motion zone that included the top and bottom white lines was selected and the Crop feature (Image>Crop) was applied for all images. Next, the background was subtracted from all

images (Process>Subtract Background; rolling ball radius of 50.0 pixels). Finally, the brightness/contrast was adjusted to enhance the difference between the white larva and the black background (Image>Adjust>Brightness/Contrast; set Maximum to the left and applied; then set Contrast to the right and applied). The preprocessed image was saved as an .avi file (File>Save as>AVI) for analysis.

TrackMate analysis

TrackMate, in Fiji, was used to analyze the speed, distance and preference/avoidance indices (Tinevez et al., 2017). Preprocessed .tif files or .avi files were opened using Fiji and TrackMate was run. In the LoG Detector box, we suggested adjusting the Estimated blob diameter, Threshold, and Median filter. For adult flies, we set the Estimated blob diameter to 27.0–40.0 pixels, Threshold to 1.0–2.5, and selected Median filter. For larvae, we set the Estimated blob diameter to about 10.0 pixels, Threshold to 1.0, and deselected the Median filter. In the Set filters on spots box, filters could be used to remove aberrant regions of interest (ROI) by choosing the *X* and *Y* region for ROI as well as the Quality of the ROI found. Alternatively, aberrant ROI can be removed manually from the All Spots statistics file. In the Simple LAP tracker box, we suggested adjusting the Linking max distance, the Gap-closing distance, and the Gap-closing max frame gap. For adult flies, we set the Linking max distance and the Gap-closing distance to the maximum *X* and *Y* pixel length of the image and the Gap-closing max frame gap to 2. For larvae, we set the Linking max distance and the Gap-closing distance to 25 pixels and the Gap-closing max frame gap to 2. In the Select an action box, Export all spots statistics was selected and then Execute was clicked. The All Spots statistics file was cross-referenced with the spot detection file in Fiji, which was used to ensure that only one spot was marked for each frame, and that erroneous duplicates and/or aberrant ROIs were deleted. Then, the All Spots statistics file was saved as a .csv file.

The moving distance from frame *n* to the next frame was calculated through the following formula:

$$\Delta\ \text{Distance} = \sqrt{(x_{n+1} - x_n)^2 + (y_{n+1} - y_n)^2}.$$

(1)

In the larval free-motion and two-choice assays, one pixel equaled about 0.493 mm. In the adult free-motion and two-choice assays, one pixel equaled about 0.060 mm.

The moving speed from frame *n* to the next frame was calculated through the following formula:

$$\text{Speed} = \frac{\Delta\ \text{Distance}}{\text{time}}.$$

(2)

The preference index (PI) or avoidance index (AI) was calculated by using the *X* position. The PI for the two-choice assay was calculated based on the time the animal spent in each temperature zone using the following formulas. For adults:

$$\text{PI} = \frac{(\text{time in } 25°\text{C}) - (\text{time in } 31°\text{C or } 11°\text{C})}{\text{Total time}}.$$

(3)

For larvae:

$$\mathrm{PI} = \frac{(\text{time in } 18°\mathrm{C}) - (\text{time in } 25°\mathrm{C})}{\text{Total time}}.$$

(4)

The AI for the adult optogenetic assay was calculated based on the time a fly spent under the infrared filter (in the ‘dark’) or in red light using the following formula:

$$\mathrm{AI} = \frac{(\text{time in the 'dark'}) - (\text{time in red light})}{\text{Total time}}.$$

(5)

Speed, distance and PI could be calculated using Excel. A Python script was developed to accelerate this process.

Statistical analysis

Statistical details of experiments are detailed in the figure legends. The normality of distributions was assessed by the Shapiro–Wilk *W* test ($P \leq 0.05$ rejected normal distribution) and statistical comparisons of normally distributed data were performed by Welch's *t*-test. For data that did not conform to a normal distribution, statistical comparisons were performed by the Mann–Whitney test. Data analysis was performed using GraphPad Prism 9 and the pseudo-F analysis was performed in R.

RESULTS

Using TrackMate to analyze larval behaviors

We first used TrackMate to track larval movement and analyzed the larval two-choice thermotactic assay. Larvae were allowed to move on a 3% agar gel. As TrackMate recognizes particles (ROI) based on their intensity, background noise signals may be recognized and mistakenly tracked as ROI. To diminish the background noise signals and increase contrast, a sheet of black matte poster paper was placed under the gel, and the ambient light was dimmed to under 10 lx. A GoPro camera was placed above the gel to record larval movement for 2 min. For the two-choice assay, a larva was released between plates held at two temperatures and recorded (Fig. 1A). The 2 min video was imported into Fiji and preprocessed, including cropping, subtracting the background, and adjusting brightness and threshold (Fig. 1C). For the two-choice assay, a line was drawn to separate different temperatures. This line must be white and must not pass through the moving path of the larva (Fig. 1G). TrackMate was then used to track larval movement and generate its trajectory (Fig. 1D,G). TrackMate also extracted *X* and *Y* positions of the larva on each frame to calculate its moving speed and distance (Fig. 1E,F). In the two-choice assay, we analyzed the *X* position of the line and the *X* position of the larva on each frame. This information allowed us to calculate the time the larva spent in each temperature zone and the PI (Fig. 1H).

We validated this method using y^{1},w^{*} (*wt*) and $Ir93a^{MI}$ larvae. IR93a is a subunit of the cool and warm receptors in dorsal organ temperature-responsive cells (Knecht et al., 2016; Hernandez-Nunez et al., 2021). $Ir93a^{MI}$ larvae moved significantly more than *wt* larvae (Fig. 1D,F,G; Movie 1). Regarding the PI, *wt* larvae preferred 18°C, consistent with previous reports (Fig. 1G,H; Movie 1) (Kwon et al., 2008, 2010; Shen et al., 2011). The $Ir93a^{MI}$ larvae

had no preference between 18 and 25°C, suggesting that IR93a is required for choosing the optimal temperature between these two (Fig. 1G,H; Movie 1).

Movie 1. https://movie.biologists.com/video/10.1242/jeb.243708/video-1

Representative trajectories of *Drosophila* adult and larval behaviors. The following behaviors are included: the *wt* (y^1, w^*) and $Ir93a^{MI}$ single-larva free-motion and two-choice thermotactic assays, *wt* (w^{1118}) and $Gr28b^{MB}$ single-fly free-motion and two-choice thermotactic assays, and *HC>CsChrimson* single-fly optogenetic assays (without and with dietary ATR)

An optogenetic assay was also analyzed by TrackMate. The optogenetic tool used in this study was the red light-shifted channel rhodopsin CsChrimson. When bound to all-trans retinal (ATR), CsChrimson is activated by red light to depolarize cells (Klapoetke et al., 2014). The larval optogenetic assay must be performed under infrared conditions while avoiding light glare. Red-light intensity should be even across the region over which the larva travels (Fig. 1B). The recording procedure and analysis method were similar to the free-motion assay. Larvae expressing CsChrimson in dorsal organ cool cells (DOCCs) showed aversive behaviors under red light with dietary ATR, such as pausing during the run, which led to a decrease in moving speed (Fig. 1I,J) (Tyrrell et al., 2021). These aversive behaviors reflected the cool avoidance driven by DOCCs and were not observed in the group without ATR (Fig. 1I,J).

The TrackMate-based automated tracking method provides an option if behavioral recordings are available and computer-based analysis is required. The analysis process may take longer when the recordings contain strong background noise signals. Fig. 1K shows an optogenetic setup that was previously used in the lab (Tyrrell et al., 2021). The light source was placed under an agar plate so that the light source and light glare were recorded (Fig. 1K). After the recordings had been converted to grayscale, the larva was detected, but a significant amount of background noise was also shown (the upper panel of Fig. 1L; the new setup had a cleaner background, as shown in the upper panel of Fig. 1I). We proposed cropping the video and using the smallest possible region for analysis. Fiji parameters, such as background, brightness and contrast, must be adjusted to diminish background noise signals. In most cases, not all background noise signals could be avoided (yellow circles in Fig. 1L). TrackMate parameters, including LoG detector, filters on spots, simple LAP tracker and filters on tracks, also had to be optimized to detect the larva in most frames (>99%) and maximally decrease noise signals. Finally, the All Spots statistics.csv file was carefully checked to ensure that all ROI were related to the larva and were not noise signals. On some frames, the larva was not detected or was counted more than once, so multiple tracks were generated. A colorful track means it is composed of multiple tracks (Fig. 1L). Although taking longer to process and analyze, these non-optimal recordings showed similar results to the optimal recordings, i.e. that DOCC expression of CsChrimson drove aversive behaviors (Fig. 1M).

Using TrackMate to analyze adult behaviors

We next used TrackMate to analyze adult behaviors. We maximally diminished the background noise signals by performing the assay on a piece of white paper (Fig. 2A). In our setup, the fly was covered by a transparent cover that only allowed it to walk, not fly. A Styrofoam box was placed over that to cover the experimental region and create a featureless environment with dim ambient light of under 10 lx. A GoPro camera was installed on the ceiling of the Styrofoam box to take time-lapse pictures (1 picture per second) for 2 min. These pictures were then imported into Fiji as an image sequence and preprocessed,

including cropping, subtracting the background, and adjusting brightness and threshold (Fig. 2C). Next, TrackMate was run to track the fly's movement, extract its *X* and *Y* positions, and generate its trajectory (Fig. 2D,G). Moving speed and distance were then calculated (Fig. 2E,F). We found that the warm receptor mutant, $Gr28b^{MB}$, moved significantly more than w^{1118} (*wt*) flies (Fig. 2D,F; Movie 1).

When TrackMate was used to analyze an adult two-choice assay, a black line was drawn to separate the two temperatures and used as a reference to calculate the PI (Fig. 2G). While *wt* flies avoided 31°C and preferred 25°C, $Gr28b^{MB}$ did not show a preference between 25 and 31°C (Fig. 2G,H). This result is consistent with previous reports (Ni et al., 2013; Simões et al., 2021; Budelli et al., 2019). Moreover, $Gr28b^{MB}$ also moved more than *wt* flies in this condition (Fig. 2F,G; Movie 1).

We also used this method to analyze the two-choice optogenetic assay. In this assay, a red-light source was placed ~457 mm above the experimental surface. Half of the transparent cover was covered by an infrared filter to create the 'dark' environment (Fig. 2B). Of note, the red light could not be directly above the cover because it caused light glares. The recording procedure and analysis method were similar to those for the larval optogenetic assay. HCs in aristae drive warm avoidance (Gallio et al., 2011; Budelli et al., 2019; Ni et al., 2013). Flies expressing CsChrimson in HCs avoided red light with dietary ATR (Fig. 2I,J; Movie 1). Without ATR, HCs were not activated and did not guide flies to avoid the red light. This hypothesis was validated by the observation that flies raised without ATR often traveled from the 'dark' zone to the red-light zone (Fig. 2I, left; Movie 1).

Drosophila species have diverse mobilities in adults

Next, we used the adult thermotactic two-choice assay to examine the temperature responses of different *Drosophila* species. We used two setups: the warm avoidance assay required flies to choose between 25 and 31°C, while the cool avoidance assay required flies to choose between 25 and 11°C. We tested 801 flies, including four genotypes of *D. melanogaster* (as controls), *D. ananassae*, *D. biarmipes*, *D. bipectinata*, *D. erecta*, *D. ficusphila*, *D. mojavensis*, *D. simulans* and *D. yakuba.* To determine their temperature preferences using thermotactic behaviors, we first excluded species that did not move or moved minimally. The behavioral recordings for each fly were analyzed using Fiji, their positions were extracted by TrackMate, and moving distances were calculated. We grouped moving distances by pseudo-F statistics and identified 10 clusters. Flies in the cluster with the shortest moving distances moved from 6.45 mm (107.584 pixels) to 47.90 mm (799.243 pixels). Independent visual analysis by four researchers agreed that flies in this cluster had limited mobility. Flies in other clusters explored both temperature zones adequately (Movie 2). Thereby, we set 47.95 mm (800 pixels) as the threshold (the dashed line in Fig. 3). Flies were omitted from PI analysis if their moving distances were shorter than 47.95 mm.

Movie 2. https://movie.biologists.com/video/10.1242/jeb.243708/video-2

Set the threshold value for moving distances. Example trajectories from flies with moving distances of about 250 pixels, 450 pixels, 650 pixels, 850 pixels, and 1050 pixels. Trajectories are shown in red.

Most fly species moved significantly more in the warm avoidance assay than in the cool avoidance assay, including w^{1118} *D. melanogaster*, *D. ananassae*, *D. biarmipes*, *D. bipectinata*, *D. erecta*, *D. mojavensis*, *D. simulans* and *D. yakuba* (Fig. 3). These data suggest that flies are more active in warm environments.

Moreover, fly species had diverse mobilities. In the warm avoidance assay, *D. erecta* moved the least and *D. mojavensis* moved the most. The average moving distance of *D. erecta* was about 1/15 that of *D. mojavensis.* In the cool avoidance assay, *D. erecta* still moved the least, but the most active flies were *D. melanogaster Ir93a*^{MI}, whose average moving distance was over 31 times that of *D. erecta* (Fig. 3). Of note, in the warm avoidance assay, moving distances from more than half of the *D. ananassae* and *D. erecta* flies did not reach the threshold (Fig. 3) and were not further analyzed. Similarly, in the cool avoidance assay, less than half of the *D. ananassae*, *D. erecta* and *D. simulans* flies reached the threshold (Fig. 3); thus, their PIs were also not calculated.

Starting temperature and sex affect PI

To understand the effects of starting temperature and sex on PI, we examined the temperature preference of male and female wild-type *w*^{1118} *D. melanogaster* under different conditions. A positive PI shows a preference for 25°C, while a negative PI indicates a preference for 31 or 11°C; a PI near zero suggests no preference.

We divided *w*^{1118} data obtained from the warm avoidance assay into four groups: males starting at 25°C, females starting at 25°C, males starting at 31°C and females starting at 31°C. As shown in Fig. 4A, males and females had similar PIs when they started at the same temperature. When flies started at different temperatures, the PIs showed a significant difference. Flies starting at 25°C preferred 25°C, while flies starting at 31°C had no preference. These data suggest that starting temperature, but not sex, affects PI in the warm avoidance assay.

In the cool avoidance assay, we also divided *w*^{1118} data into four groups: males starting at 25°C, females starting at 25°C, males starting at 11°C and females starting at 11°C (Fig. 4B). When flies started at 25°C, males had a stronger preference for 25°C than female flies did. This difference was not observed if they started at 11°C. Moreover, males starting at 25°C strongly preferred 25°C, and males starting at 11°C had no preference between 25 and 11°C. For females, flies starting at 25°C had a higher PI than those starting at 11°C, but these two groups were not significantly different. Therefore, in the cool avoidance assay, both starting temperature and sex affected PI. To understand the temperature preference of each fly species, males and females were separated and only flies starting at 25°C were analyzed.

***Drosophila biarmipes*, *D. bipectinata*, *D. mojavensis* and *D. yakuba* do not avoid warm temperatures**

Finally, we calculated PIs of different fly species. As mentioned above, only flies starting at 25°C were used. We tested four *D. melanogaster* genotypes: two wild-types, *w*^{1118} and *CS*; a cool receptor mutant, *Ir93a*^{MI}; and a warm receptor mutant, *Gr28b*^{MB} (Knecht et al., 2016; Budelli et al., 2019; Ni et al., 2013). In the warm avoidance assay, both male and female *w*^{1118} and *CS* strongly preferred 25°C (Fig. 5A,B). The PI of *Gr28b*^{MB} was significantly lower than that of *w*^{1118}, consistent with previous reports (Ni et al., 2013; Simões et al., 2021; Budelli et al., 2019) (Fig. 5A,B). *Drosophila biarmipes*, *D. bipectinata* and *D. yakuba* had similar PIs to *Gr28b*^{MB}, suggesting that they do not have a preference between 25 and 31°C (Fig. 5A,B). *Drosophila mojavensis* flies had negative PIs, indicating they prefer 31°C (Fig. 5A,B).

***Drosophila bipectinata* and *D. yakuba* do not avoid cool temperatures**

In the cool avoidance assay, male *w*^{1118} and *CS* strongly preferred 25°C (Fig. 5C). As reported previously (Enjin et al., 2016; Budelli et al., 2019), cool receptor

mutant *Ir93a*^{Ml} males had a lower PI than *w*^{1118} males (Fig. 5C). The PIs of *D. ficusphila* and *D. yakuba* males were close to 0, indicating they have no preference between 25 and 11°C (Fig. 5C). *Drosophila bipectinata* males had a negative PI, suggesting they prefer 11°C (Fig. 5C).

Regarding female flies, *w*^{1118} and *CS* also preferred 25°C (Fig. 5D). Unexpectedly, *Ir93a*^{Ml} females had a similar PI to *w*^{1118} females. *Drosophila bipectinata* and *D. yakuba* females, like their male counterparts, had PIs close to 0, indicating they have no preference between 25 and 11°C (Fig. 5D). In contrast, *D. ficusphila* females behaved differently from their males: *Drosophila ficusphila* males had no preference between 25 and 11°C, but the females had a strong preference for 25°C. These data further suggest that sex affects PI, at least in the cool avoidance assay.

DISCUSSION

In this paper, we first described an automated tracking method to analyze various *Drosophila* larval and adult behaviors, including free-motion behaviors, two-choice thermotaxis and optogenetic assays. Then, we used adult thermotactic two-choice assays to examine thermal preferences of different *Drosophila* species. We tested 801 flies, including four genotypes of *D. melanogaster* and eight other *Drosophila* species. Distinct fly species showed different temperature preferences from wild-type *D. melanogaster*. Wild-type *D. melanogaster* flies avoided the higher temperature of 31°C in the warm avoidance assay and the cooler temperature of 11°C in the cool avoidance assay. However, *D. bipectinata* and *D. yakuba* did not avoid either warm or cool temperatures in the respective assays, and *D. biarmipes* and *D. mojavensis* did not avoid the warm temperature in the warm avoidance assay. Our results also indicate that starting temperature and sex affect PI.

Drosophila melanogaster exhibit sophisticated behaviors that are widely used in studies of development, synaptic transmission, sensory physiology, and learning and memory. Many of these behaviors depend on locomotion. Locomotion analysis of larvae and adult flies is essential to gather insight into how modification of genetic components affects animal behaviors and changes their responses to stimuli. Thus, examination of their movement has become an integral part of such studies, leading to the development of tracking systems to provide a quantitative description of their behaviors (Bellen et al., 2010). Several tracking systems have been developed to track the locomotion of larvae and adult flies (Werkhoven et al., 2019; Branson et al., 2009; Valente et al., 2007; Straw and Dickinson, 2009; Colomb et al., 2012). However, many methods require programming skills and/or commercial software to set up or run the tracking systems, which often are obstacles for the researchers adopting these methods. Other methods only track larvae or adult movement, require specific experimental setups for data collection, or are challenging to analyze non-optimal recordings. Therefore, an automated tracking tool is required to analyze the locomotion of both larvae and adult flies. This tracking tool must be compatible with various file formats and non-optimal recordings. Ideally, this tool employs free software that does not require programming knowledge so that most laboratories can readily adopt it. We describe such a tool in this study. The Fiji plugin TrackMate is a free and open-source software. It accepts different file formats. Moreover, TrackMate can assess behavioral recordings from larvae and adult flies, even if the recordings include a lot of background noise. TrackMate extracts the *X* and *Y* positions of an animal on each frame. This position information is used to generate trajectories, calculate moving distances and speeds, and determine PIs in two-choice assays.

Clean backgrounds facilitate the analysis. TrackMate detects ROI – flies or larvae – based on their intensity. It cannot distinguish ROI from background noise signals if they have

similar sizes and/or intensities. Thereby, noise signals cause aberrant trajectories and require researchers to adjust TrackMate parameters to avoid these signals and check the All Spots statistics.csv file to delete information relating to noise signals in the file. We provide easy ways to obtain clean backgrounds – a piece of white paper or matte black poster paper can significantly decrease background noise signals.

TrackMate can analyze data recorded in image sequences and videos. In this study, we used time-lapse images to record adult free-motion and two-choice behaviors and videos to record larval behaviors and adult optogenetic assays. Thereby, analysis approaches for both recording methods are presented. Most videos contained 24–30 frames s^{-1}; their high temporal resolution resolved more behavioral details. When calculating moving distance and PI, high temporal resolution may not be necessary. In this case, time-lapse images become a better choice because they contain fewer data and take a shorter time to analyze. However, the time-lapse image resolution of the GoPro cannot distinguish the larva from the background; thus, videos were used for larval assays instead. When performing the larval optogenetic assay, we found it easier to track the larva under infrared conditions. Of note, regular cameras do not work under infrared conditions; the internal infrared filter needs to be removed and replaced by an 830 nm long-pass filter.

Based on trajectories, researchers can observe whether an animal runs or turns. Unfortunately, TrackMate cannot be used to analyze more complex behaviors, such as larval head sweeping or wing and leg movements in adult flies. We set a relatively large blob diameter to make TrackMate recognize the adult fly or larva as a single ROI. If using a smaller blob diameter, TrackMate often detects the animal as multiple ROI. However, the localization of each ROI is not defined; in other words, TrackMate cannot be used to recognize different parts of an animal, such as the head or tail. Therefore, it is challenging to use TrackMate to analyze more complex behaviors.

Two-choice assays are widely used to evaluate animal responses to environmental stimuli, such as light, odor, tastant, humidity and temperature. Many labs apply T-mazes to perform two-choice assays in adult flies, where researchers depend on the final position of animals to determine their preference (Sayeed and Benzer, 1996). However, it is challenging for T-maze-based two-choice assays to simultaneously assess the animals' ability to move, which is crucial for many behaviors. This issue can be solved by performing two-choice assays in a Petri dish, or a similar surface, as in our system (Figs 1A and 2A). By using this type of setup, researchers can constantly track animal responses to ensure that the differences in preference are not due to defects in locomotion. This study describes an automated tracking approach that allows researchers to quantify animal locomotion without programming knowledge. Moreover, we provide easy ways to obtain clean backgrounds for tracking and analysis. Finally, we adapted commercial equipment for thermotactic two-choice assays to increase reproducibility.

When using the adult thermotactic two-choice assay to examine the thermal preferences of different *Drosophila* species, we found that most fly species moved significantly more in warm environments than in cool environments. But this is not true for the cool receptor mutant *Ir93a*^{MI} and the warm receptor mutant *Gr28b*^{MB} (Knecht et al., 2016; Budelli et al., 2019; Ni et al., 2013). In these two mutants, moving distances were similar in the two assays. Moreover, these two mutants moved significantly more than wild-type *D. melanogaster w*^{1118} (Fig. 3). The reasons for these phenomena are unknown. One possibility is that these mutants per se move more. This possibility can be tested by measuring their moving distances in environments with unique temperatures. *Gr28b*^{MB} supports this possibility as it moved more than *w*^{1118} at 25°C (Fig. 2F). Interestingly, *Gr28b*^{MB} moving

speed did not show an obvious decrease over time, while w^{1118} speed did (Fig. 2E). An alternative possibility is that $Ir93a^{MI}$ and $Gr28b^{MB}$ moved more only when they were allowed to explore different temperature zones. In this case, temperature receptors help animals to not only choose an optimal temperature but also save energy. Further studies are needed to test these possibilities.

According to the w^{1118} data, starting temperature affects PI. The only pair that was not significantly different was females starting at 25 and 11°C in the cool avoidance assay. Even in this case, the PI of the former group was higher than that of the latter group (Fig. 4B). The PI is determined by the amount of time an animal spends in each temperature zone. If an animal starts at 25°C, it may know where the 25°C zone is and, thus, can quickly return to it, even if it travels to the opposite side. However, if a fly starts at 31 or 11°C, it may not realize there is a 25°C zone or where the zone is. As a result, as time spent in unfavorable temperatures increases, the PI decreases. Moreover, sex also affects PI. For example, in the cool avoidance assay, w^{1118} males had a stronger preference for 25°C than their female counterparts when they started at 25°C (Fig. 4B). In addition, *D. ficusphila* males had no preference between 25 and 11°C, but females had a strong preference for 25°C (Fig. 5C,D).

GR28BD is the warm receptor that guides animals to rapidly avoid the high temperature in the two-choice warm avoidance assay (Ni et al., 2013; Simões et al., 2021; Budelli et al., 2019). As expected, $Gr28b^{MB}$ had defects in the warm avoidance assay but not in the cool avoidance assay (Fig. 5). IR93a is a component of the cool receptor, and its mutant has been reported to be deficient in avoiding both warm and cool temperatures in the respective assays (Enjin et al., 2016; Budelli et al., 2019; Knecht et al., 2016). In the warm avoidance assay, $Ir93a^{MI}$ flies had a lower, but not significantly different, PI than that of w^{1118} (Fig. 5A,B). The difference may be because we only analyzed flies starting at 25°C. In the cool avoidance assay, the PI of $Ir93a^{MI}$ males was significantly lower than that of w^{1118} males (Fig. 5C), which is consistent with previous studies. However, $Ir93a^{MI}$ females had a similar PI to that of w^{1118} females (Fig. 5D). We suspect that this is due to the lower PI of w^{1118} females (Fig. 4B) or the lower temperature in our cool zone than in the previous study (Budelli et al., 2019). IR25a is another cool receptor component, and its mutant does not have defects in avoiding 10°C zones (Enjin et al., 2016). Further studies on the functions of the cool receptor are needed.

Compared with *D. melanogaster*, *D. biarmipes*, *D. bipectinata*, *D. mojavensis* and *D. yakuba* showed different temperature preferences in the warm avoidance assay, and *D. bipectinata* and *D. yakuba* showed different preferences in the cool avoidance assay. To our knowledge, this is the first study to compare aristal thermoreceptor-controlled thermotaxis among different *Drosophila* species. Warm and/or cool receptors from these species may offer opportunities for understanding mechanisms enabling thermoreceptors to respond to different temperatures.

In summary, in this study we developed an automated tracking method to analyze various *Drosophila* larval and adult behaviors and identified the species exhibiting different temperature preferences from those of *D. melanogaster*. In the future, the temperature preferences of other fly species should be analyzed, and thermosensory organs, neurons and molecular receptors should be compared among different fly species to understand the mechanisms underlying temperature preference.

Acknowledgements

We acknowledge Dr Jianhong Ou for the R script of the pseudo-F statistics and Dr Michael Dickinson for *CS* and *D. mojavensis* flies.

Author contributions

Conceptualization: A.H., A.A.O., L.N.; Methodology: A.H., A.A.O., A.N.C., L.N.; Software: A.A.O.; Validation: A.H., A.A.O., T.J.V., A.N.C.; Formal analysis: A.H., A.A.O., T.J.V., L.N.; Investigation: A.H., A.A.O., T.J.V., A.N.C.; Resources: L.N.; Data curation: A.H., A.A.O., T.J.V., A.N.C.; Writing - original draft: A.A.O., T.J.V., L.N.; Writing - review & editing: A.H., A.A.O., T.J.V., A.N.C., L.N.; Visualization: A.H., A.A.O., T.J.V., A.N.C.; Supervision: L.N.; Project administration: A.H., A.A.O., L.N.; Funding acquisition: L.N.

Funding

This work was supported by the National Institutes of Health (R21MH122987 to L.N. and R01GM140130 to L.N.). Deposited in PMC for release after 12 months.

Data availability

The Python script has been deposited in GitHub and can be accessed at: https://github.com/niflylab/SingleFlyAnalysis.git. Original statistics and raw data are available from
Dataverse: https://doi.org/10.7910/DVN/SNBQC2 and https://doi.org/10.7910/DVN/DNFWKI.

Competing interests

The authors declare no competing or financial interests.

References

Barbagallo, B. and Garrity, P. A. (2015). Temperature sensation in Drosophila. Curr. Opin. Neurobiol. 34, 8-13. doi:10.1016/j.conb.2015.01.002

Bellen, H. J., Tong, C. and Tsuda, H. (2010). 100 years of Drosophila research and its impact on vertebrate neuroscience: a history lesson for the future. Nat. Rev. Neurosci. 11, 514-522. doi:10.1038/nrn2839

Branson, K., Robie, A. A., Bender, J., Perona, P. and Dickinson, M. H. (2009). High-throughput ethomics in large groups of Drosophila. Nat. Methods 6, 451-457. doi:10.1038/nmeth.1328

Brown, A. W. A. (1951). Factors in the attractiveness of bodies for mosquitoes. Nature 167, 202. doi:10.1038/167202a0

Budelli, G., Ni, L., Berciu, C., Van Giesen, L., Knecht, Z. A., Chang, E. C., Kaminski, B., Silbering, A. F., Samuel, A., Klein, M. et al. (2019). Ionotropic receptors specify the morphogenesis of phasic sensors controlling rapid thermal preference in Drosophila. Neuron 101, 738-747.e3. doi:10.1016/j.neuron.2018.12.022

Celniker, S. E., Wheeler, D. A., Kronmiller, B., Carlson, J. W., Halpern, A.,Patel, S., Adams, M., Champe, M., Dugan, S. P., Frise, E. et al. (2002). Finishing a whole-genome shotgun: release 3 of the Drosophila melanogaster euchromatic genome sequence. Genome Biol. 3, research0079.1. doi:10.1186/gb-2002-3-12-research0079

Chen, Z. X., Sturgill, D., Qu, J., Jiang, H., Park, S., Boley, N., Suzuki, A. M., Fletcher, A. R., Plachetzki, D. C., Fitzgerald, P. C. et al. (2014). Comparative validation of the D. melanogaster modENCODE transcriptome annotation. Genome Res. 24, 1209-1223. doi:10.1101/gr.159384.113

Clark, A. G., Eisen, M. B., Smith, D. R., Bergman, C. M., Oliver, B., Markow, T. A., Kaufman, T. C., Kellis, M., Gelbart, W., Iyer, V. N. et al. (2007). Evolution of genes and genomes on the Drosophila phylogeny. Nature 450, 203-218. doi:10.1038/nature06341

Colomb, J., Reiter, L., Blaszkiewicz, J., Wessnitzer, J. and Brembs, B. (2012). Open source tracking and analysis of adult Drosophila locomotion in Buridan's paradigm with and without visual targets. PLoS ONE 7, e42247. doi:10.1371/ journal.pone.0042247

Corfas, R. A. and Vosshall, L. B. (2015). The cation channel TRPA1 tunes mosquito thermotaxis to host temperatures. eLife 4, e11750. doi:10.7554/eLife.11750

Dell, A. I., Pawar, S. and Savage, V. M. (2011). Systematic variation in the temperature dependence of physiological and ecological traits. Proc. Natl. Acad. Sci. USA. 108, 10591-10596. doi:10.1073/pnas.1015178108

Dillon, M. E.,Wang, G. and Huey, R. B. (2010). Global metabolic impacts of recent climate warming. Nature 467, 704-706. doi:10.1038/nature09407

Enjin, A., Zaharieva, E. E., Frank, D. D., Mansourian, S., Suh, G. S., Gallio, M. and Stensmyr, M. C. (2016). Humidity sensing in drosophila. Curr. Biol. 26, 1352-1358. doi:10.1016/j.cub.2016.03.049

Franks, S. J. and Hoffmann, A. A. (2012). Genetics of climate change adaptation. Annu. Rev. Genet. 46, 185-208. doi:10.1146/annurev-genet-110711-155511

Gallio, M., Ofstad, T. A., Macpherson, L. J.,Wang, J.W. and Zuker, C. S. (2011). The coding of temperature in the Drosophila brain. Cell 144, 614-624. doi:10.1016/j.cell.2011.01.028

Garrity, P. A., Goodman, M. B., Samuel, A. D. and Sengupta, P. (2010). Running hot and cold: behavioral strategies, neural circuits, and the molecular machinery for thermotaxis in C. elegans and Drosophila. Genes Dev. 24, 2365-2382. doi:10.1101/gad.1953710

Greppi, C., Budelli, G. and Garrity, P. A. (2015). Some like it hot, but not too hot. Elife 4, e12838. doi:10.7554/eLife.12838

Greppi, C., Laursen, W. J., Budelli, G., Chang, E. C., Daniels, A. M., Van Giesen, L., Smidler, A. L., Catteruccia, F. and Garrity, P. A. (2020). Mosquito heat seeking is driven by an ancestral cooling receptor. Science 367, 681-684. doi:10.1126/science.aay9847

Hamada, F. N., Rosenzweig, M., Kang, K., Pulver, S. R., Ghezzi, A., Jegla, T. J. and Garrity, P. A. (2008). An internal thermal sensor controlling temperature preference in Drosophila. Nature 454, 217-220. doi:10.1038/nature07001

Hernandez-Nunez, L., Chen, A., Budelli, G., Berck, M. E., Richter, V., Rist, A., Thum, A. S., Cardona, A., Klein, M., Garrity, P. et al. (2021). Synchronous and opponent thermosensors use flexible cross-inhibition to orchestrate thermal homeostasis. Sci. Adv. 7, eabg6707. doi:10.1126/sciadv.abg6707

Hoskins, R. A., Carlson, J. W., Kennedy, C., Acevedo, D., Evans-Holm, M., Frise, E., Wan, K. H., Park, S., Mendez-Lago, M., Rossi, F. et al. (2007).

Sequence finishing and mapping of Drosophila melanogaster heterochromatin. Science 316, 1625-1628. doi:10.1126/science.1139816

Howlett, F. M. (1910). The influence of temperature upon the biting of mosquitoes. Parasitology 3, 479-484. doi:10.1017/S0031182000002304

Hu, T. T., Eisen, M. B., Thornton, K. R. and Andolfatto, P. (2013). A second generation assembly of the Drosophila simulans genome provides new insights into patterns of lineage-specific divergence. Genome Res. 23, 89-98. doi:10.1101/gr.141689.112

Klapoetke, N. C., Murata, Y., Kim, S. S., Pulver, S. R., Birdsey-Benson, A., Cho, Y. K., Morimoto, T. K., Chuong, A. S., Carpenter, E. J., Tian, Z. et al. (2014). Independent optical excitation of distinct neural populations. Nat. Methods 11, 338-346. doi:10.1038/nmeth.2836

Klein, M., Afonso, B., Vonner, A. J., Hernandez-Nunez, L., Berck, M., Tabone, C. J., Kane, E. A., Pieribone, V. A., Nitabach, M. N., Cardona, A. et al. (2015). Sensory determinants of behavioral dynamics in Drosophila thermotaxis. Proc. Natl. Acad. Sci. USA. 112, E220-E229. doi:10.1073/pnas.1421697112

Knecht, Z. A., Silbering, A. F., Ni, L., Klein, M., Budelli, G., Bell, R., Abuin, L., Ferrer, A. J., Samuel, A. D., Benton, R. et al. (2016). Distinct combinations of variant ionotropic glutamate receptors mediate thermosensation and hygrosensation in Drosophila. eLife 5, e17879. doi:10.7554/eLife.1787910

Kwon, Y., Shim, H. S., Wang, X. and Montell, C. (2008). Control of thermotactic behavior via coupling of a TRP channel to a phospholipase C signaling cascade. Nat. Neurosci. 11, 871-873. doi:10.1038/nn.2170

Kwon, Y., Shen, W. L., Shim, H. S. and Montell, C. (2010). Fine thermotactic discrimination between the optimal and slightly cooler temperatures via a TRPV channel in chordotonal neurons. J. Neurosci. 30, 10465-10471. doi:10.1523/JNEUROSCI.1631-10.2010

Ni, L., Bronk, P., Chang, E. C., Lowell, A. M., Flam, J. O., Panzano, V. C., Theobald, D. L., Griffith, L. C. and Garrity, P. A. (2013). A gustatory receptor paralogue controls rapid warmth avoidance in Drosophila. Nature. 500, 580-584.doi:10.1038/nature12390

Powell, J. R. (1997). Progress and Prospects in Evolutionary Biology: The Drosophila Model. Oxford University Press, Incorporated. Sa´nchez-Alcan˜iz, J. A., Silbering, A. F.,

Croset, V., Zappia, G., Sivasubramaniam, A. K., Abuin, L., Sahai, S. Y., Mu¨ nch, D., Steck, K., Auer, T. O. et al. (2018). An expression atlas of variant ionotropic glutamate receptors identifies a molecular basis of carbonation sensing. Nat. Commun. 9, 4252. doi:10.1038/s41467-018-06453-1 Sayeed, O. and Benzer, S. (1996). Behavioral genetics of thermosensation and hygrosensation in Drosophila. Proc. Natl. Acad. Sci. USA. 93, 6079-6084.doi:10.1073/pnas.93.12.6079

Schindelin, J., Arganda-Carreras, I., Frise, E., Kaynig, V., Longair, M., Pietzsch, T., Preibisch, S., Rueden, C., Saalfeld, S., Schmid, B. et al. (2012). Fiji: an open-source platform for biological-image analysis. Nat. Methods 9, 676-682. doi:10.1038/nmeth.2019

Sengupta, P. and Garrity, P. (2013). Sensing temperature. Curr. Biol. 23, R304-R307. doi:10.1016/j.cub.2013.03.009

Shen,W. L.,Kwon, Y., Adegbola, A. A., Luo, J., Chess, A. and Montell, C. (2011). Function of rhodopsin in temperature discrimination in Drosophila. Science 331, 1333-1336. doi:10.1126/science.1198904

Simões, J. M., Levy, J. I., Zaharieva, E. E., Vinson, L. T., Zhao, P., Alpert, M. H., Kath, W. L., Para, A. and Gallio, M. (2021). Robustness and plasticity in Drosophila heat avoidance. Nat. Commun. 12, 2044. doi:10.1038/s41467-021-22322-w

Stark, A., Lin, M. F., Kheradpour, P., Pedersen, J. S., Parts, L., Carlson, J. W., Crosby, M. A., Rasmussen, M. D., Roy, S., Deoras, A. N. et al. (2007). Discovery of functional elements in 12 Drosophila genomes using evolutionary signatures. Nature 450, 219-232. doi:10.1038/nature06340

Straw, A. D. and Dickinson, M. H. (2009). Motmot, an open-source toolkit for realtime video acquisition and analysis. Source Code Biol. Med. 4, 5. doi:10.1186/1751-0473-4-5

Tinevez, J.-Y., Perry, N., Schindelin, J., Hoopes, G. M., Reynolds, G. D., Laplantine, E., Bednarek, S. Y., Shorte, S. L. and Eliceiri, K. W. (2017). TrackMate: an open and extensible platform for single-particle tracking. Methods 115, 80-90. doi:10.1016/j.ymeth.2016.09.016

Tyrrell, J. J., Wilbourne, J. T., Omelchenko, A. A., Yoon, J. and Ni, L. (2021). Ionotropic Receptor-dependent cool cells control the transition of temperature preference in Drosophila larvae. PLoS Genet. 17, e1009499. doi:10.1371/journal.pgen.1009499

Valente, D., Golani, I. and Mitra, P. P. (2007). Analysis of the trajectory of Drosophila melanogaster in a circular open field arena. PLoS ONE 2, e1083. doi:10.1371/journal.pone.0001083

Werkhoven, Z., Rohrsen, C., Qin, C., Brembs, B. and De Bivort, B. (2019). MARGO (Massively Automated Real-time GUI for Object-tracking), a platform for high-throughput ethology. PLoS One 14, e0224243. doi:10.1371/journal.pone.0224243